

# UC San Diego

## UC San Diego Electronic Theses and Dissertations

### Title

Physical and biological dynamics of surfzone bacterial pollution : sources, transports, and removal mechanisms

### Permalink

<https://escholarship.org/uc/item/1qd3m3w9>

### Author

Rippy, Megan Anjuli

### Publication Date

2012

Peer reviewed|Thesis/dissertation

UNIVERSITY OF CALIFORNIA, SAN DIEGO

Physical and Biological Dynamics of Surfzone Bacterial Pollution: Sources,  
Transports, and Removal Mechanisms

A dissertation submitted in partial satisfaction of the requirements for the degree  
Doctor of Philosophy

in

Oceanography

by

Megan Anjuli Rippy

Committee in charge:

Professor Peter J. S. Franks, Chair  
Professor Farooq Azam  
Professor Douglas Bartlett  
Professor Falk Feddersen  
Professor Joshua Graff Zivin  
Professor Stanley Grant  
Professor Robert Guza

2012

Copyright

Megan Anjuli Rippy, 2012

All rights reserved.

The Dissertation of Megan Anjuli Rippy is approved, and it is acceptable in quality  
and form for publication on microfilm and electronically:

---

---

---

---

---

---

---

---

---

---

Chair

University of California, San Diego

2012

## DEDICATION

To Mom and Dad, with love. You never doubted this day would come. This one is for you.

## EPIGRAPH

“Essentially, all models are wrong, but some are useful.”

*George E. P. Box*

## TABLE OF CONTENTS

Signature page.....	iii
Dedication.....	iv
Epigraph.....	v
Table of Contents.....	vi
List of Figures.....	ix
List of Tables.....	xv
Acknowledgements.....	xvi
Vita.....	xx
Abstract.....	xxi
Chapter 1: Introduction.....	1
Fecal indicator bacteria (FIB) as indicators of human health risk.....	1
Mortality of fecal indicator bacteria .....	4
Growth of fecal indicator bacteria.....	6
Fluid dynamics and FIB transport in coastal systems.....	7
Tying it all together: physical-biological assessment.....	12
But what about management?.....	15
Dissertation goals.....	17
Literature Cited.....	20
Chapter 2: Physical factors controlling variability in nearshore fecal pollution: fecal indicator bacteria as passive particles.....	31
Abstract.....	31
Introduction.....	31
Methods.....	33
<i>Field site description</i> .....	33
<i>FIB sampling program</i> .....	33
<i>2D Individual based FIB model</i> .....	35
Results and Discussion.....	39
<i>Physical environment</i> .....	39
<i>Bacterial patterns at Huntington Beach</i> .....	40
<i>Spatial structure of FIB decay</i> .....	41
<i>Model Sensitivity Analysis: Initial Patch Size</i> .....	41

<i>Best-fit model-data comparisons: Physical factors controlling FIB patchiness</i> .....	42
Acknowledgements.....	45
Literature Cited.....	46
Tables.....	48
Figures.....	49
Appendix 2.1.....	55
Appendix 2.2.....	56
 Chapter 3: Factors controlling variability in nearshore fecal pollution: the effects of mortality. ....	 62
Abstract.....	62
Introduction.....	62
Methods.....	65
<i>Sampling design</i> .....	65
<i>Enterococcus species identification</i> .....	65
<i>Solar insolation studies</i> .....	66
<i>2D Individual based FIB models</i> :.....	68
Results and Discussion.....	72
<i>Spatial patterns in Enterococcus species distribution</i> .....	72
<i>Solar insolation vs. decay</i> .....	74
<i>Mortality models: Best-fit parameter values</i> .....	75
<i>Best-fit model-data comparisons: physical and physical-mortality models compared</i> .....	76
<i>Best-fit model-data comparisons: FIB mortality mechanisms</i> .....	76
Acknowledgements.....	79
Literature Cited.....	81
Tables.....	84
Figures.....	85
Appendix 3.1.....	93
 Chapter 4: The effects of the bloom forming dinoflagellate <i>Lingulodinium polyedrum</i> on the mortality of <i>Enterococcus faecium</i> in seawater: mortality rates, water quality impacts, and monitoring implications.....	 99
Abstract.....	99
Introduction.....	100
Methods.....	103
<i>FIB-phytoplankton microcosm experiments</i> .....	103
<i>Model evaluation: the effects of phytoplankton on a surfzone pollutant patch</i> .....	104
<i>Direct correlations: detecting FIB-phytoplankton interactions in marine systems</i> .....	107
Results and Discussion.....	112



<i>Microcosm experiments</i> .....	112
<i>The effects of phytoplankton on a surfzone pollutant patch</i> .....	116
<i>Detecting FIB-phytoplankton interactions using direct correlations</i>	118
Summary and Conclusions.....	122
Acknowledgements.....	124
Literature Cited.....	125
Tables.....	131
Figures.....	132
Appendix 4.1.....	141
 Chapter 5: Beach nourishment impacts on bacteriological water quality and phytoplankton bloom dynamics.....	 142
Abstract.....	142
Introduction.....	143
Methods.....	145
<i>Field site description</i> .....	145
<i>Beach nourishment</i> .....	146
<i>Biological monitoring program</i> .....	146
<i>Enterococci in nourishment sediments</i> .....	148
<i>Water quality assessment: correlations and predictive statistical models</i> .....	149
<i>Surfzone residence time of Enterococcus</i> .....	150
<i>Enterococcus inactivation microcosm experiments</i> .....	151
Results and Discussion.....	152
<i>Physical environment</i> .....	152
<i>Water quality assessment: phytoplankton</i> .....	153
<i>Water quality assessment: Enterococcus</i> .....	156
<i>Sediment Enterococcus levels</i> .....	159
<i>Surfzone residence time: Enterococcus</i> .....	160
<i>Enterococcus inactivation: microcosm experiments</i> .....	161
Acknowledgements.....	164
Literature Cited.....	166
Figures.....	173
Appendix 5.1.....	183
Appendix 5.2.....	188
 Chapter 6: Summary and Conclusions.....	 192
Literature Cited.....	201

## LIST OF FIGURES

<p><b>Figure 2.1:</b> Schematic of the HB06 experiment. White boxes mark the location of bacterial sampling stations. Alongshore sampling sites were the Santa Ana River (SAR), the Talbert Marsh (TM), a station 500 m north of the Santa Ana River (FHM), and the first surfzone frame (F1). Cross-shore sampling sites were located at the first (F1), third (F3), fifth (F5), and seventh (F7) surfzone frames as well as an offshore buoy (OM). Depth and distance offshore of cross-shore sites are shown in the inset, where blue circles mark the location of ADV's.....</p>	49
<p><b>Figure 2.2:</b> (A) Significant wave height and (B) 20-minute mean alongshore current (red = surfzone and black = offshore), measured at cross-shore frames F1-F7. (C) Mean water depth measured at F3 versus time (hours) from 1950 on October 15<sup>th</sup> to 2350 on October 16<sup>th</sup>. Midnight is at t = 0 h. Dashed boxes indicate the 5-hr HB06 FIB study period.....</p>	50
<p><b>Figure 2.3:</b> Along- and cross-shore locations of FIB particles initialized in a uniform rectangular patch at 0650 (A) and advected back in time using measured alongshore currents for six (B), and 11 (C) hours. Surfzone FIB particles are black and offshore FIB particles are red. Particle locations reflect cross-shore shear in the alongshore current, with surfzone FIB originating to the north and offshore FIB originating to the south. The origins of surfzone FIB appear stable around 600 – 1500 m N, while the origins of offshore FIB are time dependent (B &amp; C).....</p>	51
<p><b>Figure 2.4:</b> Contour plots of (A) <i>E. coli</i> (ln MPN 100 ml<sup>-1</sup>) &amp; (B) <i>Enterococcus</i> (ln CFU 100 ml<sup>-1</sup>) concentrations at HB06 as a function of cross-shore distance (m), alongshore distance (m), and time (hours). Plots are oriented as though the viewer is standing on the beach, looking offshore. On the alongshore axis, the northernmost station is located at 0 m, with negative values indicating stations to the south. The location of each sampling station is shown by a dashed white line..</p>	52
<p><b>Figure 2.5:</b> Bar graph of measured exponential decay rates for <i>Enterococcus</i> (black bars) and <i>E. coli</i> (gray bars), and FIB modeled using the AD model (red bars). (A) Alongshore sampling stations and (B) cross-shore sampling stations. FIB decay rates from the AD model are averages of 10 model runs, shown with standard error. Boxes link stations for <i>Enterococcus</i> (black), <i>E. coli</i> (blue) and the AD model (red) with decay rates that are not significantly different from one another (<math>p &lt; 0.05</math>). See SI Fig 1 for exponential fits to FIB data.....</p>	53
<p><b>Figure 2.6:</b> A) Contour plot of best-fit AD model particle concentrations as a function of cross-shore distance (m), alongshore distance (m), and time (hours). Axes are same as figure 3. B) Bar graph of station-specific skill for AD model - FIB data comparisons; <i>Enterococcus</i> (blue) and <i>E. coli</i> (red).....</p>	54

<b>Figure 3.1:</b> Species composition of onshore (SAR, TM, FHM, and F1) vs. offshore (F5 and F7) HB06 <i>Enterococcus</i> isolates. Note that the percentage of <i>E. faecium</i> exceeds that of <i>E. mundtii</i> at onshore, but not offshore, stations.....	85
<b>Figure 3.2:</b> <i>E. coli</i> and <i>Enterococcus</i> decay rate vs. solar insolation dose averaged over shoreline (black) and offshore (red) locations. The lines are best-fit slopes. The regression skill ( $R^2 = 0.22$ ) is significant ( $p < 0.05$ ) for offshore <i>Enterococcus</i> , but not for <i>E. coli</i> or shoreline <i>Enterococcus</i> .....	86
<b>Figure 3.3:</b> Contour plots of <i>E. coli</i> data, and best-fit model outputs as a function of cross-shore distance (m), alongshore distance (m), and time (hours). On the alongshore axis, the northernmost station (F1) is located at 0 m, with negative values indicating stations to the south. Color bar units are in natural log Most Probable Number (MPN) for <i>E. coli</i> data, and natural log of particle concentration for the mortality models. Note the over retention of <i>E. coli</i> particles at offshore stations with the AD, ADC, and ADI models.....	88
<b>Figure 3.4:</b> Contour plots of <i>Enterococcus</i> data. Axes are the same as figure 3. Color bar units are in natural log Colony Forming Units (CFU) for <i>Enterococcus</i> data, and natural log of particle concentration for the mortality models. Note the over retention of <i>Enterococcus</i> particles at offshore stations with the AD, ADC, and ADI models.....	90
<b>Figure 3.5:</b> Station-specific and total skill for best-fit <i>E.coli</i> (A) and <i>Enterococcus</i> (B) models, where total skill refers to a bulk estimate calculated across all sampling stations. All mortality models improve model skill relative to the AD model at each sampling station, for both FIB groups. Model skill is highest for the models allowing for cross-shore variable FIB mortality (ADS, ADG, ADSI, and ADGI).....	91
<b>Figure 3.6:</b> Decay rate differences (model – data) at each sampling station, for each best-fit model: (A) <i>E. coli</i> and (B) <i>Enterococcus</i> . An asterisk indicates decay rate differences that are not significantly different from zero ( $p < 0.05$ ).....	92
<b>Figure 4.1:</b> A) Observed water depth (m) and B) chlorophyll a (Chl a) concentration ( $\mu\text{g L}^{-1}$ ) at Huntington Beach, California, in fall 2006. Time (days) is on the $x$ -axis for both plots. A yellow (day) and black (night) dashed colored line is used to depict day-night cycles. In A) red dots mark high tide, which was used to force FIB release events in our NP, LP, NP + L and LP + L models. In B) a green dashed line indicates the bloom threshold used to force a binary response to phytoplankton concentration in our LP and LP + L models. The bloom threshold was exceeded 3 times, although one was minor. The two larger events (bloom 1 and 2) are marked with black boxes. All models were run for 5 days to allow them to stabilize. The end of this spin-up phase is marked by a black dashed line.....	132

**Figure 4.2:** Biphasic mortality of *Enterococcus faecium* in seawater microcosm treatments with (red) or without (black) the phytoplankter *Lingulodinium polyedrum*. Curve fits and mortality rates were estimated using the equation in the box to the right. 95% confidence intervals for fits are shown using dashed lines..... 133

**Figure 4.3:** Along and cross-shore transport of FIB particles at Huntington Beach, under three model scenarios: **A)** shows the AD (advection + diffusion) model, **B)** shows the AD\_NP (advection + diffusion + no phytoplankton) model, and **C)** shows the AD\_LP (advection + diffusion + *L. poyedrum*) model. All plots are oriented with alongshore distance (m) on the long axis. Distance is relative to the alongshore location of the cross-shore transect at 0 m (F1, F3, F5, F7, OM). Negative alongshore values are to the south of the transect (FHM, TM, and SAR), and positive alongshore values are to the north of the transect. Cross-shore distance (m) is on the short axis, with F1 at the shoreline and OM ~ 300 m offshore. Time (h) is on the vertical axis, increasing upwards. The colorbar is natural log of FIB particle concentration (ln MPN 100 ml<sup>-1</sup>). In all models FIB particles were released at 1850 (high tide), between 500 and 1000 m in the alongshore. Black dots mark the along and cross-shore progression of the 35 MPN 100 ml<sup>-1</sup> EPA geometric mean standard for *Enterococcus*..... 134

**Figure 4.4:** Plot of percent difference in particle retention between the AD\_LP model (with phytoplankton) and the AD\_NP model (without phytoplankton). Plot orientation is the same as in Fig. 4.3. The colorbar is percent model difference. This statistic is calculated by taking the difference between particle concentration in the AD\_LP and AD\_NP models, and normalizing by the AD\_LP model. At 0650, the average percent increase in FIB particle retention for the AD\_LP model was 21% (black line on colorbar)..... 135

**Figure 4.5:** Timeseries of modeled *Enterococcus* and Huntington Beach chlorophyll a concentrations. For both plots time (days) is on the x-axis, chlorophyll a concentration (µg L<sup>-1</sup>) is on the right y-axis, and *Enterococcus* concentration (MPN 100 ml<sup>-1</sup>) is on the left y-axis. A yellow (day) and black (night) dashed colored line depicts day-night cycles. The dashed green line is the phytoplankton bloom threshold, and the dashed black line marks the end our our model spin-up phase. *Enterococcus* data generated from models where mortality was (LP and LP + L) or was not (NP and NP + L) a function of phytoplankton concentration are shown with black and blue dots, respectfully. Daily average *Enterococcus* concentrations are shown using solid lines of the corresponding color. Results from dark models (NP and LP), with no solar FIB mortality, are shown in **A)**. Results from light models (NP + L and LP + L), where mortality was a function of solar radiation, are shown in **B)**..... 136

**Figure 4.6:** **A & B)** *Enterococcus* – chlorophyll a correlation coefficients

(Spearman's Rho) evaluated at all possible sampling hours. Sampling hour is on the  $x$ -axis, with 0100 (the first timepoint) corresponding to samples at 1 am, and 2400 (the last timepoint) to midnight samples. All estimates of Spearman's Rho are shown with 95% confidence intervals. Correlation coefficients for models where FIB mortality was a function of phytoplankton concentration (LP and LP + L) are shown in black. Models where FIB and phytoplankton concentrations are independent (NP and NP + L) are shown in blue. **C & D**) Bar graphs showing the percent of sampling hours with positive, negative or non-significant correlations between *Enterococcus* and chlorophyll a. Significance category (positive, negative, or non-significant) is on the  $x$ -axis, and the percent of sampling hours that fall within each category is on the  $y$ -axis. The color scheme is identical to **A** and **B**. Models where FIB were solar sensitive are on the bottom (**B & D**). Dark models are on the top (**A & C**)..... 138

**Figure 4.7: A & B**) *Enterococcus* – chlorophyll a correlation coefficients (Spearman's Rho) evaluated at high tide, and every hour following high tide, for a total of 11 hours. The  $x$ -axis is sampling hour relative to high tide which occurs at  $t = 0$  h). Otherwise, plot orientation and color is identical to Fig. 4.6. **C & D**) Bar graphs showing the percent of (tidal) sampling hours with positive, negative, or non-significant correlations between *Enterococcus* and chlorophyll a. Plot orientation and color is also identical to Fig. 4.6..... 140

**Figure 5.1:** Schematic of field sampling at Boarder Fields State Beach. Samples were taken along a 3.3 km alongshore transect (dashed red line). Sample locations are labeled with white boxes. *Enterococcus*, nitrate, nitrite, ammonium, phosphate, silicate, sands, and fines were monitored at all stations. Chlorophyll concentrations were monitored at TJR, HT, and BF. Tide height, alongshore current direction and temperature were measured at F1 and at five additional locations spanning 130 m in the cross-shore (solid red line). Sediments for the beach nourishment came from the Goat Canyon Retention Basin (white dashed box)..... 173

**Figure 5.2:** 130 m cross-shore averaged **(A)** alongshore currents and **(B)** temperature. **(C)** Mean water depth (a proxy for tide height) measured ~130 m offshore (at F6) versus time (days) from 9/21/09 – 10/13/09. Red circles mark when water samples were collected, and yellow boxes mark nourishment events.. 174

**Figure 5.3:** Concentrations of **(A)** chlorophyll ( $\mu\text{M}$ ) and all parameters significantly correlated with chlorophyll at the  $p < 0.05$  (\*) or  $p < 0.01$  (\*\*) level; **(B)** nitrate ( $\mu\text{M}$ ), **(C)** water depth (m), and **(D)** cross-shore averaged alongshore current velocity ( $\text{ms}^{-1}$ ). The  $x$ -axis for **A-D** is time (days). The  $y$ -axis is alongshore distance (m) **(A-B)** or parameter magnitude **(C-D)**. A red dashed line marks the beach nourishment location (HT) **(A-B)**, and yellow boxes indicate individual nourishment events. Subplots **(E-G)** show direct correlations between chlorophyll ( $x$ -axis) and **(E)** nitrate, **(F)** water depth, or **(G)** alongshore velocity ( $y$ -axis). Spearman's correlation coefficients ( $\rho$ ) are shown in the upper right hand corner

of each correlation plot..... 176

**Figure 5.4:** (A-H) Best-fit GLM output for *Enterococcus* (fines only) compared with presence/absence data. The *x*-axis is time (days) and the *y*-axis is the probability of bacterial detection using the fine sediment GLM. Model predictions are shown as white circles, and *Enterococcus* data is shown as colored bars; presence (red bar) and absence (black bar). (I-K) Best-fit GLM outputs for chlorophyll (red or blue) compared with chlorophyll data (black). The *x*-axis is time (days) and the *y*-axis is the actual or predicted chlorophyll concentration (uM). The nitrate + tides model is shown in red, and the nitrate + tides + interaction term model is shown in blue. All plots (A-K) are organized by sampling station, with the northernmost station at the top (F1) and the southernmost station at bottom (BF for enterococci and HT for chlorophyll) (see Fig. 1). For both enterococci and chlorophyll, best-fit GLM's were spatially variable. The percent deviance explained (see upper right hand corner of A, B, F, I, J, and K) was highest at HT station. This pattern was most pronounced for enterococci..... 177

**Figure 5.5:** Concentrations of (A) *Enterococcus* (MPN 100 ml<sup>-1</sup>) and all parameters significantly correlated with *Enterococcus* at the  $p < 0.05$  (\*) or  $p < 0.01$  (\*\*) level; (B) fine sediment (gL<sup>-1</sup>), (C) silicate (uM), and (D) phosphate (uM). The *x*-axis for A-D is time (days). The *y*-axis is alongshore distance (m). All color bars are log concentration. A red dashed line marks the beach nourishment location (HT) and yellow boxes indicate individual nourishment events. Subplots (E-G) show direct correlations between *Enterococcus* (*x*-axis) and (E) fine sediment, (F) silicate or (G) phosphate (*y*-axis). Spearman's correlation coefficients (Rho) are shown in the lower right hand corner of each correlation plot..... 179

**Figure 5.6:** *Enterococcus* concentrations in beach nourishment sediments from six different placements spanning two nourishment dates; 9/25/09 and 10/1/09. The *x*-axis is the placement number (1:3) on each day, and the *y*-axis is *Enterococcus* concentration (MPN 100 g<sup>-1</sup>)..... 180

**Figure 5.7:** Surfzone residence time of enterococci at HT sampling station (black line). Four -hour-averaged *Enterococcus* concentrations (MPN 100 ml<sup>-1</sup>) are on the *y*-axis. Temporal averages are shown to avoid over or underestimating bacterial retention due to patchy *Enterococcus* concentrations. Time since the last nourishment event (h) is on the *x*-axis. All time-since-placement values are calculated as hours post placement + 2, to reflect the 4-hour averaging of enterococci. Decay of enterococci was exponential and occurred at a rate of 0.24 h<sup>-1</sup> (boxed equation). *Enterococcus* concentrations decayed below EPA single (blue) and geometric sample standards (red) by 1.3 and 5.8 hours, respectively. 23 hours post-placement, enterococci were almost undetectable in the surfzone.... 181

**Figure 5.8:** (A) Inactivation of enterococci in dark (black) and light (blue) microcosm treatments on 10/1/09. Inactivation was well modeled by an asymptotic exponential (see equation to the right). Fitted curves were not significantly different between light and dark treatments (see overlapping CI's). For both treatments ~ 61% of nourishment associated enterococci were sensitive to inactivation, and decayed rapidly (avg  $0.055 \text{ s}^{-1}$ ). The remaining fraction was resistant and stable. (B) Solar insolation levels ( $\mu\text{Ein m}^{-2}\text{s}^{-1}$ ) versus time (h) from 0800 to 1300. Insolation on 10/1/09 within the sediment plume (black dashed line) is compared to average surfzone insolation levels when the plume is absent (red dashed line) for days with similar light intensities (black: light intensity 10/1/09, red: average intensity on alternate days). Note the extremely reduced insolation levels on 10/1/09 within the plume..... 182

## LIST OF TABLES

<b>Table 2.1:</b> Rates of FIB decay during HB06.....	48
<b>Table 3.1:</b> Best-fit mortality parameters for FIB models.....	84
<b>Table 4.1:</b> A comparison of first-order exponential and biphasic decay models for enterococci (w & w/o phytoplankton).....	131



## ACKNOWLEDGEMENTS

This dissertation would not have been possible without the willingness of my advisor and mentor Peter Franks to accept a student with the desire to combine mathematical models (unfamiliar to her) with laboratory techniques (unfamiliar to him) and fieldwork, in order to address interdisciplinary questions in a field only distantly related to his own. This took a major leap of faith, for which I am eternally grateful. Peter taught me an entirely new skill set, and how to effectively use those skills to formulate non-verbal hypothesis tests for addressing oceanographic questions. Before coming to Scripps, I had not written a single line of computer code. Now I debug my own. Thank you Peter for taking the time to teach me this invaluable skill.

To my committee members Bob Guza, Falk Feddersen, Stan Grant, Farooq Azam, Doug Bartlett, and Josh Graff Zivin, I also express my thanks. You were always available to answer my many questions, and your comments on my analyses and manuscripts always improved my science. Special thanks to Bob and Falk who allowed me to participate in two of their interdisciplinary field programs; HB06 and IB09. These programs formed the backbone of this dissertation and data from them are featured in every chapter. Bob, you took it upon yourself to be my mentor in the field and to ensure that I had enough assistance to collect the water samples that I required. That you were willing to be there for 5am bacterial sampling at Imperial Beach, and brought your entire family to assist, will never cease to amaze me. I am eternally grateful to you for caring that much about me and my work.

I am also grateful for the cheerful and talented assistance of the many people

who assisted me in collecting water samples and/or physical measurements in the field. Thanks go out to the Integrative Oceanography Division staff (B. Woodward, B. Boyd, K. Smith, D. Darnell, I. Nagy, R. Grenzeback, and A. Gale). No one makes measurements of surfzone dynamics better (or with more humor) than you. You made it fun. I also want to thank the graduate students (D. Clark, M. Omand, A. Doria, M. Cape, and B. Carter) and Michelle Okihiro for their amazing sampling efforts. Special thanks to Brendan Carter for running well over 40 miles by my side to ensure that I was not collecting water samples by the San Diego – Mexico border all by myself at 4:30 am each morning.

For every graduate student there is at least one class that completely changes the way they do science. For me, this was Jay Barlow's Computer Intensive Statistics course, which introduced me to statistical methods like generalized linear modeling, bootstrapping, and cross-validation. In the past, I have taken many statistics courses in an increasingly desperate attempt to understand how to apply statistical analyses to biological questions. Jay, your class finally did the trick. Thanks so much for making it both computational and ecologically relevant.

Even with all of the above mentioned assistance, this dissertation would not have been possible without my cohort; Alison Cawood, Darcy Taniguchi, Jessee Powell, and Miriam Goldstein. You not only took me in when I was a floundering former Marine Biology student, but became my closest friends at SIO, commiserating and celebrating (as warranted), the many ups and downs of life as a graduate student. Even though we work on a wide range of different topics, you always provided good council, and more importantly, good fun, without which I would never have kept my

perspective. Thank you all! I also wish to thank the entire Franks lab for their support, lab-lunch fun, and incredibly useful critiques of scientific talks. You greatly improved my public speaking skills.

Outside of SIO, I would like to thank my climbing buddies (Katherine Webster, Natalie Ruben, Mike Kishi, James Sturtevant, and Allyn Hill), gaming group (Jen Harmston, Eric Wolff, and Ryan Marsh), and fiancé, Tom Hall, for the amazing places, good times, and support provided these past seven years. The mountains, deserts, and “dungeons”, of the greater San Diego area have brought me joy, and provided me with fond memories that I will carry with me wherever my future travels lead. My mother and sister were also a consistent source of support. Mom, you never doubted I'd succeed, even when I was not nearly so certain. Thank you. I also wish to thank all of my furry four legged children for bringing necessary snuggles, laughter, and mayhem into my life. Marmot and Socrates, although you are no longer with me, I know you would have approved of this manuscript, and slept/drooled on it accordingly. I miss you both. I also wish to thank my father who, although no longer here, remains a driving force in my life. Dad, I know you would find it hilarious that your computer illiterate daughter produced a dissertation with a modeling component. I'll say it once, you were right!

Chapter 2, in full, has been submitted for publication in *Marine Pollution Bulletin*, 2012, Rippey, M. A.; Franks, P. J. S.; Feddersen, F.; Guza, R. T.; Moore, D. F, Elsevier Press, 2012. The dissertation author was the primary investigator and author of this paper.

Chapter 3, in full, has been submitted to Marine Pollution Bulletin, 2012, Rippey, M. A.; Franks, P. J. S.; Feddersen, F.; Guza, R. T.; Moore, D. F, Elsevier Press, 2012. The dissertation author was the primary investigator and author of this paper.

Chapter 4, in part, is being prepared for submission to Environmental Science & Technology, 2012, Rippey, M. A.; Franks, P. J. S., ACS Publications, 2012. The dissertation author was the primary investigator and author of this paper.

Chapter 5, in part, is being prepared for submission to Environmental Science & Technology, 2012, Rippey, M. A.; Warrick., J. A.; Franks, P. J. S.; Feddersen, F.; Guza, R. T., ACS Publications, 2012. The dissertation author was the primary investigator and author of this paper.

## VITA

- 2005 Bachelor of Science, University of California, Santa Cruz
- 2011 Master of Science, University of California, San Diego
- 2011 Teaching Assistant, University of California, San Diego
- 2012 Doctor of Philosophy, University of California, San Diego

## PUBLICATIONS

- Warrick, J.A.; Rosenberger, K.; Lam, A.; Ferreira, J.; Miller, I. M.; **Rippy, M.**; Svejksky, J.; Mustain, N. 2012. Observations of coastal sediment dynamics of the Tijuana Estuary Fine Sediment Fate and Transport Demonstration Project, Imperial Beach, California, U.S. Geological Survey Open-File Report 2012-1083, 29 p and data files. (Available at <http://pubs.usgs.gov/of/2012/1083/>.)
- Rippy, M. A.**; Franks, P. J. S.; Feddersen, F.; Guza, R. T.; Moore, D. F. *in review*. Physical factors controlling variability in nearshore fecal pollution: fecal indicator bacteria as passive particles. *Marine Pollution Bulletin*.
- Rippy, M. A.**; Franks, P. J. S.; Feddersen, F.; Guza, R. T.; Moore, D. F. *in review*. Factors controlling variability in nearshore fecal pollution: the effects of mortality. *Marine Pollution Bulletin*.
- Rippy, M. A.**; Warrick, J. A.; Franks, P. J. S.; Feddersen, F.; Guza, R. T. F. *in prep*. Beach nourishment impacts on bacteriological water quality and phytoplankton bloom dynamics. *Environmental Science & Technology*.
- Rippy, M. A.**; Franks, P. J. S. *in prep*. The effects of the bloom forming dinoflagellate *Lingulodinium polyedrum* on the mortality of *Enterococcus faecium* in seawater: mortality rates, water quality impacts, and monitoring implications. *Environmental Science & Technology*.

## ABSTRACT OF THE DISSERTATION

Physical and Biological Dynamics of Surfzone Bacterial Pollution: Sources,  
Transports, and Removal Mechanisms

by

Megan Anjuli Rippy

Doctor of Philosophy in Oceanography

University of California, San Diego, 2012

Professor Peter J. S. Franks, Chair

Nearshore concentrations of fecal indicator bacteria (FIB) are controlled by a complex array of physical and biological processes. The studies herein evaluate the contribution of several such process to coastal FIB dynamics using laboratory studies, mathematical modeling, and fieldwork. Two field sites are discussed; Border Fields State Beach (BFSB) and Huntington Beach, both sites of chronic FIB contamination in Southern California. At Huntington Beach field measurements of alongshore currents and horizontal diffusion were used to parameterize a suite of individual based particle tracking models. These models were used diagnostically to evaluate the contribution of physics and mortality to FIB dynamics. Advection and diffusion were found to

explain a significant fraction of surfzone FIB decay, but played a lesser role offshore, suggesting that offshore FIB loss may be dominated by mortality rather than physics. No single mechanism was identified that best-explained FIB mortality at this beach, although cross-shore variable mortality mechanisms had higher skill than spatially constant ones. At BFSB the relative contribution of physics and mortality to nearshore FIB dynamics varied temporally rather than in the cross-shore. Generalized linear model analyses at this beach linked FIB contamination to an anthropogenic beach nourishment. Field-based microcosm experiments (using FIB from this source), in combination with surfzone bacterial monitoring, showed that FIB concentrations were controlled by rapid mortality of a “sensitive” FIB fraction and physical dilution-mixing, which became steadily more important as sensitive FIB died off, leaving behind a resistant community. Co-existing populations of sensitive and resistant FIB were also observed in laboratory experiments evaluating the effects of phytoplankton concentration on FIB mortality. Mortality in these experiments was biphasic, with loss of sensitive FIB occurring  $> 10x$  faster than resistant FIB. Notably, bloom concentrations of phytoplankton halved mortality rates of both FIB groups, enhancing survivorship. This signal was not obscured by physical transport/mixing (Huntington Beach particle tracking model), suggesting that phytoplankton have the potential to be an important factor controlling FIB concentrations. This dissertation highlights the importance of both physics and biology as factors controlling nearshore FIB and points to phytoplankton communities as an under-evaluated control on FIB growth/mortality in marine systems.

## CHAPTER 1.

### INTRODUCTION

Pathogenic bacteria are a persistent social, health, and economic problem along beachfront regions of the US, costing California ~\$1.9 billion yearly (Dufour and Wymer, 2006). The effects of bacterial pollution are concentrated in areas with moderate climate, like southern California, where recreational beach use is high year round (Ralston et al., 2011). At two Southern California beaches (Huntington Beach and Newport Beach), 36,778 cases of gastrointestinal illness per year were attributed to beach bacterial pollution, costing the state upwards of \$3.3 million (Turbow et al., 2003). Scaled up, this means that cases of gastrointestinal illness at 28 major Southern California beaches may exceed 627,800 – 1,479,200 yearly, costing California \$21 – \$51 million (Given et al., 2006).

Since the mid 1800s, pathogens and health risk in coastal waters have been monitored using fecal indicator bacteria (FIB) (Sinton et al., 1993a). FIB typically exhibit high concentrations in feces, and are easier to culture than pathogens, making them a useful proxy for tracking pathogens in coastal systems (Sinton et al., 1993a; Meays et al., 2004). The first widely used FIB group was total coliform bacteria, which are gram negative, and contain both fecal and environmental members. Today, *Escherichia coli* (a fecal coliform) is the most widely used indicator of fecal contamination in freshwater systems (Tallon et al., 2005). In marine waters, the monitoring of coliforms has largely been superseded by *Enterococcus* in the United



States, although co-monitoring with *E. coli* remains common (EPA, 2000; Kay et al., 2004).

*Enterococcus* is a genus of gram-positive bacteria that was first recognized as a fecal indicator by Lawes and Andrewes (1894). The use of *Enterococcus* as a monitoring tool, however, was not widespread until the 1940's, following biochemical and serological classification by Orla-Jensen (1919), Sherman (1937) and Lancefield (1933). Currently the genus *Enterococcus* is thought to contain ~30 species that fall into five main phylogenetic groups: the *E. faecalis* species group, the *E. faecium* species group, the *E. cecorum* species group, the *E. cassiflavus* species group, and the *E. avium* species group (Naser et al., 2005). These groups are delineated by genetic and biochemical differences, with the *E. avium* group separating out from the others based on the presence of group Q antigens, and the *E. faecium* group differentiated by the ability to ferment arabinose (Sinton et al., 1993a; Palmer et al., 2012). The two most common species isolated from human feces are *E. faecalis* and *E. faecium* (Sinton et al., 1993b). These species (in addition to their use as fecal indicators) are notable human pathogens causing urinary tract infections, nosocomial wound infections, and endocarditis (Hardie & Whiley, 1997; Morrison et al., 1997).

Current US Environmental Protection Agency (EPA) water quality standards arose from work in the late 1970's and early 1980's by Cabelli *et al.* (Cabelli et al., 1975; Cabelli et al., 1982; Cabelli et al., 1983; US EPA, 1986). This research identified clear dose-based relationships between highly credible gastrointestinal illness (HCGI; flu-like symptoms including fever, vomiting, and diarrhea) and the fecal indicators enterococci and *E. coli* (Cabelli et al., 1982; Cabelli et al., 1983).

Current marine standards, based on these relationships, identify a bacterial contamination level that, if exceeded, will result in >19 cases of HCGI per 1000 beach-goers (US EPA, 1986). These standards are 104 enterococci 100 ml<sup>-1</sup> seawater (single sample standard) or 35 enterococci 100 ml<sup>-1</sup> seawater (30 day geometric mean standard)) (US EPA, 1986).

Since their development, these water quality standards have been criticized for a variety of reasons. Reanalysis of the Cabelli data by Fleisher (1991 and 1992) revealed spatial variability in FIB dose/health risk relationships at different beaches, casting doubt on the utility of a single dose based standard for evaluating health risk. The observed variability was closely tied to environmental variables (like salinity), suggesting a link between local environmental conditions, FIB survivorship, and health risk (Fleisher et al., 1991). Subsequent studies have only highlighted the variable nature of the FIB/health risk relationship, with some supporting EPA standards (Wade et al., 2003; Haile et al., 1999), others suggesting that the criteria are too conservative (i.e., health risk is higher for a given FIB dose than we acknowledge) (Kay et al., 1994; Pruss et al., 1998), and a few showing no correlation at all between traditional indicators and health risk (Corbett et al., 1993; Colford et al., 2007).

These contrasting results have prompted evaluation of new indicator organisms, non-biological indicators (e.g. caffeine) , genetically-based techniques for monitoring pathogens themselves, and a whole field of research geared towards understanding the factors controlling FIB survivorship/transport in the environment, with the goal of better understanding where and why FIB and pathogen concentrations become uncoupled in coastal systems (Scott et al., 2002; Jiang and Chu, 2004;

Seurinck et al., 2005; Layton et al., 2006; Peeler et al., 2006). This field embraces a dynamics-based understanding of FIB that can help us assess the utility of these bacteria as indicators of health risk under differing environmental conditions.

Research effort has focused on identifying factors controlling FIB growth or mortality, the fluid mechanics of transport and dispersal, and the development of models (dynamic or statistical) that translate this information into bacterial contamination predictions that are useful from a beach management standpoint.

### **Mortality of Fecal Indicator Bacteria**

In seawater, FIB mortality typically exceeds growth, resulting in net bacterial loss from the system (Hartz et al., 2008). These losses are often diurnal, and have been ascribed to the damaging effects of solar radiation (Boehm et al., 2002a; Sinton et al., 2002; Ki et al., 2007; Boehm et al., 2009). Sunlight has been shown to damage FIB both directly via cellular damage (UV wavelengths) and indirectly through the exogenous or endogenous formation of reactive oxygen species (ROS) (visible wavelengths) (Curtis et al., 1992; Davies-Colley et al., 1999; Sinton et al., 1999; Muela et al., 2002). In the field, solar mortality has largely been attributed to UV, although surfzone ROS levels can be sufficient to result in oxidative stress or FIB lysis, suggesting that indirect photoinactivation may contribute to marine FIB mortality (Clark et al., 2008; Clark et al., 2010; Boehm et al., 2009).

In addition to solar radiation, FIB are sensitive to a suite of other abiotic stressors including pH, temperature and salinity (Solic and Krstulovic, 1992; Trousselier et al., 1998; Rozen and Belkin, 2001). Salinity and pH effects are most

notable for *E. coli*, as enterococci are halotolerant and can survive from pH 4 -10 (Rozen and Belkin, 2001; Fisher and Phillips, 2009). The halotolerance of enterococci, also observed for viral pathogens, is one reason that enterococci are preferred to *E. coli* as fecal indicators in marine systems (Gantzer et al., 1998; Kirschner et al., 2004). The relative survival of *E. coli* and enterococci in seawater, however, can be variable. This variability may be linked to FIB source, or, in the case of enterococci, species composition (Sinton et al., 2002; Anderson et al., 2005; Maraccini et al., 2012).

Although less studied than abiotic stressors, allochthonous marine and freshwater communities have been observed to affect FIB (Jenkins et al., 2011). In urban streams, enterococci and *E. coli* can undergo Lotka-Volterra like predator-prey cycling, with estimated clearance rates consistent with those of rotifers (Surbeck et al., 2010). In natural seawater, microcosm and dilution experiments suggest that grazing by heterotrophic nanoflagellates, ciliates, and even larger autotrophic flagellates, may significantly impact FIB abundances in the water column (Hartke et al., 2002; Gonzalez et al., 1992; Boehm et al., 2005). Notably, marine flagellates and ciliates appear to preferentially graze larger bacteria, with ciliates also exhibiting larger clearance rates when offered gram-positive strains (Anderson et al., 1986; Gonzalez et al., 1990a). As most marine bacterioplankton are smaller than indicator bacteria ( $0.02\text{-}0.12\ \mu\text{m}^3$  vs.  $> 0.66\ \mu\text{m}^3$ ) and gram negative, this selectivity may lead to high grazing pressure on FIB (especially gram positive enterococci) in marine systems (Lee and Fuhrman, 1987; Gonzalez et al., 1990a; Gontang et al., 2007). Some evidence suggests, however, that *E. coli* mortality due to protistan grazing may exceed mortality

of *Enterococcus* because *Enterococcus* has a thick gram positive cell wall that can reduce or inhibit its digestion by protists (Gonzalez et al., 1990b).

In addition to being grazed by protists, FIB in marine systems may also be affected by other biotic constituents. Indicator bacteria have been observed attached to copepods and associated with *Cladophora* mats, suggesting that zooplankton and algae may play a role in aggregation and/or survivorship of fecal indicators (Whitman et al., 2003; Byappanahalli et al., 2003; Signoretto et al., 2004). Research in this area, however, has been extremely limited, and evaluation of the effects of other marine constituents, like phytoplankton, is by and large absent.

### **Growth of Fecal Indicator Bacteria**

Although FIB mortality is often thought to dominate growth in marine and freshwater systems, this is not strictly true. Growth of *E. coli* and enterococci has been observed in waters with elevated concentrations of phosphorous and/or dissolved organic carbon (Surbeck et al., 2010). *E. coli* growth in freshwater has been measured coincident with enhanced turbulence, which is thought to increase nutrient encounter rates (Al-Homoud and Hondzo, 2008). FIB growth has also been observed in sterile beach sands transplanted onto contaminated beaches, and in natural beach sands subject to tidal rewetting (Whitman & Nevers, 2003; Yamahara et al., 2009). Notably, the growth of FIB in beach sands may be intermittent, as mortality has been observed to occur in dry beach sands and in some moist natural beach sands due to competition with native bacterial assemblages and/or protistan grazing (Hartz et al., 2008; Yamahara et al., 2009; Feng et al., 2010; Halliday et al., 2011).

Overall, the prevalence of environmental FIB growth has raised concern regarding the utility of FIB, as the pathogens they are intended to proxy (particularly viruses) may not replicate under similar environmental conditions (Griffin et al., 2003; Arnone and Walling, 2007). To date, however, our understanding of FIB survivorship greatly exceeds our understanding of pathogen survivorship in coastal systems (Yamahara et al., 2009). Recent work by Yamahara *et al.* (2012) showed that mortality of enterococci in dry sand microcosms was statistically identical to mortality of the pathogens *Salmonella* and *Campylobacter*. *Enterococcus* survival, however, was enhanced in wet sediments, which was not observed for either pathogen. Further work of this sort will help us understand when FIB are useful as proxies for pathogens in marine systems, and what pathogens they approximate best.

### **Fluid Dynamics and FIB Transport in Coastal Systems**

Although FIB survivorship is an important component contributing to our understanding of bacterial pollution and health risk in coastal systems, source dynamics and transport mechanisms are equally important. Physical transport and dilution may be identical for pathogens and FIB, making systems where bacterial loss is physically driven ideal candidates for monitoring pathogens with FIB proxies (Grant and Sanders, 2010; Zhu et al., 2011).

To date, the work done exploring FIB transport and source dynamics in marine or freshwater systems has involved a mixture of field sampling (e.g. direct measurements of currents, salinity, temperature, pressure gradients, isotopes, nutrients, and FIB) (Grant et al., 2001; Boehm et al., 2002b; Boehm et al., 2004; Kim et al.,

2004; Phillips et al., 2011), manipulative field experiments using fluorescent dye and drifter releases (Grant et al., 2001; Grant et al., 2005), and mathematical modeling, with models ranging in complexity from simple mass balance models to complex 3D hydrodynamic simulations (Connolly et al., 1999; Boehm et al., 2003; Kim et al., 2004; Grant et al., 2005; Liu et al., 2006; Sanders et al., 2005; Thupaki et al., 2010; de Brauwere et al., 2011; Zhu et al., 2011). The information presented here regarding physical transports in the nearshore is not intended to be a complete review of nearshore processes, and focuses only on studies that directly evaluate the importance of physical transports or source dynamics for FIB.

Several studies have emphasized the importance of cross-shore flows in controlling nearshore concentrations of FIB. Cross-shore transport by tidal or lower frequency currents has been implicated in shoreline contamination from an outfall plume in Oahu, Hawaii (Connolly et al., 1999). Similarly, internal tides have been implicated in cross-shore transport of FIB in Southern California. It is, however, uncertain whether these plume waters are a true source of FIB or a source of cool, nutrient rich water that enhances the survivorship of terrestrial derived FIB in the surfzone (Boehm et al., 2002b; Wong et al., 2012).

Smaller scale cross-shore flows may also play a role in coastal FIB transport. In 2003, Boehm *et al.* evaluated the importance of FIB dilution by rip currents using a tanks-in-series box model with breaking wave-induced alongshore current flow. It was found that rip cell dilution was significant, and controlled by wave climate. Specifically, perpendicular wave attack was found to reduce surfzone alongshore transport, maximizing cross-shore flushing of rip cells and surfzone FIB dilution

(Boehm et al., 2003). Rip cell activity has also been directly observed during dye release experiments, and linked to FIB dilution in mass transport models assuming FIB release from an estuarine point source (Grant et al., 2001; 2005). In some locations, it has been estimated that total cross-shore FIB transport can equal total alongshore transport, resulting in appreciable cross-shore dilution of FIB (Thupaki et al., 2010). Other studies, however, have observed retentive surfzone conditions, with alongshore FIB transport exceeding cross-shore transport by 50-300 times, resulting in high-concentration plumes hugging the shoreline (Grant et al., 2001, 2005; Kim et al., 2004).

Alongshore currents (like cross-shore currents) can be important controls on shoreline FIB contamination. These currents influence both the maximum spatial extent of a contaminant plume along a beach and the direction it travels from any given source. In quiet embayments where alongshore transport is minimal, high concentrations of FIB can be retained at the shoreline where people swim (Zhu et al., 2011). This is particularly true when fecal contamination is from a terrestrial source, such as leaky sewage infrastructure or dog fecal matter (Boehm et al., 2009; Zhu et al., 2011). In systems with slightly more rapid flows, like the Laurentian Great Lakes, alongshore currents can be important for transporting fecal contaminants from point sources to nearby beaches (Liu et al., 2006; Thupaki et al., 2010). Rapid alongshore current reversals are typical of these lakes and make it possible for FIB to impact beaches both left and right of a point source on any given day (Liu et al., 2006; Thupaki et al., 2010). These current reversals may also enhance coastal FIB dilution (Thupaki et al., 2010).



Although not all alongshore current reversals are tidal, tidal variability has been observed in alongshore currents seaward of the surfzone, and may be important for nearshore FIB transport (Kim et al., 2004; Grant et al., 2005). In 2004, Kim *et al.* found that > 2/3 of alongshore current reversals just outside of the surfzone at Huntington Beach, California, were tidally correlated. During flood tide, enhanced total coliform levels were measured coincident with upcoast flow of tidal currents. These currents augmented alongshore surfzone flows, increasing the transport of pollutants from the Santa Ana River to Huntington Beach proper (Kim et al., 2004). A tidal influence on alongshore current direction at Huntington Beach was also observed by Grant *et al.* (2005) using nearshore dye releases.

In addition to being an important control on FIB alongshore transport, tides are also central to FIB source dynamics. In low-flow rivers and estuaries, flood tides can result in seawater intrusion into river/estuary systems, forming a prism that blocks freshwater outflow (Grant et al., 2001, Jeong et al., 2005; Pednekar et al., 2005). Flow resumes on the ebb tide, resulting in cyclical discharge events to the surfzone. The effects of tidal flushing on pollutant transport within a river/estuary system or its receiving waters can be complex, with seawater inflow having the potential to transport pollutants into the estuary or dilute them depending on the location of point or non-point sources within the estuary itself (Sanders et al., 2005; de Brauwere et al., 2011). The effects of tidal flushing can be particularly dramatic for highly contaminated low-flow rivers, where FIB inputs to the surfzone can vary from 0 MPN 100 ml<sup>-1</sup> (flood tide) to > 240,000 MPN 100 ml<sup>-1</sup> (ebb tide) over a single tidal cycle (personal observation).

Tidal scouring and tidal pumping are two additional mechanisms by which tides can regulate nearshore FIB concentrations. In tidal pumping, changes in tide height generate pressure gradients in the beach water table that drive fluctuating pore-water flow fields (Billerbeck, 2005). The extent to which FIB are mobilized and released into the surfzone by tidal pumping is uncertain. De Sieyes *et al.* (2008) showed that groundwater discharge at Stinson Beach, California, was enhanced during neap tide. Although FIB were observed in groundwater samples, discharge itself was not associated with elevated surfzone FIB levels, suggesting that FIB may have been strained/adsorbed onto beach sands. This result is consistent with observations at other beaches (Boehm *et al.*, 2004; Phillips *et al.*, 2011).

In contrast to tidal pumping, which describes through-beach transport, tidal scouring is a process by which FIB are washed off a beach at high tide (a kind of over-beach transport). Zhu *et al.* (2011) found that tidal scouring of dog feces at a Florida beach contributed extensively to fecal contamination. At Huntington Beach, however, hydrodynamic modeling of fecal inputs from marsh birds showed that tidal scouring of fecal matter was insufficient to explain contamination in nearby Talbert Marsh (Sanders *et al.*, 2005). This same model pointed to tidally forced sediment resuspension as the primary source of FIB in marsh waters (Sanders *et al.*, 2005). This connection between sediment resuspension and FIB contamination has also been observed in other studies. Because the processes governing FIB attachment to particles are complex and not well understood, quantifying the importance of sediment resuspension and/or settling as FIB sources/sinks has been difficult (Sanders *et al.*, 2005; Thupaki *et al.*, 2010; Cho *et al.*, 2010; Suter *et al.*, 2011).

**Tying it all together: Physical – Biological assessment**

Although research regarding pertinent physical transports and source dynamics of surfzone FIB has been extensive, comparatively little work has been done evaluating the role of these processes in light of the complex FIB survivorship dynamics discussed earlier. These sorts of analyses are vital for identifying beaches where FIB dynamics are likely to be an accurate proxy for pathogen dynamics, and are necessary to help us develop useful predictive models. These models can provide a cost-effective supplement to bolster our underfunded water quality monitoring programs (Thupaki et al., 2010; Boehm et al., 2007).

To date, the most closely examined FIB mortality mechanism, in light of pertinent fluid flows and source dynamics, is solar-induced mortality (Boehm, 2003; Boehm et al., 2005; Grant et al., 2005; Boehm et al., 2009; Ziu et al., 2011). Boehm (2003) evaluated the relative contribution of dilution (via rip cell mixing) and mortality (attributed to solar insolation) to total coliform decay at Huntington Beach. Her findings suggest that dilution may dominate FIB loss at dynamic beaches. This finding was further explored in a subsequent study that expanded mortality to include grazing and solar insolation (Boehm et al., 2005). This work showed that dilution was the dominant source of loss, followed by solar insolation and grazing. The absolute contribution of these processes at any given time, however, was variable. Specifically, the importance of dilution was minimized by oblique wave angles, which increased surfzone retention, making the contribution of solar inactivation and grazing to total FIB loss more important (Boehm et al. 2005). Both of these studies used simple mass-

balance models, with alongshore currents forced by wave direction, to approximate alongshore current flow. As complex hydrodynamic simulations have become less computationally restricted, they have been used more frequently for these sorts of assessments, increasing the realism of our nearshore physical transports (Connolly et al., 1999; Sanders et al., 2005; Liu et al., 2006; Thupaki et al., 2010; Zhu et al., 2011; de Brauwere et al., 2011).

While we have been able to use hydrodynamic simulations to model FIB in fresh and marine waters, these models have been less effective than one might hope for evaluating the relative roles of physics and biology as factors controlling FIB. Many models contain parameterizations for FIB survivorship, but fail to evaluate them, making it difficult to assess the importance of mortality for model results (Connolly et al., 1999; Sanders et al., 2005). Other models are used effectively to compare physical transports and bulk ecological processes, but do not assess, or incompletely assess, the importance of individual ecological terms (Liu et al., 2006; Thupaki et al., 2010; de Brauwere et al., 2011).

For example, Liu *et al.* (2006) used a 2D (vertically integrated) hydrodynamics model of the Great Lakes that identified source loading from creeks and solar mortality as dominant processes controlling FIB dynamics. Solar mortality, however, was never evaluated on its own. Rather, a bulk mortality term (containing solar, temperature, and settlement based loss) was compared to a first-order exponential mortality term, and found to improve model-data fits. Because parameterization of the bulk mortality formulation attributed a larger fraction of loss to the solar term, solar mortality was determined to be the most important for loss. Loss terms, however, can

compensate for one another, making separate evaluation of individual components important to avoid the inclusion of redundant processes (Thupaki et al., 2010). Although time consuming, thorough analysis of individual model terms (even ones that seem unimportant for a given systems) is a requisite for understanding the roles of specific survivorship mechanisms in different physical contexts. Currently, there is the tendency to pick and choose survivorship mechanisms to include in models based on what is deemed likely to be important, without evaluating alternatives (de Brauwere et al., 2011). This has the potential to lead to models that are accurate, but imprecise, making them difficult to translate into useful predictive tools.

It is also notable that to date, even in locations where the balance between physical transports and FIB survivorship has been explored, we still only understand this balance for the most nearshore of waters. The majority of FIB data collected, and used to calibrate /test models, comes from shoreline samples in knee-deep water (Grant et al., 2001; Boehm et al., 2003; Liu et al., 2006; Thupaki et al., 2010). Recreational beach use, especially in California where surfing is a common activity, is not limited to the shoreline. This makes it important to evaluate FIB contamination and the processes controlling it over wider recreational domains. Many hydrodynamic models already have the ability to predict FIB concentrations in highly resolved along and cross-shore grids. What we lack is an understanding of how the balances between physical transports and FIB survivorship in the surfzone translate to waters beyond the surfzone, where physical processes are different, and survivorship may also change (Davies-Colley et al., 1994; Kim et al., 2004).

**But what about Management?**

Although hydrodynamic models and other dynamics-based tools for FIB prediction may eventually be useful for beach management decisions, these tools are currently computationally intensive and complex, making them difficult for management use. Consequently, a substantial amount of effort has been directed towards the development and assessment of statistical models for FIB prediction (Nevers and Whitman, 2005; Boehm et al., 2007). These models draw upon the greater pool of processes identified as important for FIB using dynamics-based models, laboratory experiments, or field work, identify easily measured environmental parameters associated with these processes, and attempt to use these parameters to predict FIB concentrations (Boehm et al., 2007; He and He, 2008; Zhang et al., 2012). Predictive statistical models have proven extremely useful in freshwater systems, and have been implemented by management in several states in the Great Lakes area (Nevers and Whitman, 2005; Francy et al., 2006; Francy, 2009). Their utility for marine beaches is only beginning to be explored (Hou et al., 2006; Boehm et al., 2007; He and He, 2008; Zhang et al., 2012).

To date, the most commonly used form of predictive statistical models are based on multiple linear regressions (MLR) with log transformed FIB data (Nevers and Whitman, 2005, 2011; Nevers et al., 2007; Frick et al., 2008). These models are often more successful at FIB prediction than traditional persistence methods, which apply FIB concentrations (cultured from water samples 18-24 hours prior) to the coming day's water quality assessment. Persistence methods have been shown to result in incorrect management decisions up to 41% of the time (Kim and Grant,

2004). At some beaches, MLR based statistical models have been shown to more than halve both Type II prediction error (beaches left open when water quality is poor) and Type I error (beaches closed when water quality is good), with respect to persistence-based methods (Nevers and Whitman., 2005). These successes prompted the development and testing of the EPA backed software Virtual Beach (VB), which provides a statistical package for beach managers that facilitates the development and use of MLR based FIB models at local beaches (Ge and Frick, 2007; Frick et al., 2008; Ge and Frick, 2009; Zhang et al., 2012).

VB software has been explored for use in marine waters by Zhang *et al.*, (2012) at Holly Beach, on the Gulf Coast. At this beach, linear VB model predictions were correlated with observed FIB data (correlation coefficient  $\sim 0.354$ ). FIB variability was underestimated, however, resulting in high root mean squared error. FIB contamination magnitude was typically over or underestimated by 10 fold, making it difficult to see how this model could be reliably used for management decisions. The performance of the VB model was similar when modified to allow for non-linear relationships between environmental variables, and, overall, VB models were found to have higher prediction error than other predictive statistical methods like Artificial Neural Network (ANN) models. (Zhang et al., 2012). ANN models have also been found to predict FIB concentrations well at other marine beaches including Torrey Pines State Beach and San Elijo State Beach in Southern California (He and He, 2008).

In addition to MLR and ANN models, partial least squares regression and regression trees have been explored as statistical methods for predicting indicator

bacteria at marine beaches (Hou et al., 2006; Boehm et al., 2007). The performance of these models has been observed to be variable, particularly in the validation phase, where model performance is evaluated using a novel data set not included in model development (Boehm et al., 2007). These difficulties with model validation, which are particularly evident for dynamic marine beaches, have led to a call for interdisciplinary studies that characterize both the extra-enteric ecology of FIB and nearshore physical transports (Boehm et al., 2007). In their 2007 publication, Boehm *et al.* state that:

“To improve models, we need to learn more about FIB sources, natural variation, and the processes that govern FIB fate and transport in the very nearshore environment”.

This call emphasizes our current need for interdisciplinary syntheses of water quality research in order to better understand and evaluate fecal pollution in coastal waters.

### **Dissertation Goals:**

It is the primary goal of this dissertation to address the above-mentioned call for interdisciplinary syntheses of extra-enteric FIB ecology, physical transports, and source dynamics. To this effect, Chapter 2 of my dissertation focuses on the development and evaluation of a physical transport model for Huntington Beach, California. The performance of this model is assessed using along and across-shore resolved FIB data, addressing the above-mentioned need to expand our evaluation of FIB dynamics into the outer surfzone and beyond. Chapter 3 of this dissertation explores the performance of six different mortality formulations in the Huntington



Beach physical transport model, allowing me to evaluate the role of different ecological processes in light of pertinent physical transports, at this beach. This evaluation centers on the importance of solar radiation, but also examines other, less frequently explored contributors to FIB mortality.

Chapter 4 of my dissertation addresses FIB extra-enteric ecology itself in more depth. Due to the paucity of studies that explore biotic (as opposed to abiotic) stressors, this chapter focuses on the importance of planktonic marine communities – specifically bloom forming dinoflagellates – for FIB survivorship. Preliminary results of FIB-phytoplankton survivorship experiments will be discussed, and the importance of the resultant mortality terms evaluated, using the physical transport model developed in Chapter 2.

Chapter 5 of my dissertation represents a transition from the dynamics-based work in my previous chapters to more deterministic, management-centered research. This chapter focuses on the water quality implications of sediment resuspension from a beach nourishment at Boarder Fields State Beach, near the San Diego-Mexico boarder. Predictive statistical approaches are used to diagnose important parameters affecting water quality during the nourishment event. The implications of this work for the use of statistical approaches to predict water quality at marine beaches will be addressed.

Chapter 6 will conclude my dissertation, providing a synthesis of the physical, ecological, and management implications of the previous chapters. It is my hope that this dissertation will become one of many that evaluate bacteriological water quality in an increasingly interdisciplinary framework. Our field lies at the intersection of

oceanography, microbiology, physics, chemistry, engineering, and human health. The discipline can only benefit from the combined efforts of each.

### Literature Cited

- Al-Homoud, A.; Hondzo, M. 2008. Enhanced uptake of dissolved oxygen and glucose by *Escherichia coli* in a turbulent flow. *Applied Microbiology and Biotechnology*. 79, 643-655.
- Anderson, A.; Larsson, U.; Hagstrom, A. 1986. Size-selective grazing by a microflagellate on pelagic bacteria. *Molecular Ecology Progress Series* 33: 51-57.
- Anderson, K. L.; Whitlock, J. E.; Harwood, V. J. 2005. Persistence and differential survival of fecal indicator bacteria in subtropical waters and sediments. *Applied and Environmental Microbiology*. 71, 3041-3048.
- Arnone, D. R.; Walling, J. P. 2007. Waterborne pathogens in urban watersheds. *Journal of Water and Health*. 5: 149-162.
- Billerbeck, M. Pore Water Transport and Microbial Activity in Intertidal Wadden Sea Sediments. Dissertation zur Erlangung des Doktorgrades der Naturwissenschaften. Universität Bremen vorgelegt von Markus Billerbeck. 2005.
- Boehm, A. B. 2003. Model of microbial transport and inactivation in the surfzone and application to field measurements of total coliform in northern Orange County, California. *Environmental Science and Technology*. 37, 5511-5517.
- Boehm, A. B.; Grant, S. B.; Kin, J. H.; Mowbray, S. L.; McGee, C. D.; Clark, C. D.; Foley, D. M.; Wellman, D. E. 2002a. Decadal and shorter period variability of surf zone water quality at Huntington Beach, California. *Environmental Science and Technology*. 36: 3885-3892.
- Boehm, A. B.; Keymer, D. P.; Shellenbarger, G. G. 2005. An analytical model of enterococci inactivation, grazing, and transport in the surfzone of a marine beach. *Water Research*. 39, 3565-3578.
- Boehm, A. B.; Sanders, B. F.; Winant, C. D. 2002b. Cross-shelf transport at Huntington Beach. Implications for the fate of sewage discharged through an offshore outfall. *Environmental Science and Technology*. 36, 1899-1906.
- Boehm, A. B.; Shellenbarger, G. G.; Paytan, A. 2004. Groundwater discharge: potential association with fecal indicator bacteria in the surf zone. *Environmental Science and Technology*. 38: 3558- 3566.
- Boehm, A. B.; Whitman, R. L.; Nevers, M. B.; Hou, D.; Weisberg, S. B. 2007

Nowcasting recreational water quality, in statistical framework for recreational water quality criteria and monitoring (ed L. J. Wymer), John Wiley & Sons, Ltd, Chichester, UK.

- Boehm, A.; Yamahara, K.; Love, D. C.; Peterson, B. M.; McNeill, K.; Nelson, K. L. 2009. Covariation and photoinactivation of traditional and novel indicator organisms and human viruses at a sewage impacted marine beach. *Environmental Science and Technology*. 43, 8046-8052.
- de Brauwere, A.; de Brye, B.; Servais, P.; Passerat, J.; Deleersnijder, E. 2011. Modeling *Escherichia coli* concentrations in the tidal Scheldt river and estuary. *Water Research*. 45: 2724-2738.
- Byappanahalli, M. N.; Shively, D. A.; Nevers, M. B.; Sadowsky, M. J.; Whitman, R. L. 2003. Growth and survival of *Escherichia coli* and enterococci populations in the macro-alga, *Cladophora* (Chlorophyta). *FEMS Microbiology Ecology*. 46, 203-211.
- Cabelli, V. J.; Dufour, A. P.; McCabe, L. J.; Levin, M. A. 1982. Swimming-associated gastroenteritis and water quality. *American Journal of Epidemiology*. 115: 606-616.
- Cabelli, V. J.; Dufour, A. P.; McCabe, L. J.; Levin, M. A. 1983. A marine recreational water quality criterion consistent with indicator concepts and risk analysis. *Journal of Water Pollution Control Federation*. 55: 1306-1314.
- Cabelli, V. J.; Levin, M. A.; Dufour, A. P.; McCabe, L. J. The development of criteria for recreational waters. In: Gameson ALH, editor. Discharge of sewage from sea outfalls. Oxford: Pergamon; 1975 p. 63-74.
- Cho, K. H.; Pachepsky, Y. A.; Kim, J. H.; Guber, A. K.; Shelton, D. R.; Rowland, R. 2010. Release of *Escherichia coli* from the bottom sediment in a first-order creek: Experiment and reach-specific modeling. *Journal of Hydrology*. 391: 322-332.
- Clark, C.; De Bruyn, W. J.; Hirsch, C. M.; Aiona, P. 2010. Diel cycles of hydrogen peroxide in marine bathing waters in Southern California, USA: *In situ* surf zone measurements. *Marine Pollution Bulletin*. 60: 2284-2288.
- Clark, C.; De Bruyn, W. J.; Jakubowski, S. D., Grant. S. B. 2008. Hydrogen peroxide production in marine bathing waters: Implications for fecal indicator bacteria mortality. *Marine Pollution Bulletin*. 56: 397-401.
- Connolly, J. P.; Blumberg, A. F.; Quadrini, J. D. 1999. Modeling fate of pathogenic organisms in coastal waters off Oahu, Hawaii. *Journal of Environmental*

*Engineering*. 125: 398-406.

- Colford, J. M.; Wade, T. J.; Schiff, K. C.; Wright, C. C.; Griffith, J. F.; Sandhu, S. K.; Burns, S.; Sobsey, M.; Lovelace, G.; Weisberg, S. B. 2007. Water quality indicators and the risk of illness at beaches with non point sources of fecal contamination. *Epidemiology*. 18: 27-35.
- Corbett, S. J.; Rubin, G. L.; Curry, G. K.; Kleinbaum, D. G. 1993. The health effects of swimming at Sydney beaches. *American Journal of Public Health*. 83: 1701-1706.
- Curtis, T. P.; Mara, D. D.; Silva, S. A. 1992. Influence of pH, oxygen and humic substances on ability of sunlight to damage fecal coliforms in waste stabilization pond water. *Applied and Environmental Microbiology*. 58: 1335-1343.
- Davies-Colley, R. J.; Bell, R. G.; Donnison, A. M. 1994. Sunlight inactivation of enterococci and fecal coliforms in sewage effluent diluted in seawater. *Applied and Environmental Microbiology*. 60: 2049-2058.
- Davies-Colley, R. J.; Donnison, A. M.; Speed, D. J.; Ross, C. M.; Nagels, J. W. 1999. Inactivation of faecal indicator microorganisms in waste stabilization ponds: interactions of environmental factors with sunlight. *Water Research*. 5, 1220-1230.
- Dufour, A. P.; Wymer, L. J. Microbes, monitoring, and human health. *Oceanography*. 2006, 19, 72-80.
- Feng, F.; Goto, D.; Yan, T. 2010. Effects of autochthonous microbial community on the die-off of fecal indicators in tropical beach sand. *FEMS Microbial Ecology*. 74: 214-225.
- Fisher, K.; Phillips, C. 2009. The ecology, epidemiology and virulence of *Enterococcus*. *Microbiology*. 155: 1749-1757
- Fleisher, J. M. 1991. A re-analysis of data supporting the US Federal bacteriological water quality governing marine recreational waters. *Journal of Water Pollution Control Federation*. 63: 259-264.
- Fleisher, J. M. US Federal bacteriological water quality standards: are-analysis of the data on which they are based. In: Kay D, editor. *Recreational water quality management: coastal bathing waters*, vol. I. Chinchester, UK: Ellis Horwood; 1992 p. 113-128.
- Francy, D. S.; Darner, R. A.; Bertke, E. E. 2006. Models for predicting recreational

water quality at lake Erie beaches. USGS Scientific Investigations Report 2 006-5192.

- Francy, D. S. 2009. Use of predictive models and rapid methods to nowcast bacteria levels at coastal beaches. *Aquatic Ecosystem Health and Management*. 12: 117-182.
- Frick, W. E.; Ge, Z.; Zepp, R. G. 2008. Nowcasting and forecasting concentrations of biological contaminants at beaches: a feasibility and case study. *Environmental Science and Technology*. 42: 4818–4824.
- Gantzer, C.; Maul, A.; Audic, J. M.; Schwartzbrod, L. 1998. Detection of infectious enteroviruses, enterovirus genomes, somatic coliphages, and *Bacteroides fragilis* phages in treated wastewater. *Applied and Environmental Microbiology*. 64: 4307-4312.
- Ge, Z; Frick, W. E. 2007. Some statistical issues related to multiple linear regression modeling of beach bacteria concentrations. *Environmental Research*. 103: 358–364.
- Ge, Z; Frick, W. E. 2009. Time-frequency analysis of beach bacteria variations and its implication for recreational water quality modeling. *Environmental Science and Technology*. 43:1128–1133.
- Given, S.L.; Pendleton, L. H.; Boehm, A. B. 2006. Regional public health cost estimates of contaminated coastal waters: a case study of gastroenteritis at southern California beaches. *Environmental Science and Technology*. 40, 4851-4867.
- Gontang, E. A.; Genical, W.; Jensen, P. R. 2007. Phylogenetic diversity of gram-positive bacteria cultured from marine sediments. *Applied and Environmental Microbiology*. 73: 3272-3282.
- Gonzalez, J. M.; Iriberry, J.; Egea, L.; Barcina, I. 1990b. Differential Rates of Digestion of Bacteria by Freshwater and Marine Phagotrophic Protozoa.. *Applied and Environmental Microbiology*, 56: 1851-1857.
- Gonzalez, J. M.; Iriberry, J.; Egea, L.; Barcina, I. 1992. Characterization of culturability, protistan grazing and death of enteric bacteria in aquatic ecosystems. *Applied and Environmental Microbiology*. 58: 998-1004.
- Gonzalez, J. M.; Sherr, E. B.; Sherr, B. F. 1990a. Size-selective grazing on bacteria by natural assemblages of estuarine flagellates and ciliates. *Applied and Environmental Microbiology*, 56: 583-589.

- Grant, S. B.; Kim, J. H.; Jones, B. H.; Jenkins, S. A.; Wasyl, J.; Cudaback, C. 2005. Surf zone entrainment, along-shore transport, and human health implications of pollution from tidal outlets. *Journal of Geophysical Research*. 110: C10025-C10045.
- Grant, S. B.; Sanders, B. F. 2010. Beach boundary layer: A framework for addressing recreational water quality impairment at enclosed beaches. *Environmental Science and Technology*. 44: 8804-8813.
- Grant, S. B.; Sanders, B. F.; Boehm, A. B.; Redman, J. A.; Kim, J. H.; Mrse, R. D.; Chu, A. K.; Gouldin, M.; McGee, C. D.; Gardiner, N. A.; Jones, B. H.; Svejksky, J.; Leipzig, G. V.; Brown, A. 2001. Generation of enterococci bacteria in a coastal saltwater marsh and its impact on surf zone water quality. *Environmental Science and Technology*. 35, 2407-2416.
- Griffin, D. W.; Donaldson, K. A.; Paul, J. H.; Rose, J. B. 2003. Pathogenic human viruses in coastal waters. *Clinical Microbiology Reviews*. 16: 129-143.
- Haile, R. W.; Witte, J. S.; Gold, M.; Cressey, R.; McGee, C.; Millikan, R. C.; Glasser, A.; Harawa, N.; Ervin, C.; Harmon, P.; Harper, J.; Dermard, J.; Alamillo, J.; Barret, K.; Nides, M.; Wang, G. 1999. The health effects of swimming in ocean water contaminated by storm drain runoff. *Epidemiology*. 10: 355-363.
- Halliday, E.; Gast, R. J.; 2011. Bacteria in beach sands: an emerging challenge in protecting coastal water quality and bather health. *Environmental Science and Technology*. 45, 370-379.
- Hardie, J. M.; Whiley, R. A. 1997. Classification and overview of the genera *Streptococcus* and *Enterococcus*. *Journal of Applied Microbiology Symposium Supplement*. 83: 1S-11S.
- Hartke, A.; Lemarinier, S.; Pichereau, V.; Auffray, Y. 2002. Survival of *Enterococcus faecalis* in seawater microcosms is limited in the presence of bacterivorous zooflagellates. *Current Microbiology* 44, 329-335.
- Hartz, A.; Cuvelier, M.; Noqosielski, K.; Bonilla, T. D.; Green, M.; Esiobu, N.; McCorquodale, D. S.; Rogerson, A. 2008. Survival potential of *Escherichia coli* and enterococci in subtropical beach sand: implications for water quality managers. *Journal of Environmental Quality*. 37: 898-905.
- He, L. M.; He, Z. L. 2008. Water quality prediction of marine recreational beaches receiving watershed baseflow and stormwater runoff in southern California, USA. *Water Research*. 42: 2563-2573.
- Hou, D., Rabinovici, S. J. M. Boehm, A. B. 2006. Enterococci predictions from partial

- least squares regression models in conjunction with a single-sample standard improve the efficacy of beach management advisories. *Environmental Science and Technology*. 40: 1737-1743.
- Jenkins M. B.; Fisher, D. S.; Endale, D. M.; Adams, P. 2011. Comparative die-off of *Escherichia coli* 0157:H7 and fecal indicator bacteria in pond water. *Environmental Science and Technology*. 45: 1853–1858.
- Jiang, S. C.; Chu, W. 2004. PCR detection of pathogenic viruses in Southern California urban rivers. *Journal of Applied Microbiology*. 97: 17-28.
- Jeong, Y.; Grant, S. B.; Ritter, S.; Pednekar, A.; Candelaria, L.; Winant, C. 2005. Identifying pollutant sources in tidally mixed systems: case study of fecal indicator bacteria from marinas in Newport Bay, Southern California. *Environmental Science and Technology*. 39, 9083- 9093.
- Kay, D.; Bartram, J.; Pruss, A.; Ashbolt, N.; Wyer, M. D.; Rleisher, J. M.; Fewtrell, L.; Rogers, A.; Rees, G. 2004. Derivation of numerical values for the World Health Organization guidelines for recreational waters. *Water Research* 1296-1304.
- Kay, D.; Fleisher, J. M.; Salmon, R. L.; Jones, F.; Wyer, M. D.; Godfree, A. F.; Zelenauch-Joquette, Z.; Shore, R. 1994. Predicting likelihood of gastroenteritis from sea bathing: results from randomized exposure. *Lancet*. 344: 905-909.
- Ki, S. J.; Ensari, S.; Kim, J. H. 2007. Solar and tidal modulations of fecal indicator bacteria in coastal waters at Huntington Beach, California. *Environmental Management*. 39, 867-875.
- Kim, J. H.; Grant, S. B.; McGee, C. D.; Sanders, B. F.; and Largier, J. L. 2004. Locating sources of surf zone pollution: a mass budget analysis of fecal indicator bacteria at Huntington Beach, California. *Environmental Science and Technology*. 38: 2626-2636.
- Kim, J. H.; Grant, S. B. 2004. Public mis-notification of coastal water quality: a probabilistic evaluation of posting errors at Huntington Beach, California. *Environmental Science and Technology*. 8: 2479-2504.
- Kirschner, K. A.; Zechmeister, T. C.; Kavka, G. G.; Beiwl, C.; Herzig, A.; Mach, R. L.; Farnleitner, A. H. 2004. Integral strategy for evaluation of fecal indicator performance in bird-influenced saline inland waters. *Applied and Environmental Microbiology*. 40: 7396-7403.
- Lancefield R. C. 1933. A serological differentiation of human and other groups of hemolytic streptococci. *Journal of experimental medicine*. 57: 571-595.



- Lawes, J. P.; Andrewes, F. W. 1894. Report on the result of investigations of the microorganisms of sewage: *Report to London City Council*.
- Layton, A.; McKay, L.; Williams, D.; Garrett, V.; Gentry, R.; Sayler, G. 2006. Development of *Bacteriodes* 16S rRNA gene TaqMan-based real-time PCR assays for estimation of total, human, and bovine fecal pollution in water. *Applied Environmental Microbiology* 72: 4212-4224.
- Lee, S.; Fuhrman, J. A. 1987. Relationships between biovolume and biomass of naturally derived marine bacterioplankton. *Applied and Environmental Microbiology*. 53: 1298-1303.
- Liu, L.; Phanikumar, M. S.; Molloy, S. L.; Whitman, R. L.; Shively, D. A.; Nevers, M. B.; Schwab, D. J.; Rose, J. B. 2006. Modeling the transport and inactivation of *E. coli* and enterococci in the near-shore region of lake Michigan. *Environmental Science and Technology*. 40: 5022-5028.
- Maraccini, P. A.; Ferguson, D. M.; Boehm, A. B. 2012. Diurnal variation in *Enterococcus* species composition in polluted ocean water and a potential role for the enterococcal carotenoid in protection against photoinactivation. *Applied and Environmental Microbiology*. 78: 305-310.
- Meays, C. L.; Broersma, K.; Nordin, R.; Mazumder, A. 2004. Source tracking fecal bacteria in water: a critical review of current methods. *Journal of Environmental Management*. 73: 71-79.
- Morrison, D.; Woodford, N.; Cookson, B. 1997. Enterococci as emerging pathogens of humans. *Journal of Applied Microbiology*. 83: 89S – 99S.
- Muela, A.; Garcia-Bringas, J. M.; Seco, C.; Arana, I.; Barcina, I. 2002. Participation of oxygen and the role of exogenous and endogenous sensitizers in the photoinactivation of *Escherichia coli* by photosynthetically active radiation, UV-A and UV-B. *Microbial Ecology*. 44, 354-364.
- Naser, S.; Thompson, F. L.; Hoste, B.; Gevers, D.; Vandemeulebroeke, K.; Cleenwerck, I.; Thompson, C. C.; Vancanneyt M.; Swings, J. 2005. Phylogeny and identification of enterococci by *atpA* gene sequence analysis. *Journal of Clinical Microbiology*. 43: 2224-2230.
- Neevers, M. B.; Whitman, R. L. 2005. Nowcast modeling of *Escherichia coli* concentrations at multiple urban beaches of southern Lake Michigan. *Water Research*. 39: 5250-5260.
- Nevers, M. B.; Whitman, R. L. 2011. Efficacy of monitoring and empirical predictive

- modeling at improving public health protection at Chicago beaches. *Water Research*. 4: 1659–1668.
- Nevers, M. B.; Whitman, R. L.; Frick, W. E.; Ge, Z. 2007. Interaction and influence of two creeks on *Escherichia coli* concentrations of nearby beaches: exploration of predictability and mechanisms. *Journal of Environmental Quality*. 36: 1338-1345.
- Orla-Jensen, S. 1919. The lactic acid bacteria. *Mem. Acad. Roy. Sci. Danemark Sect. Sci. Ser.* 5: 81-197.
- Palmer, K. L.; Godfrey, P.; Griggs, A.; Kos, N. V.; Zucker, J.; Desjardins, C.; Cerqueira, G.; Gevers, D.; Walker, S.; Wortman, J.; Feldgarden, M.; Haas, B.; Birren, B.; Gilmore, M. S. 2012. Comparative genomics of enterococci: variation in *Enterococcus faecalis*, clade structure in *E. faecium*, and defining characteristics of *E. gallinarium* and *E. casseliflavus*. *MBio*. 1:e00318-11.
- Pednekar, A. M.; Grant, S. B.; Jeong, Y.; Poon, Y.; Oancea, C. 2005. Influence of climate change, tidal mixing, and watershed urbanization on historical water quality in Newport Bay, a saltwater wetland and tidal embayment in Southern California. *Environmental Science and Technology*. 39: 9071-9082.
- Peeler, K. A.; Opsuhl, S. P.; Chanton, J. P. 2006. Tracking anthropogenic inputs using caffeine, indicator bacteria, and nutrients in rural, freshwater, and urban marine systems. *Environmental Science and Technology*. 40: 7616-7622.
- Phillips, M. C.; Solo-Gabriele, H. M.; Reniers, A. J. H. M.; Wang, J. D. Kiger, R. T.; Abdel-Mottaleb, N. 2011. Pore water transport of enterococci out of beach sediments. *Marine Pollution Bulletin*. 62: 2293-2298.
- Pruss, A. 1998. Review of epidemiological studies on health effects from exposure to recreational water. *International Journal of Epidemiology*. 27: 1-7.
- Ralston, E. P.; Kite-Powell, H.; Beet, A. 2011. An estimate of the cost of acute health effects from food and water-borne marine pathogens and toxins in the United States. *Journal of Water and Health*. 9: 680-694.
- Rozen, Y.; Belkin, S. 2001. Survival of enteric bacteria in seawater. *FEMS Microbiology Reviews*, 25: 513-529.
- Sanders, B. F.; Arega, F.; Sutula, M. 2005. Modeling the dry-weather tidal cycling of fecal indicator bacteria in surface waters of an intertidal wetland. *Water Research*. 39: 3394-3408.
- Scott, T. M.; Rose, J. B.; Jenkins, T. M.; Farrah, S. R.; Lukasik, J. 2002. Microbial

- source tracking: current methodology and future directions. *Applied and Environmental Microbiology* 68: 5796-5803.
- de Sieyes, N. R.; Yamahara, K. M.; Layton, B. A.; Joyce, E. H.; Boehm, A. B. 2008. Submarine discharge of nutrient-enriched fresh groundwater at Stinson beach, California is enhanced during neap tides. *Limnology and Oceanography*. 53: 1434-1445.
- Signoretto, C.; Burlacchini, G.; Lleo, M. M.; Pruzzo, C.; Zampini, M.; Pane, L.; Franzini, G.; Canepari, P. 2004. Adhesion of *Enterococcus faecalis* in the nonculturable state to plankton is the main mechanism responsible for persistence of this bacterium in both lake and seawater. *Applied and Environmental Microbiology*. 70: 6892-6896.
- Sinton, L. W.; Donnison, A. M.; Hastie, C. M. 1993a. Faecal streptococci as faecal pollution indicators: a review. Part 1: Taxonomy and Enumeration. *New Zealand Journal of Marine and Freshwater Research*. 27, 101-115.
- Sinton, L. W.; Donnison, A. M.; Hastie, C. M. 1993b. Faecal streptococci as faecal pollution indicators: a review. Part II: Sanitary Significance, Survival and Use. *New Zealand Journal of Marine and Freshwater Research*. 27: 117-137.
- Sinton, L. W.; Finlay, R. K.; Lynch, P. A. 1999. Sunlight inactivation of fecal bacteriophages and bacteria in sewage-polluted seawater. *Applied and Environmental Microbiology*. 65, 3605-3613.
- Sinton, L. W.; Hall, C. H.; Lynch, P. A.; Davies-Colley, R. J. 2002. Sunlight inactivation of fecal indicator bacteria and bacteriophages from waste stabilization pond effluent in fresh and saline waters. *Applied and Environmental Microbiology* 68, 1122-1131.
- Sherman, J. M. 1937. The Streptococci. *Bacteriol. Rev.* 1: 3-97.
- Seurinck, S.; Verstraete, W.; Siciliano, S. D. 2005. Microbial source tracking for identification of fecal pollution. *Reviews in Environmental Science and Bio/Technology*. 4: 19-37.
- Solic, M.; Krstulovic, N. 1992. Separate and combined effects of solar radiation, temperature, salinity, and pH in the survival of fecal coliforms in seawater. *Marine Pollution Bulletin*. 24, 411-416.
- Surbeck, C. Q.; Jiang, S. C. Grant, S. B. 2010. Ecological control of fecal indicator bacteria in an urban stream. *Environmental Science and Technology* 44, 631-637.

- Suter, E.; Juhl, A. R.; O'Mullan, G. D. 2011. Particle association of *Enterococcus* and total bacteria in the lower Hudson River estuary, USA. *Journal of Water Resource and Protection*. 3: 715-725.
- Tallon, P.; Magajina, B.; Lofranco, C.; Leung, T. K. 2005. Microbial indicators of faecal contamination in water: a current perspective. *Water, Air, and Soil Pollution*. 116: 139-166.
- Thupaki, P.; Phannikumar, M. S.; Beletsky, D.; Schwab, D. J.; Nevers, M. B.; Whitman, R. L. 2010. Budget analysis of *Escherichia coli* at a southern Lake Michigan beach. *Environmental Science and Technology*. 44: 1010-1016.
- Troussellier, M.; Bonnefont, J.; Courties, C.; Derrien, A.; Dupray, E.; Gauthier, M.; Gourmelon, M.; Joux, F.; Lebaron, P.; Martin, Y.; Pommepuy, M. 1998. Responses of enteric bacteria to environmental stresses in seawater. *Oceanologica Acta*. 21, 965-981.
- Turbow, D. J.; Osgood, N. D.; Jiang, S. C. 2003. Evaluation of recreational health risk in coastal waters based on *Enterococcus* densities and bathing patterns. *Environmental Medicine*. 111: 598-603.
- USEPA. 1986. Bacteriological ambient water quality criteria for marine and fresh recreational waters. EPA 440/5-84-002. U.S. Environmental Protection Agency, Office of Research and Development, Cincinnati, OH.
- USEPA. 2000. Improved enumeration methods for the recreational water quality indicators: enterococci & *Escherichia coli*. EPA/821/R-97/004. U.S. Environmental Protection Agency, Office of Science and Technology.
- Wade, J. T.; Pai, N.; Eisenberg, J. N. S. Colford, J. M. Jr. 2003. Do U.S. Environmental Protection Agency water quality guidelines for recreational waters prevent gastrointestinal illness? A systematic review and meta-analysis. *Environmental Health Perspectives*. 111: 1102-1109.
- Whitman, R. L.; Nevers, M. B. 2003. Foreshore sand of *Escherichia coli* in nearshore water of a Lake Michigan beach. *Applied and Environmental Microbiology*. 69: 5555-5562.
- Whitman, R. L.; Shively, D. A.; Pawlik, H.; Nevers, M. B.; Byappanahalli, M. N. 2003. Occurrence of *Escherichia coli* and enterococci in *Cladophora* (Chlorophyta) in nearshore water and beach sand of Lake Michigan. *Applied and Environmental Microbiology*. 69: 4714-4719.
- Wong, S. H. C.; Santoro, A. E.; Nidzieko, N. J.; Hench, J. L.; Boehm, A. B. 2012. Coupled physical, chemical, and microbiological measurements suggest a

connection between internal waves and surf zone water quality in the Southern California Bight. *Continental Shelf Research*. 34: 64-78.

Yamahara, K. M.; Sassoubre, L. M.; Goodwin, K. D.; Boehm, A. B. 2012. Occurrence and persistence of bacterial pathogens and indicator organisms in beach sand along the California coast. *Applied and Environmental Microbiology*. 78: 1733-1745.

Yamahara, K. M.; Walters, S. P.; Boehm, A. B. 2009. Growth of enterococci in unaltered, unseeded beach sands subjected to tidal wetting. *Applied and Environmental Microbiology*. 75: 1517-1524.

Zhang, Z.; Zhiqiang, D.; Rusch, K. A. 2012. Development of predictive models for determining enterococci levels at Gulf Coast beaches. *Water Research*. 46: 465-474.

Zhu, X.; Wang, J. D.; Solo-Gabriele, H. M.; Fleming, L. E. 2011. A water quality modeling study of non-point sources at recreational marine beaches. *Water Research*. 45: 2985-2995.

## CHAPTER 2.

### PHYSICAL FACTORS CONTROLLING VARIABILITY IN NEARSHORE FECAL POLLUTION: FECAL INDICATOR BACTERIA AS PASSIVE PARTICLES

#### **Abstract**

We present results from a 5-hour field program (HB06) that took place at California's Huntington State Beach. We assessed the importance of physical dynamics in controlling fecal indicator bacteria (FIB) concentrations during HB06 using an individual based model including alongshore advection and cross-shore variable horizontal diffusion. The model was parameterized with physical (waves and currents) and bacterial (*E. coli* and *Enterococcus*) observations made during HB06. The model captured surfzone FIB dynamics well (average surfzone model skill: 0.84 {*E. coli*} and 0.52 {enterococci}), but fell short of capturing offshore FIB dynamics. Our analyses support the hypothesis that surfzone FIB variability during HB06 was a consequence of southward advection and diffusion of a patch of FIB originating north of the study area. Offshore FIB may have originated from a different, southern, source. Mortality may account for some of the offshore variability not explained by the physical model.

#### **Introduction**

Approximately 90% of California's beach closures are due to elevated levels of fecal indicator bacteria (FIB) (Dufour and Wymer, 2006). FIB are nonpathogenic enteric bacteria, present at high concentrations in human and animal wastes, that are

used to track bacterial pathogens in coastal systems (Sinton et al., 1993). FIB are released from contaminated sources – often non-point source run-off or riverine discharge – become suspended in the surfzone (coastal waters shoreward of the breaker line), and are transported to beaches (Boehm et al., 2002; Boehm et al., 2005; Grant et al., 2005). The spatial and temporal distribution of FIB sources, and the dynamics of the surfzone through which FIB are transported, play an important role in regulating the extent and intensity of beach bacterial contamination. Furthermore, because FIB survival in the surfzone determines the duration of transport, factors regulating FIB growth and mortality in coastal waters are also central to our understanding of bacterial pollution (Anderson et al., 2005; Boehm, 2003; Boehm et al., 2005).

Beach pollution events are often poorly predicted, and about 40% of contamination postings are erroneous (Kim and Grant, 2004). With over 550 million annual person-visits to California beaches, this inaccuracy impacts both individual beach goers and California's multi-billion dollar coastal tourism industry (Grant et al., 2001). Predictive modeling of bacterial pollution using readily measured (or modeled) physical parameters (wave height/direction, river flow, rainfall, etc.) could be a cost-effective way to improve the accuracy of beach contamination postings. However, to be effective in a range of settings, these models require mechanistic understanding of bacterial sources, transports, and extra-enteric growth or decay. Mechanistic understanding moves beyond correlations, and examines the effects of individual processes structuring beach pollution. Past mechanistic studies have been limited by a lack of physical (fluid) and biological observations with suitable spatial and temporal

resolution.

We present results from a field program with joint physical and bacterial observations designed to identify the dominant mechanisms controlling local FIB variability. In the present paper we focus on quantifying the contribution of physical processes (advection and diffusion) to the observed FIB patterns, and developing a best-fit physical model from this analysis. The contribution of biological processes to nearshore FIB variability is addressed in Rippey et al. (submitted ms.).

## **Methods**

### ***Field Site Description:***

Southern California's Huntington State Beach is ~3.2 km long, with chronically poor surfzone water quality (Grant et al., 2001; Kim et al., 2004). At its southern end, the beach receives brackish flows from the Talbert Marsh (TM) and the Santa Ana River (SAR), both of which have been implicated as sources of surfzone FIB (Kim et al., 2004). In fall 2006, a multi-institutional field campaign ("HB06") focused on observing nearshore waves, currents, temperature, phytoplankton, and FIB at this beach. The present study concerns the bacterial component of HB06, a 5-hour FIB survey with high spatial and temporal resolution conducted on October 16<sup>th</sup> along transects extending 1 km north of the TM/SAR outlets, and 300 m offshore.

### ***FIB Sampling Program:***

#### **Sample Collection & Processing:**

FIB concentrations were measured at 8 stations: 4 in knee-deep water along a



1000 m alongshore transect north of SAR (SAR, TM, FHM, F1; Fig. 2.1), and 4 along a 300 m cross-shore transect starting at F1 (knee-deep water), and terminating at an offshore Orange County Sanitation District mooring (OM) in ~8 m mean water depth (F1, F3, F5, F7, OM; Fig. 2.1). Every 20 minutes, from 0650 h to 1150 h PDT, 100 ml water samples were taken at all stations. Samples were stored on ice and transported to the Orange County Sanitation District (OCSD) within 6 h of collection. All samples were analyzed for *E. coli* (IDEXX Colilert) and *Enterococcus* (EPA method 1600) concentrations by OCSD personnel.

*Spatial & Temporal Patterns in Bacterial Decay:*

Temporal rates of FIB loss were estimated for each station from regressions of log(FIB) versus time. We refer to these FIB loss rates as “decay”, where decay includes removal/dilution due to advection and diffusion as well as biological mortality. In contrast, the term “mortality” will be used to denote the portion of decay that is due to FIB senescence alone, and is *not* caused by the measured physical processes.

At stations where FIB concentrations dropped below minimum sensitivity standards for our bacterial assays (< 10 MPN / 100 ml for *E. coli* or < 2 CFU / 100 ml for enterococci) prior to the end of the study period, decay rates were calculated using only data up until these standards were reached (SI Fig. 2.1). Decay rates were compared across sampling stations to look for spatial patterns in bacterial loss. Decay rates were also compared across FIB groups (*E. coli* vs. enterococci) to identify group-specific patterns. Statistical analyses were performed using MATLAB (Mathworks,

Natick, MA).

*Nearshore Instrumentation:*

Pressure sensors and Acoustic Doppler velocimeters (ADV's) (Sontek, 2004), both sampling at 8 Hz, were placed in the nearshore to monitor the wave and current field during our study. All instruments were mounted on tripod frames fixed on the seafloor at seven locations (F1-F7) along the shoreward-most 150 m of the cross-shore transect shown in (Fig. 2.1). Cross-shore resolved estimates of the alongshore current field were determined using 20 minute averaged alongshore water velocities from each ADV.

***2D Individual Based FIB Model:***

The contribution of physical processes in structuring FIB concentrations during HB06 was quantified using a 2D ( $x$  = alongshore,  $y$  = cross-shore) individual-based advection-diffusion or “AD” model for FIB (informed by the model of Tanaka and Franks, 2008). Only alongshore advection, assumed to be uniform alongshore, was included in the model. Both cross-shore and alongshore diffusivities were also included. These were assumed to be equal at any point in space, and alongshore uniform. The cross-shore variation of diffusivity was modeled as:

$$\kappa_h = \kappa_0 + \frac{(\kappa_1 - \kappa_0)}{2} \left( 1 - \tanh \left( \frac{(y - y_0)}{y_{scale}} \right) \right) \quad (1)$$

Here,  $k_0$  is the background (offshore) diffusivity,  $k_l$  is the elevated surfzone diffusivity (Reniers et al., 2009; Spydell et al., 2007),  $y_0$  is the observed cross-shore midpoint of the transition between  $k_0$  and  $k_l$  (i.e., the offshore edge of the surfzone) and  $y_{scale}$  determines the cross-shore transition width. Representative values of  $k_l$  ( $0.5 \text{ m}^2 \text{ s}^{-1}$ ) and  $k_0$  ( $0.05 \text{ m}^2 \text{ s}^{-1}$ ) were chosen based on incident wave height and alongshore current measurements (Clark et al., 2010; Spydell et al., 2009). The observed width of the surfzone (i.e., the region of breaking waves) was used to determine  $y_0$ . Significant wave height was maximum at F4 and low at F1 and F2, suggesting that the offshore edge of the surfzone was between F2 and F4 (Fig. 2.2 a); thus  $y_0 = 50 \text{ m}$ , near F3. To give a rapid cross-shore transition between surfzone (F2) and offshore (F4) diffusivity,  $y_{scale}$  was set to 5 m (SI Fig. 2.2). The AD model was only weakly sensitive to the parameterization of  $y_{scale}$ ,  $k_0$  and  $k_l$ , with sensitivity varying by station (SI Fig. 2.3). Cross-shore advection was not included in the model, as alongshore samples were taken from the same water depth each time (i.e., following the tidal excursion). Neglecting cross-shore advection (including rips, etc.) will generally lead to conservative estimates of the contribution of physical dilution to FIB decay.

Particle Motions:

In the AD model, FIB particles are advected alongshore by 20 minute average currents ( $u$ ), that vary in the cross-shore ( $y$ ). FIB particles diffuse along- and cross-shore by horizontal diffusion ( $k_h$ ). For a particle starting at  $(x_t, y_t)$ , its position at  $(x_{t+\Delta t}, y_{t+\Delta t})$  is

$$x_{t+\Delta t} = x_t + \frac{\partial \kappa_h(y_t)}{\partial y} \Delta t \quad (2)$$

$$+ R \left( \frac{2\kappa_h \left( y_t + \frac{1}{2} \frac{\partial \kappa_h}{\partial y} \Delta t \right) \Delta t}{r} \right)^{\frac{1}{2}} + u \Delta t$$

$$y_{t+\Delta t} = y_t + \frac{\partial \kappa_h(y_t)}{\partial y} \Delta t \quad (3)$$

$$+ R \left( \frac{2\kappa_h \left( y_t + \frac{1}{2} \frac{\partial \kappa_h}{\partial y} \Delta t \right) \Delta t}{r} \right)^{\frac{1}{2}}$$

where  $R$  is a random number with zero mean and variance  $r$ . For this model,  $r = 1/3$ , giving  $R$  a uniform distribution with range  $[-1, 1]$  (Ross and Sharples, 2004; Tanaka and Franks, 2008). The time step was  $\Delta t = 1$  s for all model runs. A reflecting boundary condition was used at the shoreline; otherwise particles could move anywhere in the domain.

*Model Initialization:*

The AD model was initialized at  $t_0 = 0650$  h (the earliest FIB sampling time)

with 80,000 bacterial particles distributed uniformly within a rectangular  $(x,y)$  patch. Each particle represents a number of FIB (concentration  $C$ ); the actual number of FIB per particle can be scaled to match the data, provided the same scaling is applied to every particle. Our scaling constants were determined such that the space-time mean of AD modeled FIB equaled the space-time mean of measured FIB (*E. coli* or *Enterococcus*).

Initial patch boundaries (along and cross-shore) were identified by varying patch boundary locations over reasonable ranges to maximize the skill between the AD model and HB06 FIB data (Krause et al., 2005). Skill is defined as:

$$\text{Skill} = 1 - \frac{\text{mean}(C_{obs} - C_{mod})^2}{\text{mean}(C_{obs} - \bar{C}_{obs})^2} \quad (4)$$

where,  $C_{obs}$  are log FIB concentration data,  $C_{mod}$  are log AD model outputs, and  $\bar{C}_{obs}$  is the space-time mean of  $\log(C_{obs})$  for all stations and times. Here, skill is a measure of how much better (or worse) the model explains fluctuations in the data than the data mean. A value of 0 indicates that the model performs the same as the data mean. A value of 1 indicates that the model explains all the variance after removing the mean, and a negative value indicates that the model performs worse than the data mean. Depending on the context, the numerator for skill was calculated for individual stations, groups of stations, or all stations together; the denominator was always the same (all stations).

HB06 FIB observations showed the offshore FIB patch edge to be ~140 - 300

m from the shoreline. The effect of this range of possible offshore patch edges was explored in the model. The northernmost patch edge was varied from 0-2000 m north of the sampling region, and the southernmost patch edge was varied from 0-2000 m south of the sampling region. The initial patch always included the 1 km-long sampling region. Initial patch sizes that maximized alongshore and cross-shore station skill were used to initialize a “best-fit” AD model for subsequent comparisons between modeled and observed FIB concentrations and decay rates. The robustness of the model to alternative initial patch shapes is discussed briefly below (for details see Appendix 2.1 and SI Fig. 2.4).

## **Results and Discussion**

### ***Physical Environment:***

On October, 16<sup>th</sup>, 2006, the surfzone was between 40 and 70 m wide, with wave breaking beginning between F2 and F4. The maximum significant wave height was about 0.8 m, at F4 (Fig. 2.2 a). The alongshore current direction ( $u$ ) was variable both in time and with distance across shore. During the 5 h of FIB sampling, inner surfzone  $u$  (F1 and F2) was typically southward, while outer surfzone  $u$  (F3) and offshore  $u$  (F4-F7) were initially northward, and then reversed between 0750 h and 0930 h (Fig. 2.2 b). The reason for the current reversal at F3 and farther offshore is unknown, but may be linked to tidal phase, which transitioned from flood to ebb at 0710 h (Fig. 2.2 c).

The cross-shore sign reversal of the alongshore currents during the first hour of FIB sampling was also observed in the 12 h prior to FIB sampling (Fig. 2.2 b). During

this time, the average surfzone current was flowing south ( $0.03 \text{ m s}^{-1}$ ), and the average offshore current was flowing north ( $0.05 \text{ m s}^{-1}$ ) (Fig. 2.2 b), suggesting that offshore and surfzone FIB could have originated from different alongshore sources separated by as much as 5 km.

To identify possible source locations for the bacterial pollution observed on October 16<sup>th</sup> in more detail, the advection diffusion (AD) model (described above) was initialized with a uniform rectangular patch of particles spanning the study region (150 m cross-shore by 1000 m alongshore). The model was then run backwards in time (hindcast) to sundown of the previous evening using measured alongshore currents and no diffusion. These analyses showed that the surfzone FIB may have originated from a source 600-1500 m north of the study area, whereas the offshore FIB probably originated from a southern source, anywhere from 2-5 km south of the study area (Fig. 2.3).

#### ***Bacterial Patterns at Huntington Beach:***

At 0650 h on Oct. 16<sup>th</sup>, *E. coli* and *Enterococcus* concentrations exceeded EPA single-sample standards (104 *Enterococcus* /100 ml and 235 *E. coli* /100 ml) at most stations (88% for *E. coli* and 75% for *Enterococcus*). FIB concentrations were near zero offshore at OM, and concentrations at TM were approximately half those of the other stations (Fig. 2.4). The low concentrations at OM are consistent with prior research suggesting shoreline sources of FIB at Huntington Beach (Grant et al., 2001; Kim et al., 2004), and the retentive nature of the surfzone (Clark et al., 2010; Grant et al., 2005; Spydell et al., 2009). The low concentrations at TM, however, were

unexpected, as prior research at Huntington Beach has shown a connection between *Enterococcus* concentrations and bird feces in the marsh (Grant et al., 2001; Kim et al., 2004).

By 1150 h, FIB concentrations at all sampling locations were well below morning levels (Fig. 2.4). FIB decay was exponential in time at all stations, with *Enterococcus* concentrations decaying significantly faster than *E. coli* concentrations (Table 1).

#### ***Spatial Structure of FIB decay:***

*E. coli* and *Enterococcus* decay rates varied spatially, and were faster to the north than the south. FIB decay rates were not always significantly different at adjacent alongshore stations, but decay at SAR (southernmost station) was always slower than at F1 (northernmost station; Fig. 2.5 a). There were no significant differences in FIB decay rates across shore for either FIB group (Fig. 2.5 b). The similar along- and across shore spatial patterns in decay observed for *E. coli* and *Enterococcus* suggest that, although the magnitude of decay may vary with FIB group (mentioned above), both groups are affected by similar overarching processes such as physical dilution by advection and diffusion. We will quantify the contribution of advection and diffusion to measured FIB decay using our AD model.

#### ***Model Sensitivity Analysis: Initial Patch Size***

Due to predominately southward advection during the sampling period, the AD model was sensitive to initial (0650 h) offshore and northern patch boundaries, but not



the southern boundary. We modified equation 4 to calculate skill at alongshore or cross-shore stations only, as we varied the northern and offshore edges of the initial patch, respectively. Alongshore skill was maximum when the initial northern patch edge was 200 m N of F1 for enterococci and 600 m north of F1 for *E. coli* (Skill = 0.60 and 0.85, respectively) (SI Fig. 2.5 a). Notably, however, alongshore skill was relatively constant for initial northern patch edges between 100 - 900 m north (*E. coli*) or 100 – 600 m north (enterococci) (SI Fig. 2.5 a). For subsequent AD model runs, the northern patch edge was set to 600 m north; this value lies within the region of high model skill for *E. coli* and *Enterococcus* (SI Fig. 2.5 a). It is also consistent with the results of our hindcast model (Fig. 2.3), which indicated that surfzone FIB originated 600-1500 m north of the study area..

Overall, cross-shore AD model skill was lower than alongshore skill.

Maximum cross-shore skill occurred when the initial offshore patch edge was 160 m offshore for both FIB groups (Skill = 0.16 and 0.29, respectively) (SI Fig. 2.5 b).

The optimal northern and offshore initial patch boundaries identified in this manner (600 m north and 160 m offshore) were relatively robust to initial patch shape. Initializing the model with a rectangular patch that had diffused for five hours, instead of a rectangular patch with sharp edges, identified similar patch boundaries (700 m north and 160 m offshore) with reduced model skill, especially in the cross-shore (SI Fig. 2.4; SI Fig. 2.5).

### ***Best-Fit Model-Data Comparisons: Physical factors controlling FIB patchiness***

The AD (advection and diffusion) model reproduced a statistically significant

amount of FIB variability at alongshore stations during HB06. Modeled FIB concentrations decayed markedly (especially at northern stations) by 1150 h, as was observed in the field (Fig. 2.4; Fig. 2.6 a). Station-specific model skill was typically high (Skill = 0.74 - 0.90 for *E. coli*, and 0.45 – 0.66 for *Enterococcus*), with lower skill observed for *Enterococcus* (Fig. 2.6 b). Modeled station-specific FIB decay – driven only by advection and diffusion – was exponential for all alongshore stations (SI Fig. 2.6), and exhibited a spatial pattern similar to HB06 FIB data, with significantly faster decay observed at northern stations than southern stations (Fig. 2.5 a). Although the spatial patterns of decay estimated by the AD model matched those of HB06 FIB well, the actual magnitudes of the decay rates were lower than observed (Fig. 2.5). The only station where the AD model captured FIB decay rates accurately ( $p < 0.05$ ) was SAR, for *E. coli* (Fig. 2.5 a). At all other stations, AD modeled FIB decay accounted for  $\leq 50\%$  of observed decay (Fig. 2.5). This underestimation of FIB decay rates suggests that an additional source of decay must be included in the model to accurately reproduce FIB dynamics during HB06. This additional decay is likely to be intrinsic to the FIB taxa, as the amount of unexplained FIB decay during HB06 was group-specific (Fig. 2.5).

In the cross-shore, the AD model successfully reproduced FIB patterns for surfzone stations (F1, F3) and the offshore mooring (*Enterococcus* only), where FIB concentrations were consistently near zero. It failed, however, to reproduce FIB patterns for offshore stations exhibiting FIB contamination (F5, F7) (Fig. 2.6 b). Poor model-data fits at these stations likely reflect over-retention of offshore FIB (Fig. 2.4; Fig. 2.6 a). Modeled FIB decay at these stations was significantly slower than decay

at F1 and F3, while observed FIB decay rates were constant across-shore (Fig. 2.5 b). Together, the relatively poor model-data fits and decay-rate estimates for offshore stations suggest that, although the AD model performs well in the surfzone, it is missing a dominant process structuring offshore FIB concentrations during HB06.

Through a synthesis of field observations and models, we have shown that a model including only horizontal advection and diffusion can explain a significant portion of the variability in FIB concentrations at Huntington Beach, especially in the alongshore (Skill of 0.45 to 0.90 at alongshore stations and -0.23 to 0.74 at cross-shore stations, Fig. 2.6 b). HB06 was the first study to perform high-resolution monitoring of FIB, waves, and currents in the nearshore, providing an opportunity to directly quantify the importance of these physical processes in structuring nearshore FIB pollution. The strong role of advection and diffusion in structuring patterns of FIB during HB06 was somewhat surprising given the temporal decays observed at each sampling station often attributed to solar insolation (e.g., Ki et al., 2007). Our analyses suggest, however, that a significant portion of this decay (mean of 38 % for *E. coli*, and 14 % for *Enterococcus*) was due to southward advection and diffusion of FIB patches through the study area (Fig. 2.5). This resulted in faster FIB decay to the north than the south, as the FIB patch was mixed and advected past northern stations first.

Although the AD model captured FIB dynamics during HB06 well overall, the underestimation of FIB decay rates (especially at offshore stations) suggests that it is missing important processes governing FIB decay. Given the reported sensitivity of FIB to variations in solar insolation, organic matter, pH, salinity, etc., it is likely that

some form of extra-enteric FIB mortality may have contributed to the FIB decay observed during HB06 (Anderson et al., 2005; Curtis et al., 1992; Sinton et al., 2002). The contribution of mortality to nearshore FIB variability is addressed in Rippey et al. (submitted ms.).

### **Acknowledgements**

This work was supported by NSF, ONR, CA SeaGrant, the California Coastal Conservancy, the California Department of Boating and Waterways, and NOAA. Tests for FIB analysis were provided and performed by the Orange County Sanitation District. Special thanks to volunteers and staff from the Integrative Oceanography Division (B. Woodward, B. Boyd, D. Clark, K. Smith, D. Darnell, I. Nagy, J. Leichter, M. Omand, M. Okihiro, M. Yates, M. McKenna, S. Henderson, D. Michrokowski) for their assistance in data collection. Chapter 2, in full, has been submitted for publication in *Marine Pollution Bulletin*, 2012, Rippey, M. A.; Franks, P. J. S.; Feddersen, F.; Guza, R. T.; Moore, D. F, Elsevier Press, 2012. The dissertation author was the primary investigator and author of this paper.

### Literature Cited

- Anderson, K. L.; Whitlock, J. E.; Harwood, V. J. 2005. Persistence and differential survival of fecal indicator bacteria in subtropical waters and sediments. *Applied and Environmental Microbiology*. 71, 3041-3048.
- Boehm, A. B.; Grant, S. B.; Kim, J. H.; Mowbray, S. L.; McGee, C. D.; Clark, C. D.; Foley, D. M.; Wellman, D. E. 2002. Decadal and shorter period variability of surf zone water quality at Huntington Beach, California. *Environmental Science & Technology*. 36, 3885-3892.
- Boehm, A. B. 2003. Model of microbial transport and inactivation in the surf zone and application to field measurements of total coliform in northern Orange County, California. *Environmental Science & Technology*. 37, 5511-5517.
- Boehm, A. B.; Keymer, D. P.; Shellenbarger, G. G. 2005. An analytical model of enterococci inactivation, grazing, and transport in the surf zone of a marine beach. *Water Research*. 39, 3565-3578.
- Clark, D. B.; Feddersen, F.; Guza, R. T. 2010. Cross shore surfzone tracer dispersion in an alongshore current. *Journal of Geophysical Research*. 115, C10035-C10053.
- Curtis, T. P.; Mara, D. D.; Silva, S. 1992. Influence of pH, oxygen, and humic substances on ability of sunlight to damage fecal coliforms in waste stabilization pond water. *Applied and Environmental Microbiology*. 58, 1335-1343.
- Dufour, A. P.; Wymer, L. J. 2006. Microbes, monitoring, and human health. *Oceanography*. 19, 72-80.
- Grant, S. B.; Sanders, B. F.; Boehm, A. B.; Redman, J. A.; Kim, J. H.; Mrse, R. D.; Chu, A. K.; Gouldin, M.; McGee, C. D.; Gardiner, N. A.; Jones, B. H.; Svejksky, J.; Leipzig, G. V.; Brown, A. 2001. Generation of enterococci bacteria in a coastal saltwater marsh and its impact on surf zone water quality. *Environmental Science & Technology*. 35, 2407-2414.
- Grant, S. B.; Kim, J. H.; Jones, B. H.; Jenkins, S. A.; Wasyl, J.; Cudaback, C. 2005. Surf zone entrainment, along-shore transport, and human health implications of pollution from tidal outlets. *Journal of Geophysical Research*. 110, C10025-C10045.
- Ki, J.; Ensari, S.; Kim H. J. 2007. Solar and tidal modulations of fecal indicator bacteria in coastal waters at Huntington Beach, California. *Environmental*

*Management*. 39, 867-875.

- Kim, J. H.; Grant, S. B. 2004. Public mis-notification of coastal water quality: a probabilistic evaluation of posting errors at Huntington Beach. *Environmental Science & Technology*. 8, 2479-2504.
- Kim, J. H.; Grant, S. B.; McGee, C. D.; Sanders, B. F.; and Largier, J. L. 2004. Locating sources of surf zone pollution: a mass budget analysis of fecal indicator bacteria at Huntington Beach, California. *Environmental Science & Technology*. 38, 2626-2636.
- Krause, P.; Boyle, D. P.; Base, F. 2005. Comparison of different efficiency criteria for hydrological model assessment. *Advances in Geosciences*. 5, 89-97.
- Reniers, A. J. H. M.; MacMahan, J. H.; Thornton, E. B.; Stanton, T. P.; Henriquez, M.; Brown, J. W.; Brown, J. A.; Gallagher, E. 2009. Surf zone surface retention on a rip-channeled beach. *Journal of Geophysical Research*. 114, C10010-C10022.
- Ross, O. N.; Sharples, J. 2004. Recipe for 1-D Lagrangian particle tracking models in space-varying diffusivity. *Limnology and Oceanography: Methods*. 2, 289-302.
- Sinton, L. W.; Donnison, A. M.; Hastie, C. M. 1993. Faecal streptococci as faecal pollution indicators: a review. part 1: taxonomy and enumeration. *New Zealand Journal of Marine and Freshwater Res.* 27, 101-115.
- Sinton, L. W.; Hall, C. H.; Lynch, P. A.; Davies-Colley, R. J. 2002. Sunlight inactivation of fecal indicator bacteria and bacteriophages from waste stabilization pond effluent in fresh and saline waters. *Applied and Environmental Microbiology*. 68, 1122-1131.
- Sontek. 2004. *Sontek ADV Field Acoustic Doppler Velocimeter: Technical Documentation*. Sontek/YSI, San Diego.
- Spydell, M.; Feddersen, F.; Guza, R. T.; Schmidt, W. E. 2007. Observing surf-zone dispersion with drifters. *Journal of Physical Oceanography*. 37, 2920-2939.
- Spydell, M. S.; Feddersen, F.; Guza, R. T. 2009. Observations of drifter dispersion in the surfzone: the effect of sheared alongshore currents. *Journal of Geophysical Research*. 114, C07028-C07045.
- Tanaka, Y.; Franks, P. J. S. 2008. Vertical distributions of Japanese sardine (*Sardinops melanosticus*) eggs: a comparison of observations and a wind-forced Lagrangian mixing model. *Fisheries Oceanography*. 17, 89-100.

**Table 2.1:** Rates of FIB decay during HB06.

Station	<i>E. coli</i> Decay <sup>a</sup> (MPN s <sup>-1</sup> ) x 10 <sup>-4</sup>	<i>E. coli</i> R <sup>2</sup>	<i>Enterococcus</i> Decay <sup>a</sup> (CFU s <sup>-1</sup> ) x 10 <sup>-4</sup>	<i>Enterococcus</i> R <sup>2</sup>	<i>E. coli</i> vs <i>Ent.</i> Decay ANCOVA F-stat
<b>SAR</b>	-0.37	0.48*	-1.40	0.91**	41.66 **
<b>TM</b>	-0.69	0.50*	-1.96	0.85**	21.61 **
<b>FHM</b>	-0.11	0.80**	-2.41	0.91**	36.06 **
<b>F1</b>	-2.04	0.89**	-3.85	0.89**	19.59 **
<b>F3</b>	-2.08	0.89**	-3.32	0.81*	12.70 *
<b>F5</b>	-2.16	0.89**	-3.71	0.91**	19.64 **
<b>F7</b>	-2.29	0.87**	-4.41	0.89**	18.90 **
<b>OM</b>	-1.24	0.18	0.00	0.00	--

\* indicates significance at  $p < 0.01$

\*\* indicates significance at  $p < 0.001$

a: FIB decay rates (and R<sup>2</sup> estimates) were calculated from exponential regressions of logged FIB data vs time

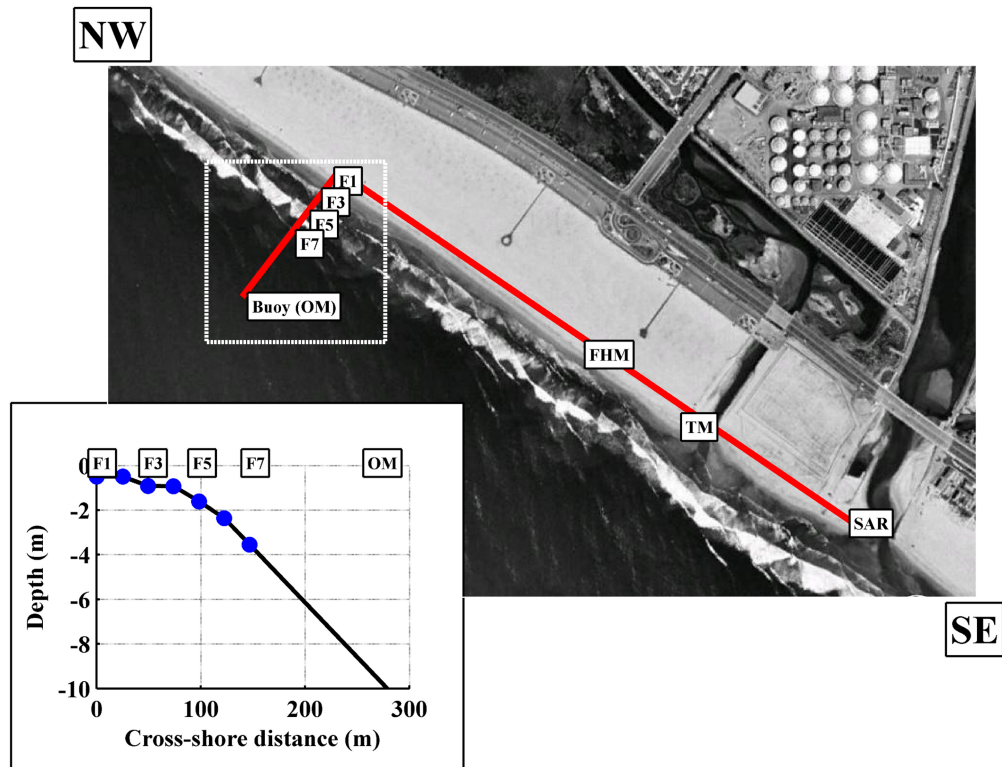


**Figure 2.1:** Schematic of the HB06 experiment. White boxes mark the location of bacterial sampling stations. Alongshore sampling sites were the Santa Ana River (SAR), the Talbert Marsh (TM), a station 500 m north of the Santa Ana River (FHM), and the first surfzone frame (F1). Cross-shore sampling sites were located at the first (F1), third (F3), fifth (F5), and seventh (F7) surfzone frames as well as an offshore buoy (OM). Depth and distance offshore of cross-shore sites are shown in the inset, where blue circles mark the location of ADV's.



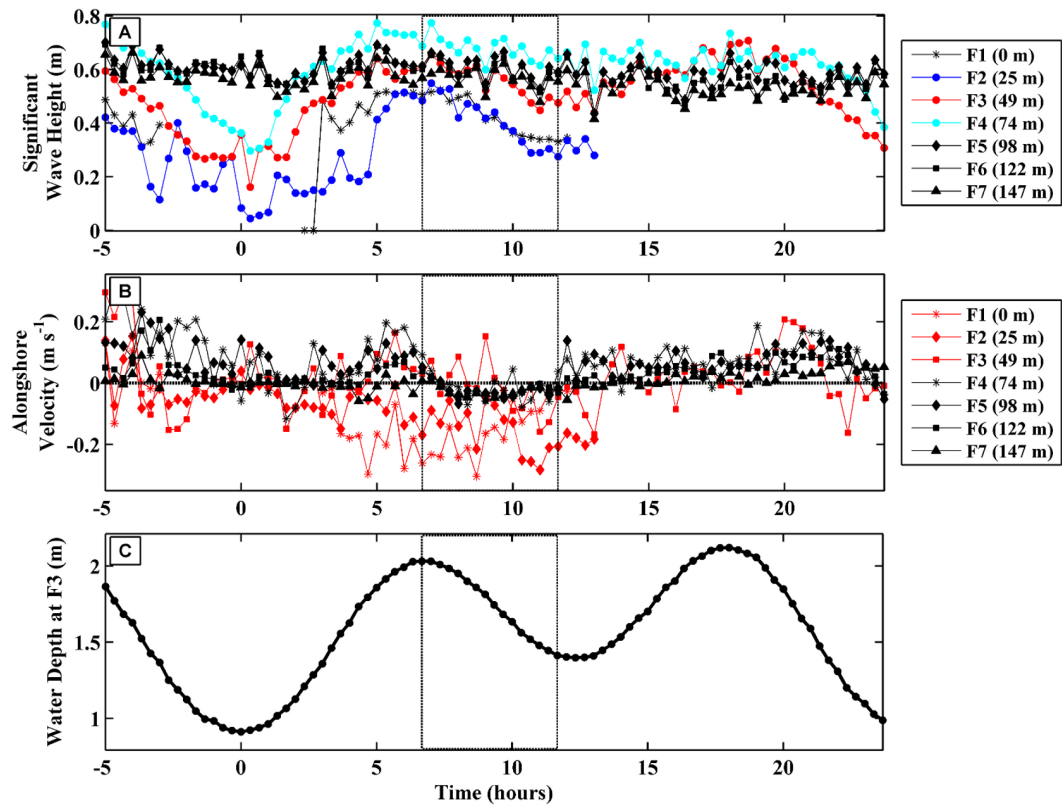


**Figure 2.2:** (A) Significant wave height and (B) 20-minute mean alongshore current (red = surfzone and black = offshore), measured at cross-shore frames F1-F7. (C) Mean water depth measured at F3 versus time (hours) from 1950 on October 15<sup>th</sup> to 2350 on October 16<sup>th</sup>. Midnight is at  $t = 0$  h. Dashed boxes indicate the 5-hr HB06 FIB study period.

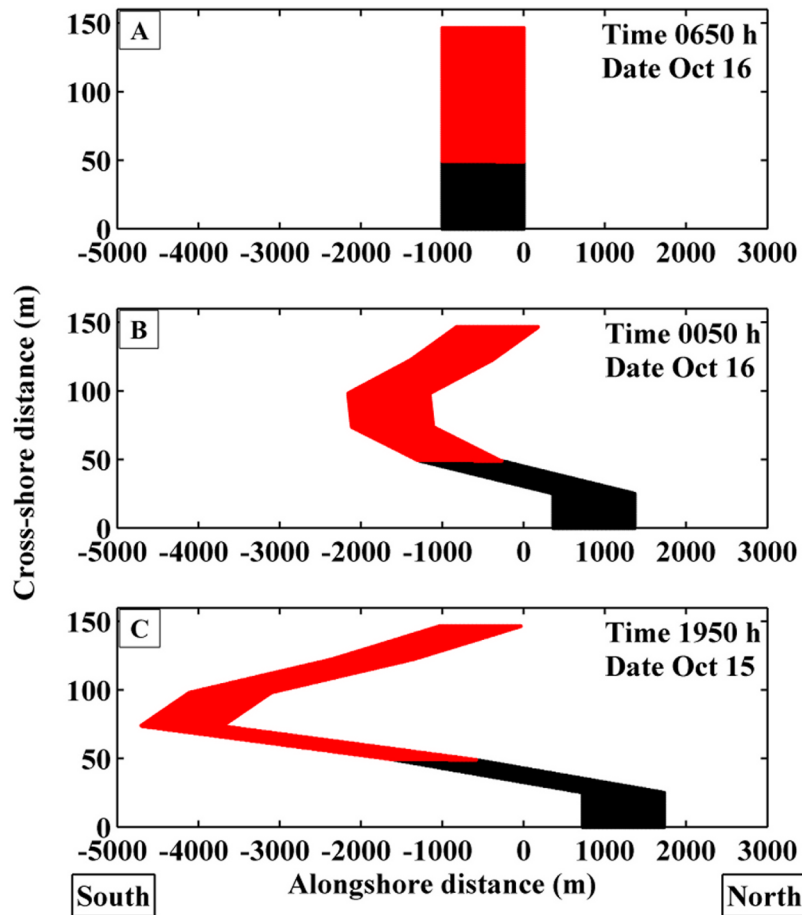


**Figure 2.3:** Along- and cross-shore locations of FIB particles initialized in a uniform rectangular patch at 0650 (A) and advected back in time using measured alongshore currents for six (B), and 11 (C) hours. Surfzone FIB particles are black and offshore FIB particles are red. Particle locations reflect cross-shore shear in the alongshore current, with surfzone FIB originating to the north and offshore FIB originating to the south. The origins of surfzone FIB appear stable around 600 – 1500 m N, while the origins of offshore FIB are time dependent (B & C).

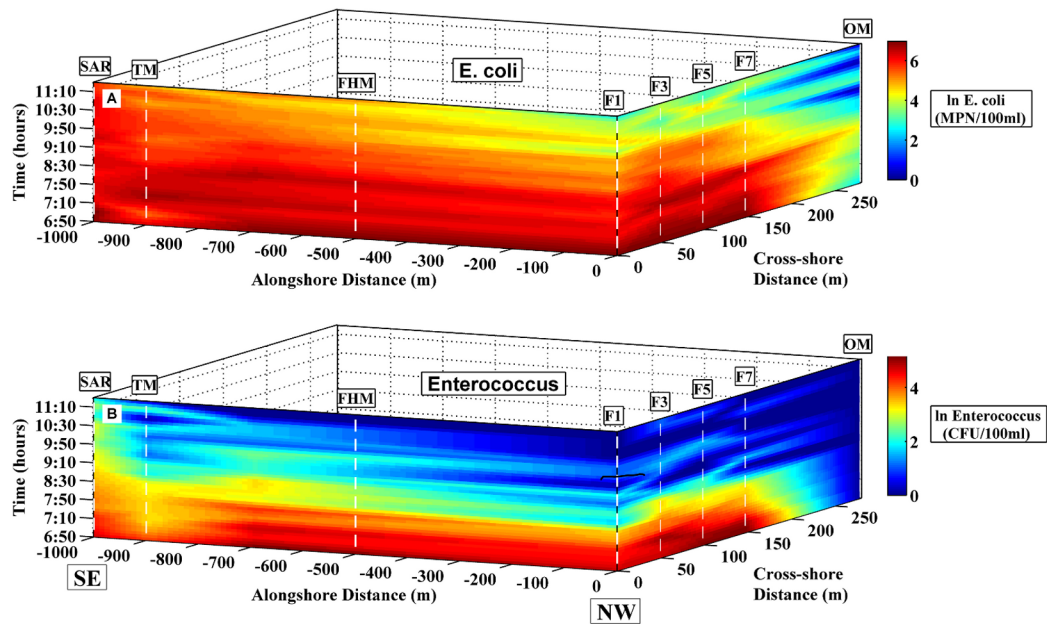


**Figure 2.4:** Contour plots of (A) *E. coli* (ln MPN 100 ml<sup>-1</sup>) & (B) *Enterococcus* (ln CFU 100 ml<sup>-1</sup>) concentrations at HB06 as a function of cross-shore distance (m), alongshore distance (m), and time (hours). Plots are oriented as though the viewer is standing on the beach, looking offshore. On the alongshore axis, the northernmost station is located at 0 m, with negative values indicating stations to the south. The location of each sampling station is shown by a dashed white line.

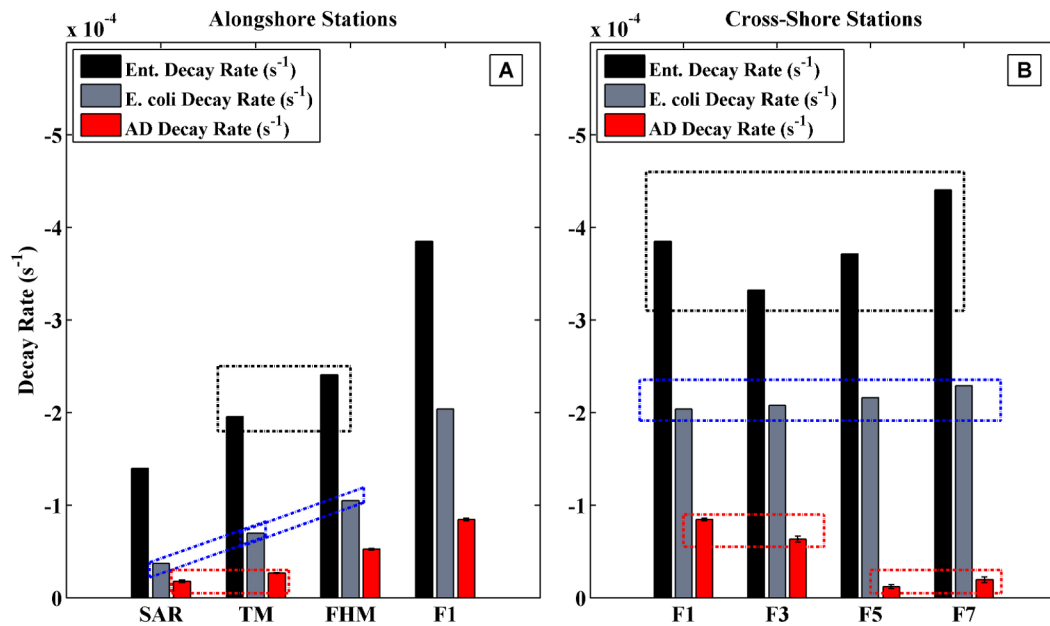


**Figure 2.5:** Bar graph of measured exponential decay rates for *Enterococcus* (black bars) and *E. coli* (gray bars), and FIB modeled using the AD model (red bars). (A) Alongshore sampling stations and (B) cross-shore sampling stations. FIB decay rates from the AD model are averages of 10 model runs, shown with standard error. Boxes link stations for *Enterococcus* (black), *E. coli* (blue) and the AD model (red) with decay rates that are not significantly different from one another ( $p < 0.05$ ). See SI Fig 1 for exponential fits to FIB data.

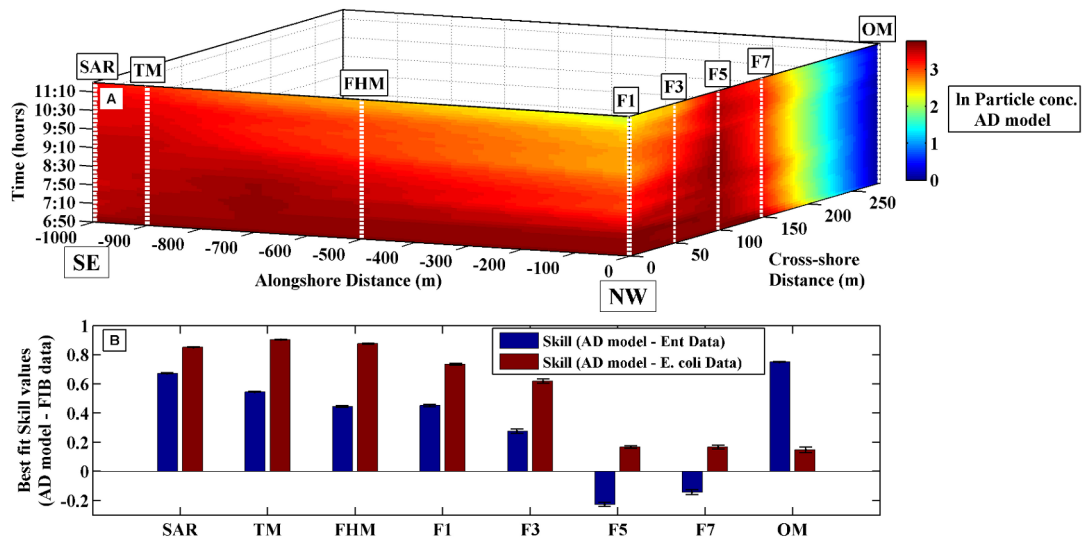


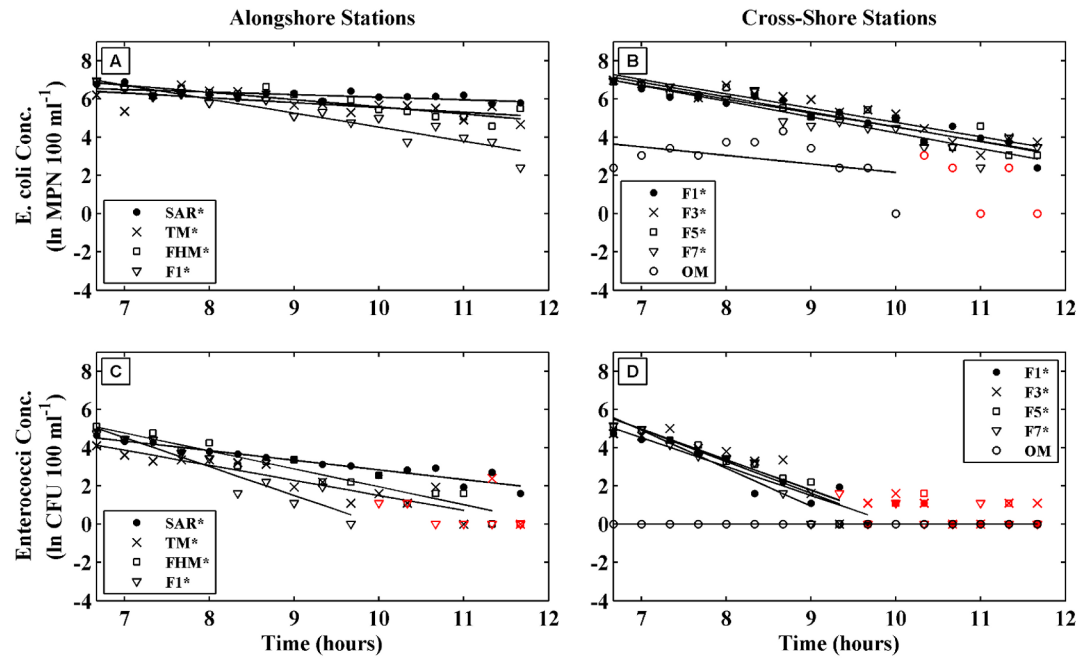
**Figure 2.6:** **A)** Contour plot of best-fit AD model particle concentrations as a function of cross-shore distance (m), alongshore distance (m), and time (hours). Axes are same as figure 3. **B)** Bar graph of station-specific skill for AD model - FIB data comparisons; *Enterococcus* (blue) and *E. coli* (red).

## Appendix 2.1: Supplementary Methods

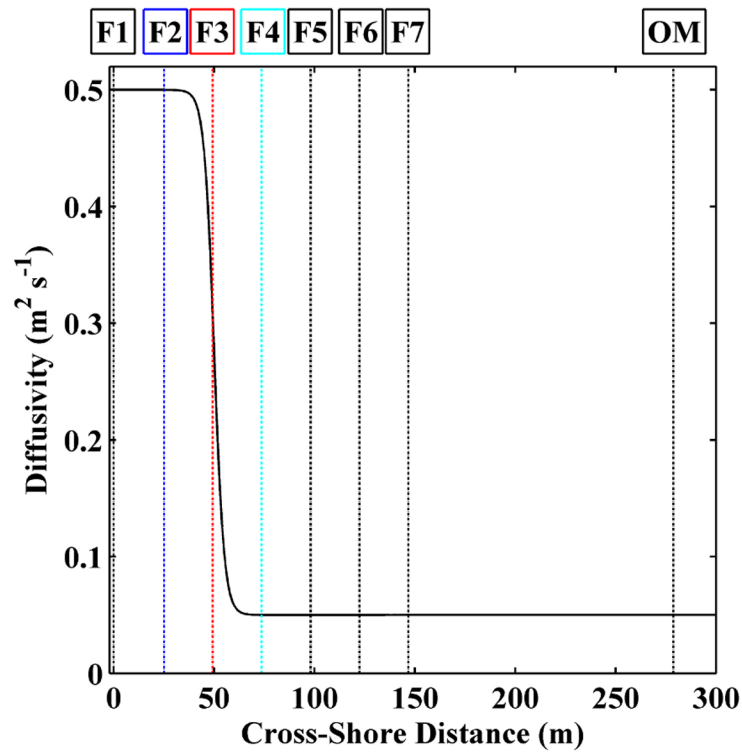
### ***AD Model: Initial Patch Shape***

The AD model developed during this study was typically initialized with a uniform rectangular patch of FIB at 0650 h. A rectangular patch was chosen because FIB concentrations at 0650 h were similar at most sampling stations. Beyond study bounds, however, a FIB patch could take on any shape. For this reason, in our exploration of northern and offshore FIB patch edges, we explored the effects of alternate (non uniform rectangular) initial patch shapes on AD model skill. These alternate patch shapes were constructed by pre-diffusing a uniform rectangular patch for 1, 2, or 5 hours, according to the diffusion formulation of the AD model. The resultant FIB patch was then used to initialize the AD model (SI Fig. 4). Similar skill was observed when the AD model was initialized with either pre-diffused or uniform rectangular initial patch shapes, although the pre-diffused FIB patch typically yielded poorer skill values (SI Fig. 5).

## Appendix 2.2: Supplementary Figures.

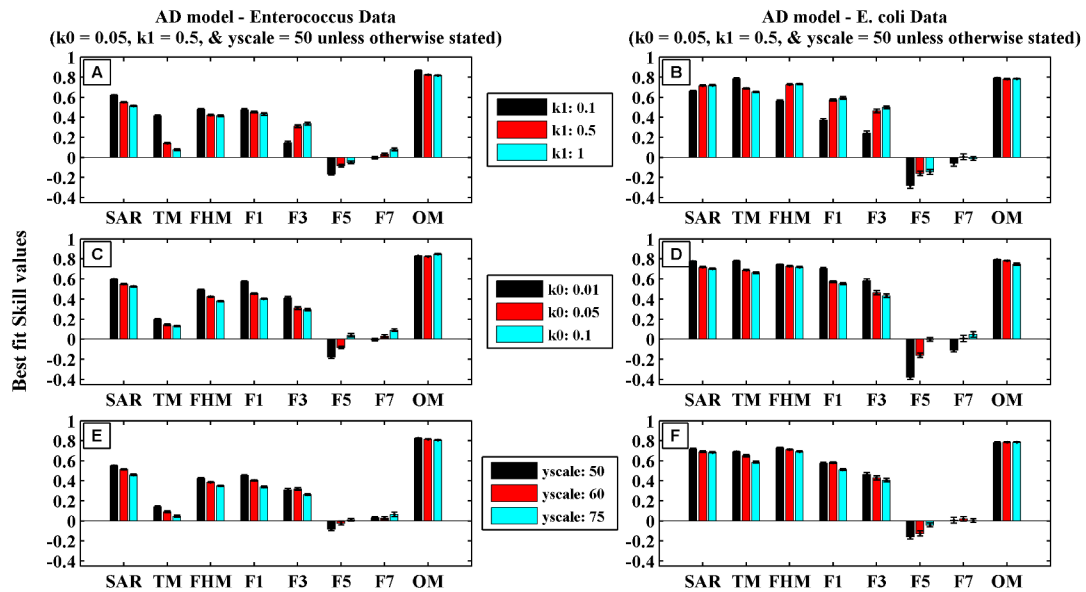


**SI Fig. 2.1:** Time series of FIB concentration (A & B = *E. coli* & B & C = *Enterococcus*) at alongshore (A & C) and cross-shore (B & D) stations. All fits are exponential. Significant fits ( $p < 0.01$ ) are denoted by asterisks (see legends). Data (red) occur after FIB concentrations at each station drop to zero. These data are near the lower detection limit of Enterolert ( $\ln 10 / 100 \text{ ml}$  for *E. coli*, or  $\ln 2 / 100 \text{ ml}$  for *Enterococcus*) and were not used for decay rate fits.

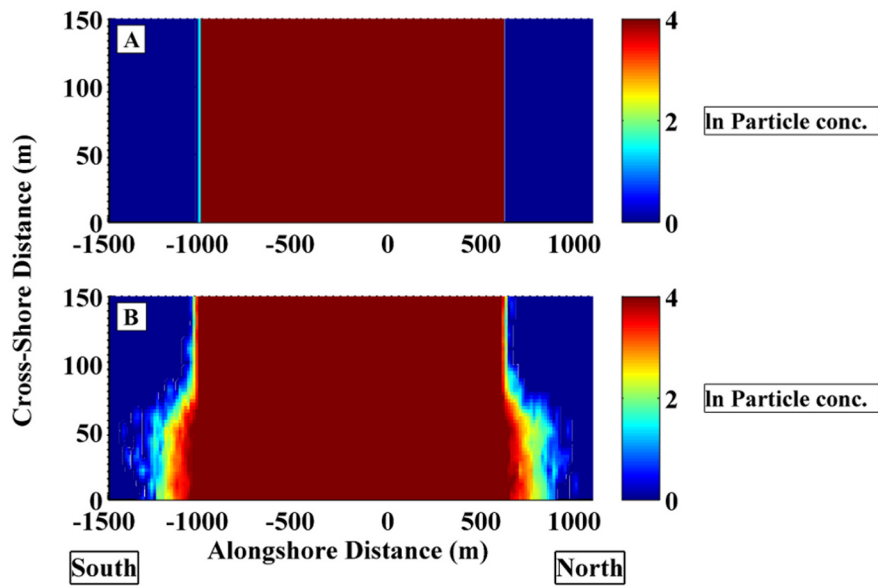


**SI Figure 2.2:** Cross-shore profile of diffusivity for the AD model. Cross-shore distance  $x$  is defined so that tripod F1 is located at 0 m. Frame location is demarcated by dashed vertical lines with text boxes. The transition between surfzone and offshore occurs at 50 m (F3), shown in red, with F2 (blue) occurring solidly within the surfzone, and F4 (cyan) just beyond it. Color scheme corresponds to Fig 2a.

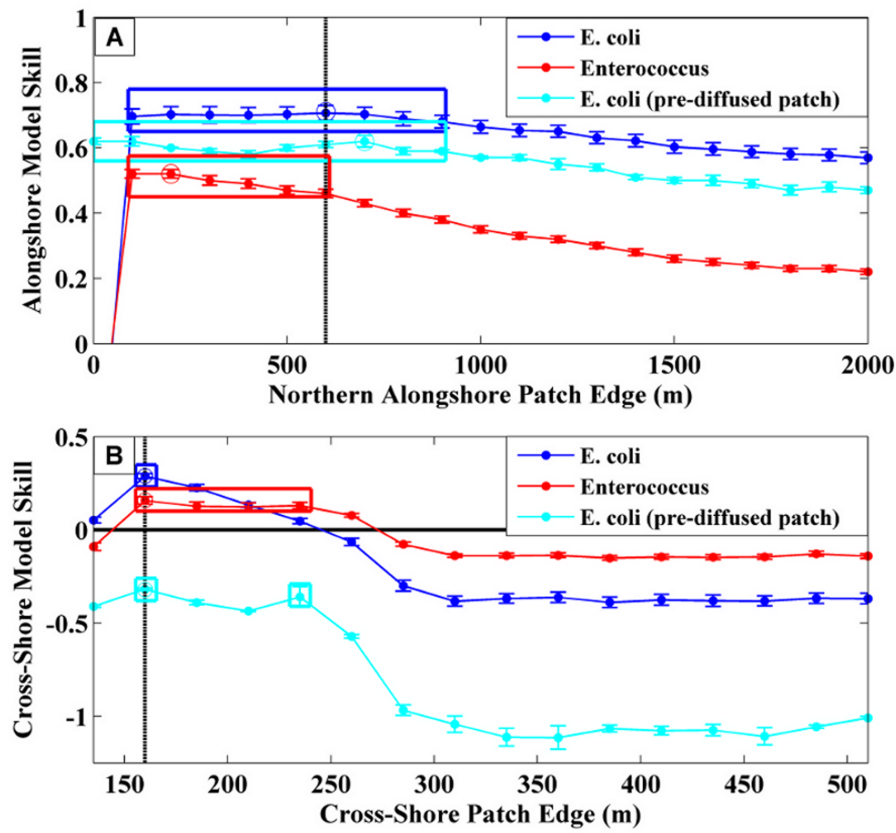




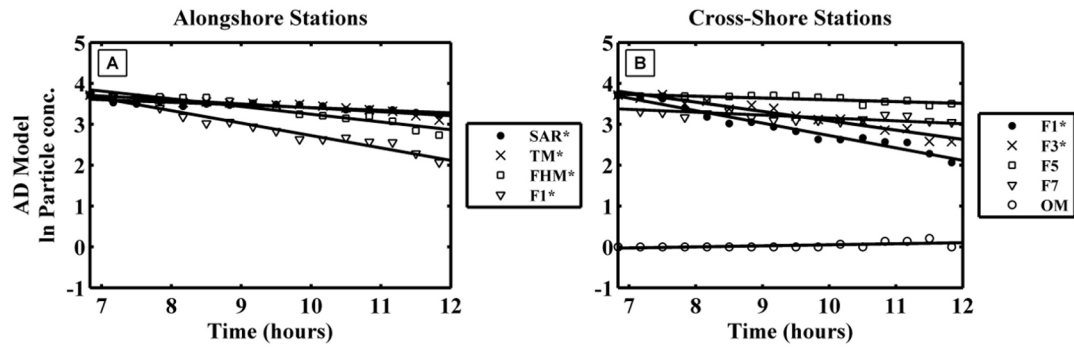
**SI Figure 2.3:** Sensitivity plots for  $\kappa_1$  (offshore diffusivity ( $\text{m}^2 \text{s}^{-1}$ )) (A, B),  $\kappa_0$  (surfzone diffusivity ( $\text{m}^2 \text{s}^{-1}$ )) (C, D), and  $y_{scale}$  (width of surfzone – offshore transition (m)) (E, F). Analyses for *Enterococcus* are on the left (A, C, E), and analyses for *E. coli* are on the right (B, D, F). For all plots the x-axis is sampling station, and the y-axis is AD model skill. The AD model is fairly insensitive to the selection of  $\kappa_1$ ,  $\kappa_0$ , and  $y_{scale}$ . For many stations, the chosen parameter set of  $\kappa_1 = 0.5 \text{ m}^2 \text{ s}^{-1}$ ,  $\kappa_0 = 0.05 \text{ m}^2 \text{ s}^{-1}$ , and  $y_{scale} = 50 \text{ m}$  produces the best fits.



**SI Figure 2.4:** Plots of log particle concentration for two different AD model initial conditions. Alongshore distance (m) is on the  $x$ -axis, and cross-shore distance (m) is on the  $y$ -axis. **A)** FIB are released in a uniform rectangular patch. **B)** FIB are released in a pre-diffused patch, where diffusion has been allowed to run for 5 hours.



**SI Figure 2.5:** Model skill versus patch extent averaged over (A) alongshore and (B) cross-shore stations. Skill is defined as in equation 4, but with the numerator summed over alongshore stations (alongshore skill) or cross-shore stations (cross-shore skill) instead of all stations (total skill). The effects of offshore patch extent on skill at alongshore stations was negligible, so skill in A (red = *Enterococcus* and blue = *E. coli*) has been averaged across all possible offshore patch extents. The effects of northern patch extent on skill at cross-shore stations was also negligible, so skill in B has been averaged across all possible northern patch extents. Best-fit patch extents for each FIB group are indicated by open circles and colored boxes indicate the +/- 0.05 skill range around the maximum skill value for each FIB group. Light blue open circles show best-fit AD model skill for *E. coli* when the AD model is initialized with a patch that has been pre-diffused for 5 hours, instead of a rectangular one with sharp edges. For both FIB groups and initial patch shapes the best offshore patch edge was 160 m offshore. The AD model was fairly insensitive to northern patch extent, but model skill was high 100-900 m N of F1 (*E. coli*) or 100-600 m N of F1 (*Enterococcus*). 600 m N was selected as the initial northern patch extent because model skill was high there for both FIB groups, and because the hindcast model (see SI Fig. 5c) supports northern patch origins between 600 and 1500 m N of F1.



**SI Figure 2.6:** Time series of best-fit AD model particle concentration at alongshore (A) and cross-shore (B) stations during HB06. All fits except F5, F7, and OM are exponential and significant at the  $p < 0.01$  level. Significant fits are denoted by asterisks (see legends).

CHAPTER 3.  
FACTORS CONTROLLING VARIABILITY IN NEARSHORE FECAL  
POLLUTION: THE EFFECTS OF MORTALITY

**Abstract**

A suite of physical-biological models was used to explore the importance of mortality and fluid dynamics in controlling concentrations of fecal indicator bacteria (FIB) at Huntington Beach, CA. An advection-diffusion (AD) model provided a baseline to assess improvements in model skill with the inclusion of mortality. Six forms of mortality were modeled. All mortality models performed better than the AD model, especially at offshore sampling stations, where model skill increased from  $< 0.18$  to  $> 0.50$  (*E. coli*) or  $< -0.14$  to  $> 0.30$  (*Enterococcus*). Models including cross-shore variable mortality rates reproduced FIB decay accurately ( $p < 0.05$ ) at more stations than models without. This finding is consistent with analyses that revealed cross-shore variability in *Enterococcus* species composition and solar dose response. No best model was identified for *Enterococcus*, as all models including cross-shore variable mortality performed similarly. The best model for *E. coli* included solar-dependent and cross-shore variable mortality.

**Introduction**

Human pathogenic bacteria are a persistent social, health, and economic problem at beaches around the world. The significant health risks and economic losses associated with beach bacterial pollution have prompted extensive monitoring

programs and concerted research efforts aimed at predicting pollution events (Boehm, 2003; Boehm et al., 2005; Sanders et al., 2005).

Multiple mechanisms have been identified that introduce pathogens and associated fecal indicator bacteria (FIB) into the surfzone, including: tidal pumping from estuaries (Grant et al., 2001) and groundwater (Boehm et al., 2004), river flow (Gersberg et al., 2006), and re-suspension from sediments (Yamahara et al., 2007). Similarly, many factors governing rates of FIB mortality in seawater have been identified, including: solar insolation (Sinton et al., 2002, 2007), temperature (Solic and Krstulovic, 1992), dissolved organic nutrients (Hartke et al., 1998), dissolved oxygen (Curtis et al., 1992), and protistan grazing (Hartke et al., 2002). What is often absent from efforts to understand nearshore FIB persistence, however, are syntheses of physical and biological dynamics. Only a handful of studies have attempted to quantify the importance of different physical or biological processes in controlling the extent and intensity of FIB pollution in the surfzone (Boehm et al., 2005; Boehm et al., 2009; Grant et al., 2001). Even fewer use models as vehicles to test hypotheses concerning the accuracy with which different combinations of mechanisms can reproduce actual FIB data (Boehm, 2003; Boehm et al., 2005, Sanders et al., 2005). Here, we present a study designed specifically for this purpose.

Data were acquired during a 5-hour field program at Huntington Beach, CA, on October 16<sup>th</sup>, 2006, that monitored nearshore FIB concentrations, waves, and currents. In this manuscript we explore the effects of biological dynamics (in this case mortality) in controlling the spatial and temporal variability of FIB at Huntington Beach. Six different mortality functions representing different FIB mortality

mechanisms were added to an individual based model of FIB that contained alongshore advection and cross-shore variable horizontal diffusion (the AD model). These new mortality models, together with additional data (*Enterococcus* species distribution and time dependent solar insolation dose observations), are used to evaluate hypotheses regarding FIB mortality mechanisms in the nearshore.

The mortality mechanisms explored in this paper are: spatially and temporally constant mortality (null hypothesis), spatially constant solar-induced mortality, stationary cross-shore mortality gradients, FIB source-dependent mortality, and two combinations of the above. Solar-induced mortality was explored because insolation is often posited as a dominant source of mortality for nearshore FIB, and has been suggested to affect FIB at Huntington Beach (Boehm et al., 2002; Sinton et al., 2002). Cross-shore mortality gradients were examined because surfzone and offshore waters often have different dynamics, which can result in cross-shore gradients of properties affecting FIB mortality, like temperature, grazers and turbidity (Omand et al., 2011; Reniers et al., 2009; Smith and Largier, 1995). Turbidity gradients, in particular, can affect the penetration of solar insolation, which, if FIB are solar sensitive, may result in cross-shore variable FIB mortality gradients that the organisms move through as they are advected and diffused across shore (Alkan et al., 1995; Whitman et al., 2004). One of our two combination mortality functions includes both cross-shore mortality gradients and solar sensitivity to depict this particular mortality mechanism. Lastly, source-specific FIB mortality was examined because FIB from different sources can have different mortality rates (Sinton et al., 2002), and multiple FIB sources have been identified at Huntington Beach (Boehm et al., 2004; Grant et al., 2001; Rippey et al.,

submitted ms.).

## Methods

### ***Sampling Design:***

Details of the HB06 FIB experiment are reported in Rippy et al. (submitted ms.). Briefly, FIB concentrations at Huntington Beach (which runs approximately north-south) were measured for five hours on October 16<sup>th</sup>, 2006, at 8 stations. Four of these stations spanned a 1000 m alongshore transect from the Santa Ana River, north. The remaining 4 stations were on a 300 m cross-shore transect starting at the northernmost alongshore station and terminating at an offshore mooring (Rippy et al., submitted ms., their Fig. 2.1). Water samples (100 ml) were collected at all stations, every 20 minutes, from 0650 to 1150 PDT. All samples were analyzed for *E. coli* (IDEXX Colilert) and *Enterococcus* (USEPA method 1600) concentrations by Orange County Sanitation District personnel.

Acoustic Doppler velocimeters (ADV's) mounted on fixed tripod frames were used to measure currents along the shoreward-most 150 m of the cross-shore transect (Rippy et al., submitted ms., their Fig. 2.1). These data were used to force alongshore currents in the 2D FIB models discussed below.

### ***Enterococcus Species Identification:***

*Enterococcus* species identification was performed to detect spatial patterns that could indicate the presence of multiple *Enterococcus* sources (potentially exhibiting differing mortality rates) in the nearshore. Species were identified at the



Orange County Public Health Laboratory using presumptive *Enterococcus* colonies grown up from water samples on mEI agar plates. Three presumptive *Enterococcus* colonies were examined per plate when colony counts allowed, corresponding to 3 colonies per water sample. Initial colony identification was performed using a Microscan Walk-Away 96 system containing Microscan Pos Combo Type 12 panels (Dade Bering Inc., West Sacramento, CA). The type 12 panel contains 27 dried biochemical tests for the identification of gram-positive bacteria. The software database for this system contains 42 gram-positive cocci, including seven species of *Enterococcus*. Additional biochemical tests were also used for identification purposes including carbohydrate fermentation in brain heart infusion broth with 1% sucrose (35 °C), a motility test using motility medium with Triphenyl Tetrazolium Chloride (30 °C), and a pigment production assay using Trypticase soy agar with 5% sheep's blood (35 °C). Final identification was determined utilizing published standard biochemical identification charts (Moore et al., 2008).

Due to the retentive nature of the surfzone (Reniers et al., 2009), special attention was paid to cross-shore variability of *Enterococcus* species distributions. All identified *Enterococcus* isolates were classified based on their collection location as either “onshore” (SAR, TM, FHM, and F1) or “offshore” (stations  $\geq$  50 m seaward of the surfzone: F5 and F7). Species composition onshore vs. offshore was compared using a Pearson chi-squared test.

#### ***Solar Insolation Studies:***

Solar insolation data were collected using a Davis Vantage Pro Plus cosine

pyranometer stationed 3.2 km inland of Huntington Beach, with a sampling frequency of once per minute (SI Fig. 3.1). This sensor was part of a weather station managed by the Golden West College Observatory. Solar radiation dosages were calculated by integrating solar insolation over the 20-minute FIB sampling interval. All statistical analyses were performed using MATLAB (Mathworks, Natick, MA).

To assess the role of solar insolation as a factor controlling temporal decay in FIB concentrations at Huntington Beach, decay rates were calculated for both *Enterococcus* and *E. coli* at each sampling station and compared to solar insolation dose. FIB decay rates were calculated as  $r = \log[N(t)/N(t-\Delta t)]/(\Delta t)$ , where  $r$  is the FIB-specific decay rate,  $N(t)$  is population at time  $t$ , and the time interval  $\Delta t$  is 20 min, the FIB sampling interval. Note that these decay rates include all processes leading to local losses of FIB, including advection, diffusion and mortality. Here, the term *decay rate* will always refer to total change in FIB concentration (from data or model outputs) with time, regardless of the processes forcing those changes. In contrast, the term *mortality rate* will be used to denote the portion of FIB decay that is due to FIB senescence alone, and not caused by advection or diffusion.

Solar penetration may be significantly decreased in the surfzone due to turbidity and bubbles (Alkan et al., 1995; Smith and Largier, 1995). To determine whether or not the relationship between solar dose and FIB decay differed in the surfzone vs. farther offshore, FIB sampling stations were divided into “onshore” and “offshore” locations (see *Enterococcus* species identification above). The solar dose/decay rate data for these sets of stations were pooled, and a regression line was fit to each set to determine onshore- and offshore solar dose-FIB decay rate

relationships.

## ***2D Individual Based FIB Models:***

### *Model Structure: AD*

Rippy et al. (submitted ms.) constructed a 2D ( $x$  = alongshore,  $y$  = cross-shore) individual-based FIB model (AD) and parameterized it based on literature values, HB06 physical measurements, and model fits to HB06 FIB data (*E. coli* and *Enterococcus*). The AD model includes alongshore advection,  $u(y,t)$ , given by the cross-shore transect of ADV's mentioned above, and horizontal diffusion ( $k_h$ ), acting both along- and across-shore. Advection and horizontal diffusion were assumed to be uniform alongshore. The local magnitude of horizontal diffusion was defined as,

$$\kappa_h = \kappa_0 + \left( \frac{\kappa_1 - \kappa_0}{2} \right) \left( 1 - \tanh \left( \frac{(y - y_0)}{y_{scale}} \right) \right) \quad (1)$$

where  $k_0$  is the background (offshore) diffusivity,  $k_1$  is the elevated surfzone diffusivity,  $y_0$  is the cross-shore midpoint of the transition between  $k_0$  and  $k_1$  (i.e., the offshore edge of the surfzone) and  $y_{scale}$  determines the width of this transition in the cross-shore. The  $k_0$ ,  $k_1$ ,  $y_0$ , and  $y_{scale}$  values used here are those that provided the best AD model fits to Huntington Beach FIB data:  $0.05 \text{ m}^2 \text{ s}^{-1}$ ,  $0.5 \text{ m}^2 \text{ s}^{-1}$ , 50 m and 5 m, respectively (Rippy et al., submitted ms.). The fit metric used to assess this, and all other model-data fits presented in this paper, was model skill (Krause et al., 2005):

$$\text{Skill} = 1 - \frac{\text{mean}(C_{obs} - C_{mod})^2}{\text{mean}(C_{obs} - \bar{C}_{obs})^2} \quad (2)$$

Here,  $C_{obs}$  is log observed FIB concentration,  $C_{mod}$  is log modeled FIB concentration, and  $\bar{C}_{obs}$  is the mean of  $\log(C_{obs})$  over all stations and times. Skill represents the degree to which variability in the data is better explained by the model than by the global space-time mean of the data. Depending on context, skill was calculated for individual stations, groups of stations, or all stations together, by changing the numerator of equation 2.

Model Initialization:

For all model formulations, 80,000 bacterial particles containing a concentration of FIB ( $C$ ) were initialized in a uniform grid extending 160 m offshore, and from the Santa Ana River to 600 m north of F1 (the northernmost sampling frame) in the alongshore. These along- and across-shore boundaries for the initial FIB patch were determined to produce the best fits between FIB data and the AD model (Rippy et al., submitted ms).

Model Structure: Mortality Models

All mortality models were of the form

$$\frac{dC}{dt} = -MC \quad (3)$$

where  $C$  is FIB concentration and  $M$  is a FIB mortality function. In the AD model,  $M$  was set to zero, and the concentration of FIB in each initial particle was fixed.  $M$  was non-zero for all mortality models. Equation (3) was solved numerically using the Euler finite-difference method. Six different functional forms of  $M$  were examined, two of which (ADC and ADI) contain only one mortality parameter ( $m$ ). The remaining four (ADS, ADG, ADSI, and ADGI) contain two mortality parameters each ( $m_0$  and  $m_1$ ), allowing FIB mortality to vary across shore.

#### One Parameter Mortality Models: ADC and ADI

In the one-parameter models FIB mortality was set either to a constant rate  $m$  (units:  $s^{-1}$ ) (ADC model) or a time-dependent rate determined by measured solar insolation  $I(t)$  scaled by maximum solar insolation  $I_{max}$  (ADI model):

$$\text{ADC model: } M = m \quad (4)$$

$$\text{ADI model: } M = \frac{mI(t)}{I_{max}} \quad (5)$$

Appropriate test ranges for the mortality parameters were selected from literature (Boehm et al., 2005; Sinton et al., 2002; Troussellier et al., 1998). Final parameter values for both models, and those described below, were those that maximized the skill between modeled and observed FIB concentrations (*E. coli* and *Enterococcus*).

Two-Parameter Mortality Models: source-specific

In all source-specific mortality models, particles initialized 0-50 m cross-shore were considered “onshore” particles and those initialized 50 -160 m cross-shore were considered “offshore” particles. Particle mortality was set according to the particle’s initial onshore or offshore location (its “source”) and was either constant (onshore =  $m_0$  and offshore =  $m_1$ ) (ADS model), or dependent on scaled solar insolation (ADSI model):

$$\text{ADS model: } M = \begin{cases} m_0 & \text{Initial Particle Location} < 50 \text{ m Cross - shore} \\ m_1 & \text{Initial Particle Location} > 50 \text{ m Cross - shore} \end{cases} \quad (6)$$

$$\text{ADSI model: } M = \begin{cases} \frac{m_0 I(t)}{I_{max}} & \text{Initial Particle Location} < 50 \text{ m Cross - shore} \\ \frac{m_1 I(t)}{I_{max}} & \text{Initial Particle Location} > 50 \text{ m Cross - shore} \end{cases} \quad (7)$$

Note that in the ADS and ADSI models, mortality rate is an intrinsic property of each particle, and tracks individual particles in a Lagrangian manner.

Two-Parameter Mortality Models: cross-shore mortality gradient

In all cross-shore gradient-dependent mortality models the mortality function  $M$  was determined either by the cross-shore location of the particle (ADG), or by the

cross-shore location of the particle and scaled solar insolation (ADGI). The cross-shore dependence of  $M$  was similar to the horizontal diffusion function used in all models (equation 1):

$$\text{ADG model: } M = m_1 + \left( \frac{m_0 - m_1}{2} \right) \left( 1 - \tanh \left( \frac{y - y_0}{y_{scale}} \right) \right) \quad (8)$$

$$\text{ADGI model: } M = \left( m_1 + \left( \frac{m_0 - m_1}{2} \right) \left( 1 - \tanh \left( \frac{y - y_0}{y_{scale}} \right) \right) \right) \left( \frac{I(t)}{I_{max}} \right) \quad (9)$$

where  $m_0$  is surfzone mortality,  $m_1$  is offshore mortality,  $y_0$  is the offshore edge of the surfzone, and  $y_{scale}$  determines the cross-shore scale of the surfzone/offshore transition. Values for  $y_0$  and  $y_{scale}$  were 50 m and 5 m, respectively, the same values used to parameterize diffusivity (equation 1). Note that in the ADG and ADGI models, mortality is not an intrinsic property of a given particle (as in the ADS and ADSI models). Instead, particles move through stationary cross-shore mortality gradients and take on different mortality rates based on their cross-shore location within those gradients.

## **Results and Discussion:**

### ***Spatial Patterns in Enterococcus Species Distribution:***

All presumptive *Enterococcus* isolates were found to come from one of nine different groups. Five of these groups were common fecal (*E. faecalis*, *E. faecium*, *E.*

*hirae*) and plant-associated (*E. casseliflavus*, *E. mundtii*) *Enterococcus* species, and one group contained rare *Enterococcus* biotypes (“other” *Enterococcus*). Three additional non-enterococcal groups were also isolated. These organisms grow and produce enterococcus-like reactions on mEI agar (blue halo) but are not *Enterococcus*. These organisms were *Streptococcus bovis*, found in ruminant guts, *Aerococcus viridans*, and a group of unidentified non-enterococcal organisms collectively called the “not *Enterococcus*” group. During HB06, *E. casseliflavus* (~32%) was the dominant *Enterococcus* species observed, while *E. faecalis* (~22%) and *E. faecium* (~15%) were also common (SI Fig. 3.2). The dominance of *E. casseliflavus* during HB06 is notable, as *E. casseliflavus* is a plant- rather than fecal-associated species. Its dominance in the surfzone at Huntington Beach, and other nearby beaches (Ferguson et al., 2005, Moore et al., 2008), suggests that the use of total *Enterococcus* counts without subsequent species identification may lead to spurious identification of surfzone fecal pollution.

Statistically significant differences were observed in the *Enterococcus* species composition onshore vs. offshore (Chi-square p-value < 0.01). Onshore, *E. casseliflavus*, *E. faecalis* and *E. faecium* all occurred at high percentages (>17% each), while offshore, concentrations of *E. faecium* were only ~8%, reducing it from a major (onshore) to a minor (offshore) constituent. Furthermore, the percentage of *E. mundtii* was much higher offshore than onshore (14 vs. 7 %), and *E. hirae*, *A. viridans*, rare *Enterococcus* biotypes, and nonenterococcal organisms were more prevalent offshore (Fig. 3.1). The differences in *Enterococcus* species composition across shore are consistent with the results of the hindcast model (Rippy et al., submitted ms., their Fig.



2.3), which identified two sources of *Enterococcus* (a northern onshore source and a southern offshore source) at Huntington Beach. These results also lend credence to the source-specific mortality formulations in the ADS and ADSI models, which parameterize the mortality of onshore and offshore FIB differently based on the assumption that different FIB sources can have different exposure histories or species compositions, and thus different mortality rates (Sinton et al., 2002).

***Solar Insolation vs. Decay:***

October 16<sup>th</sup>, 2006, was partially cloudy with maximum solar insolation levels of  $445 \text{ J m}^{-2}\text{s}^{-1}$  measured at 13:00 (SI Fig. 3.1). No significant relationship was detected between solar insolation dose ( $\text{J m}^{-2}$ , integrated over the 20 min sampling interval) and *E. coli* decay rate at any station over the study period. Measured *Enterococcus* decay rates, however, increased significantly with solar insolation dose, but only at offshore stations (50-150 m offshore) (Fig. 3.2).

The general lack of correlation between solar insolation dose and FIB decay (especially for *E. coli*) was unexpected, as prior research has indicated a clear relationship between sunlight and FIB mortality in seawater (Boehm et al., 2005; Sinton et al., 2002; Troussellier et al., 1998). It is possible, however, that solar insolation did contribute to FIB decay at Huntington Beach, and that detection of this effect was obscured by the contribution of physical dilution (via advection and diffusion) to decay (Rippy et al., submitted ms.).

The significant correlation found between solar insolation dose and FIB decay for offshore enterococci (Fig. 3.2) supports the role of solar insolation in regulating

*Enterococcus* mortality seaward of the surfzone. This finding motivates testing insolation-dependent mortality models for this FIB group, particularly those that allow the relationship between solar insolation dose and FIB decay to vary across shore (ADSI and ADGI models).

### ***Mortality Models: Best-Fit Parameter Values***

All mortality models were sensitive to the selection of mortality parameters:  $m$  for the one-parameter models (ADC & ADI) and  $m_0$  and  $m_1$  (surfzone and offshore mortality) for the two-parameter models (ADS, ADSI, ADG & ADGI) (SI Figs. 3.3-3.6). For all two-parameter mortality models, skill was more sensitive to changes in the offshore mortality parameter than the surfzone mortality parameter (SI Fig. 3.5; SI Fig. 3.6). This indicates that mortality may be a dominant processes contributing to FIB decay offshore, where the influences of advection and diffusion are weaker (Rippy et al., submitted ms).

Mortality parameters for *Enterococcus* were larger overall than those for *E. coli* for every model (Table 3.1). This is consistent with the slower overall decay observed for *E. coli* during the HB06 study (Rippy et al., submitted ms). For the ADS, ADSI, ADG, and ADGI models, the offshore mortality parameter ( $m_1$ ) was always higher than the surfzone mortality parameter ( $m_0$ ) for both FIB groups (Table 3.1), indicating that cross-shore variable FIB mortality is needed to accurately reproduce observed FIB concentrations.

Best-fit mortality values for *E. coli* (all models) corresponded roughly to values reported for *E. coli* mortality in seawater ( $1.3 \times 10^{-6} - 8.1 \times 10^{-4} \text{ s}^{-1}$ ) (Sinton et

al., 2007; Troussellier et al., 1998) (Table 3.1). For all two-parameter *E. coli* models, offshore mortality rates were at the lower edge of reported mortality rate ranges, and surfzone mortality rates were at the upper edge (Sinton et al., 2007; Troussellier et al., 1998) (Table 3.1). Best-fit mortality values for *Enterococcus* (ADC, ADI, ADS & ADG) also corresponded roughly to reported *Enterococcus* mortality rates ( $4.4 \times 10^{-5}$  -  $4.7 \times 10^{-4} \text{ s}^{-1}$ ) (Boehm et al., 2005) (Table 3.1). Notably, maximum offshore *Enterococcus* mortality values for the ADSI and ADGI models (range:  $7.6 \times 10^{-5}$  -  $2 \times 10^{-3}$ ) exceeded reported rates (Boehm et al., 2005) (Table 3.1).

***Best-Fit Model-Data Comparisons: Physical and Physical-Mortality models compared***

The mortality models performed better than the AD model in reproducing FIB concentrations during HB06. The superior performance of the mortality models is most notable at offshore stations F5 and F7, where AD modeled FIB concentrations were too high (Fig. 3.3; Fig. 3.4). Including mortality significantly improved model skill at these offshore stations, with skill estimates increasing from  $< 0.05$  (AD model) to  $> 0.37$  (Mortality models) for both FIB groups (Fig. 3.5). Model skill also improved at surfzone stations, but these improvements were smaller in magnitude (Fig. 3.5). This underscores the importance of mortality as a factor contributing to FIB decay in offshore waters.

***Best-Fit Model-Data Comparisons: FIB Mortality Mechanisms***

Although all forms of mortality improved model predictions, FIB

concentrations (Fig. 3.3; Fig. 3.4) and station-specific decay rates (Fig. 3.6) were most accurately reproduced by mortality functions with cross-shore dependence – either onshore/offshore sources (ADS, ADSI) or a persistent cross-shore mortality gradient (ADG, ADGI). This finding is consistent with the *Enterococcus* speciation and solar insolation dose results discussed above, which revealed differences in onshore vs. offshore *Enterococcus* species composition and response to solar insolation dose (Fig. 3.1; Fig. 3.2).

It is notable, given the emphasis on solar-induced mortality in FIB literature (Boehm et al., 2005; Sinton et al., 2002; Troussellier et al., 1998), that mortality functions with cross-shore variability in mortality rates had higher skill than those including only time-dependent solar mortality. This is not to say that coastal FIB decay is not a function of solar insolation dose; the insolation-dependent ADGI and ADSI models performed extremely well for both *E. coli* and *Enterococcus* (Fig. 3.5; Fig. 3.6). ADI performance, however, was significantly worse than either ADG or ADS, suggesting that the importance of time-dependent solar dose was secondary to the importance of cross-shore variability of mortality (Fig. 3.5; Fig. 3.6).

No best-fit mortality model was identified for *Enterococcus* – all models with cross-shore variable FIB mortality (ADS, ADSI, ADG, and ADGI) had similar skill and predicted *Enterococcus* decay rates accurately ( $p < 0.05$ ) at the same number of sampling stations (6 of 7) (Fig. 3.5; Fig. 3.6). For *E. coli*, cross-shore variable mortality models also had similar skill (Fig. 3.5). That said, the ADGI model (including both cross-shore variable and solar-induced mortality) performed slightly better than the other three, reproducing *E. coli* decay rates accurately ( $p < 0.05$ ) at the

greatest number of sampling stations (6 of 7) (Fig. 3.6).

The superior performance of cross-shore variable mortality models for both FIB groups at Huntington Beach highlights the need for further research regarding the spatial variability of FIB mortality in nearshore systems. Our data were insufficient to distinguish among the various cross-shore variable FIB mortality hypotheses we explored, and thus the mechanisms underlying this variability remain unknown. Given the superior performance of the ADGI model for *E. coli*, however, special attention should be paid to processes that cause cross-shore gradients of insolation, such as turbidity. Field-based microcosm experiments could be useful in this regard.

Based on the exponential FIB decay observed during our study our models focused on extra-enteric FIB mortality. FIB, however, have been reported to grow and/or undergo inactivation/repair cycles in aquatic systems (Boehm et al., 2009; Surbeck et al., 2010). For this reason our estimated mortality rates are better interpreted as net rates, including some unknown combination of mortality, inactivation, and growth. *E. coli*, for example, has been shown to exhibit elevated growth rates in highly turbulent flows (Al-Homoud and Hondzo, 2008). Thus one interpretation of our cross-shore variable net mortality rates for *E. coli* (low in the surfzone and higher offshore) could be a relatively constant baseline mortality rate with some level of additional growth (lower net mortality) in the surfzone. Similarly, it is possible that some portion of the FIB loss we attribute to mortality (surfzone or offshore) is instead inactivation due to photodamage, and that some of these damaged FIB could undergo repair and recover. This would make actual FIB mortality rates lower than those estimated from our models (Boehm et al., 2009). More extensive

experiments, monitoring a broader range of biological parameters, are required to piece together the processes contributing to the patterns in net FIB mortality revealed by our Huntington Beach FIB models.

Although observed FIB decay has often been attributed to mortality alone, and can likewise be attributed to physical processes alone (e.g., the AD model), we have shown the importance of including both mortality and advection/diffusion in models predicting nearshore FIB concentrations. Furthermore, our study shows the importance of understanding the functional form of mortality, emphasizing that mortality can vary in both space and time. Because of this, accurate predictive FIB models are likely to be location-specific, with mortality functions reflecting dominant local FIB sources and/or spatial gradients in bacterial stressors. Our success at modeling short-term changes in FIB concentrations at Huntington Beach is encouraging, and further study (more extensive data sets, spanning longer time periods and spatial extents) is warranted to explore the effectiveness of individual based models for long-term FIB prediction.

### **Acknowledgements**

This work was supported by NSF, ONR, CA SeaGrant, the California Coastal Conservancy, the California Department of Boating and Waterways, and NOAA. Tests for FIB analysis were provided and performed by the Orange County Sanitation District and the Orange County Public Health Laboratory. Special thanks to volunteers from the Integrative Oceanography Division (B. Woodward, B. Boyd, D. Clark, K. Smith, D. Darnell, I. Nagy, J. Leichter, M. Omand, M. Yates, M. McKenna,

S. Henderson, D. Michrokowski) for their assistance in data collection. Chapter 3, in full, has been submitted to Marine Pollution Bulletin, 2012, Rippy, M. A.; Franks, P. J. S.; Feddersen, F.; Guza, R. T.; Moore, D. F, Elsevier Press, 2012. The dissertation author was the primary investigator and author of this paper.

### Literature Cited

- Al-Homoud, A.; Hondzo, M. 2008. Enhanced uptake of dissolved oxygen and glucose by *Escherichia coli* in a turbulent flow. *Applied Microbiology and Biotechnology* 79, 643-655.
- Alkan, U.; Elliot, D. J.; Evison, L. M. 1995. Survival of enteric bacteria in relation to simulated solar radiation and other environmental factors in marine waters. *Water Research*. 29, 2071-2081.
- Boehm, A. B.; Grant, S. B.; Kim, J. H.; Mowbray, S. L.; McGee, C. D.; Clark, C. D.; Foley, D. M.; Wellman, D. E. 2002. Decadal and shorter period variability of surf zone water quality at Huntington Beach, California. *Environmental Science & Technology*. 36, 3885-3892.
- Boehm, A. B. 2003. Model of microbial transport and inactivation in the surf zone and application to field measurements of total coliform in northern Orange County, California. *Environmental Science & Technology*. 37, 5511-5517.
- Boehm, A. B.; Shellenbarger, G. G.; Paytan, A. 2004. Groundwater discharge: potential association with fecal indicator bacteria in the surf zone. *Environmental Science & Technology*. 38, 3558-3566.
- Boehm, A. B.; Keymer, D. P.; Shellenbarger, G. G. 2005. An analytical model of enterococci inactivation, grazing, and transport in the surf zone of a marine beach. *Water Research*. 39, 3565-3578.
- Boehm, A.; Yamahara, K.; Love, D. C.; Peterson, B. M.; McNeill, K.; Nelson, K. L. 2009. Covariation and photoinactivation of traditional and novel indicator organisms and human viruses at a sewage-impacted marine beach. *Environmental Science & Technology*. 43, 8046-8052.
- Curtis, T. P.; Mara, D. D.; Silva, S. 1992. Influence of pH, oxygen, and humic substances on ability of sunlight to damage fecal coliforms in waste stabilization pond water. *Applied and Environmental Microbiology*. 58, 1335-1343.
- Ferguson, D. M.; Moore, D. F.; Getrich, M. A.; Zhouandai, M. H. 2005. Enumeration and speciation of *Enterococci* found in marine and intertidal sediments and coastal water in southern California. *Journal of Applied Microbiology*. 99, 598-608.
- Gersberg, R. M.; Rose, A. M.; Robles-Sikisaka, R.; Dhar, A. K. 2006. Quantitative detection of hepatitis A virus and enteroviruses near the United States-Mexico



- border and correlation with levels of fecal indicator bacteria. *Applied and Environmental Microbiology*. 72, 7438-7444.
- Grant, S. B.; Sanders, B. F.; Boehm, A. B.; Redman, J. A.; Kim, J. H.; Mrse, R. D.; Chu, A. K.; Gouldin, M.; McGee, C. D.; Gardiner, N. A.; Jones, B. H.; Svejksky, J.; Leipzig, G. V.; Brown, A. 2001. Generation of *Enterococci* bacteria in a coastal saltwater marsh and its impact on surf zone water quality. *Environmental Science & Technology*. 35, 2407-2414.
- Hartke, A.; Giard, J.; Laplace, J.; Auffray, Y. 1998. Survival of *Enterococcus faecalis* in an oligotrophic microcosm: changes in morphology, development of general stress resistance, and analysis of protein synthesis. *Applied and Environmental Microbiology*. 64, 4238-4245.
- Hartke, A.; Lemarinier, S.; Pichereau, V.; Auffray, Y. 2002. Survival of *Enterococcus faecalis* in seawater microcosms is limited in the presence of bacterivorous zooflagellates. *Current Microbiology*. 44, 329-335.
- Krause, P.; Boyle, D. P.; Base, F. 2005. Comparison of different efficiency criteria for hydrological model assessment. *Advances in Geosciences*. 5, 89-97.
- Moore, D. F.; Guzman, J. A.; McGee, C. 2008. Species distribution and antimicrobial resistance of *Enterococci* isolated from surface and ocean water. *Journal of Applied Microbiology*. 105, 1017-1025.
- Omand, M. M.; Leichter, J. J.; Franks, P. J. S.; Guza, R. T.; Lucas, A. J.; Feddersen, F. 2011. Physical and biological processes underlying the sudden surface appearance of a red tide in the nearshore. *Limnology and Oceanography*. 56, 787-801.
- Reniers, A. J. H. M.; MacMahan, J. H.; Thornton, E. B.; Stanton, T. P.; Henriquez, M.; Brown, J. W.; Brown, J. A.; Gallagher, E. 2009. Surf zone surface retention on a rip-channeled beach. *Journal of Geophysical Research*. 114, C10010-C10022.
- Sanders, B. F.; Arega, F.; Sutula, M. 2005. Modeling the dry-weather tidal cycling of fecal indicator bacteria in surface waters of an intertidal wetland. *Water Research*. 39, 3394-3408.
- Sinton, L. W.; Hall, C. H.; Lynch, P. A.; Davies-Colley, R. J. 2002. Sunlight inactivation of fecal indicator bacteria and bacteriophages from waste stabilization pond effluent in fresh and saline waters. *Applied and Environmental Microbiology*. 68, 1122-1131.
- Sinton, L.; Hall, C.; Braithwaite, R. 2007. Sunlight inactivation of *Campylobacter*

- jejuni* and *Salmonella enterica*, compared with *Escherichia coli*, in seawater and river water. *Journal of Water and Health*. 5, 357-365.
- Smith, J. A.; Largier, L. 1995. Observations of nearshore circulation: rip currents. *Journal of Geophysical Research*. 100, C10967-C10975.
- Solic, M.; Krstulovic, N. 1992. Separate and combined effects of solar radiation, temperature, salinity, and pH in the survival of fecal coliforms in seawater. *Marine Pollution Bulletin*. 24, 411-416.
- Surbeck, C. Q.; Jiang, S. C. Grant, S. B. 2010. Ecological control of fecal indicator bacteria in an urban stream. *Environmental Science & Technology*. 44, 631-637.
- Troussellier, M.; Bonnefont, J.; Courties, C.; Derrien, A.; Dupray, E.; Gauthier, M.; Gourmelon, M.; Joux, F.; Lebaron, P.; Martin, Y.; Pommepuy, M. 1998. Responses of enteric bacteria to environmental stresses in seawater. *Oceanologica Acta*. 21, 965-981.
- Whitman, R. L.; Nevers, M. B.; Korinek, G. C.; Byappanahalli, M. N. 2004. Solar and temporal effects on *Escherichia coli* concentration at a Lake Michigan swimming beach. *Applied and Environmental Microbiology*. 70, 4276-4285.
- Yamahara, K. M.; Layton, B. A.; Santoro, A. E.; Boehm, A. B. 2007. Beach sands along the California coast are diffuse sources of fecal bacteria to coastal waters. *Environmental Science & Technology*. 41, 4515-4521.

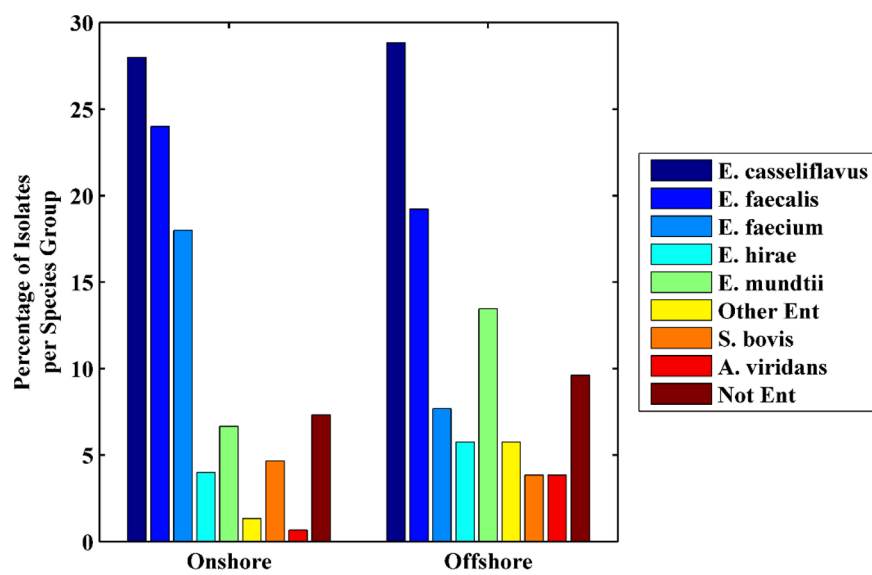
**Table 3.1:** Best-fit mortality parameters for FIB models

<i>E. coli</i> Models	Model Formulation									
	Mortality Param. (s <sup>-1</sup> )	AD	ADC	ADI	ADS	ADG	ADSI	ADGI		
1 parameter models	$m$	--	$7.5 \times 10^{-5}$	$1.2 \times 10^{-4}$	--	--	--	--	--	--
	range of $m^*$	--	--	$6.1 \times 10^{-6} - 1.2 \times 10^{-4}$	--	--	--	--	--	--
2 parameter models	$m_0^a$	--	--	--	$1.0 \times 10^{-6}$	$1.0 \times 10^{-6}$	$1.0 \times 10^{-6}$	$1.0 \times 10^{-6}$	$1.0 \times 10^{-6}$	$1.0 \times 10^{-6}$
	range of $m_0^*$	--	--	--	--	--	--	$5.1 \times 10^{-8} - 1.0 \times 10^{-6}$	$5.1 \times 10^{-8} - 1.0 \times 10^{-6}$	$5.1 \times 10^{-8} - 1.0 \times 10^{-6}$
	$m_I^b$	--	--	--	$2.0 \times 10^{-4}$	$2.0 \times 10^{-4}$	$4.0 \times 10^{-4}$	$4.0 \times 10^{-4}$	$4.0 \times 10^{-4}$	$4.0 \times 10^{-4}$
	range of $m_I^*$	--	--	--	--	--	--	$2.0 \times 10^{-5} - 4.0 \times 10^{-4}$	$2.0 \times 10^{-5} - 4.0 \times 10^{-4}$	$2.0 \times 10^{-5} - 4.0 \times 10^{-4}$
<i>Enterococcus</i> Models										
Model Formulation										
Mortality Param. (s <sup>-1</sup> )	AD	ADC	ADI	ADS	ADG	ADSI	ADGI			
1 parameter models	$m$	--	$1.0 \times 10^{-4}$	$2.0 \times 10^{-4}$	--	--	--	--	--	--
	range of $m^*$	--	--	$1.0 \times 10^{-5} - 2.0 \times 10^{-4}$	--	--	--	--	--	--
2 parameter models	$m_0^a$	--	--	--	$1.6 \times 10^{-4}$	$1.0 \times 10^{-4}$	$2.5 \times 10^{-4}$	$2.5 \times 10^{-4}$	$2.5 \times 10^{-4}$	$2.0 \times 10^{-4}$
	range of $m_0^*$	--	--	--	--	--	$1.3 \times 10^{-5} - 2.5 \times 10^{-4}$	$1.3 \times 10^{-5} - 2.5 \times 10^{-4}$	$1.0 \times 10^{-5} - 2.0 \times 10^{-4}$	$1.0 \times 10^{-5} - 2.0 \times 10^{-4}$
	$m_I^b$	--	--	--	$4.0 \times 10^{-4}$	$4.0 \times 10^{-4}$	$2.0 \times 10^{-3}$	$2.0 \times 10^{-3}$	$2.0 \times 10^{-3}$	$1.5 \times 10^{-3}$
	range of $m_I^*$	--	--	--	--	--	$1.0 \times 10^{-4} - 2.0 \times 10^{-3}$	$1.0 \times 10^{-4} - 2.0 \times 10^{-3}$	$7.6 \times 10^{-5} - 1.5 \times 10^{-3}$	$7.6 \times 10^{-5} - 1.5 \times 10^{-3}$

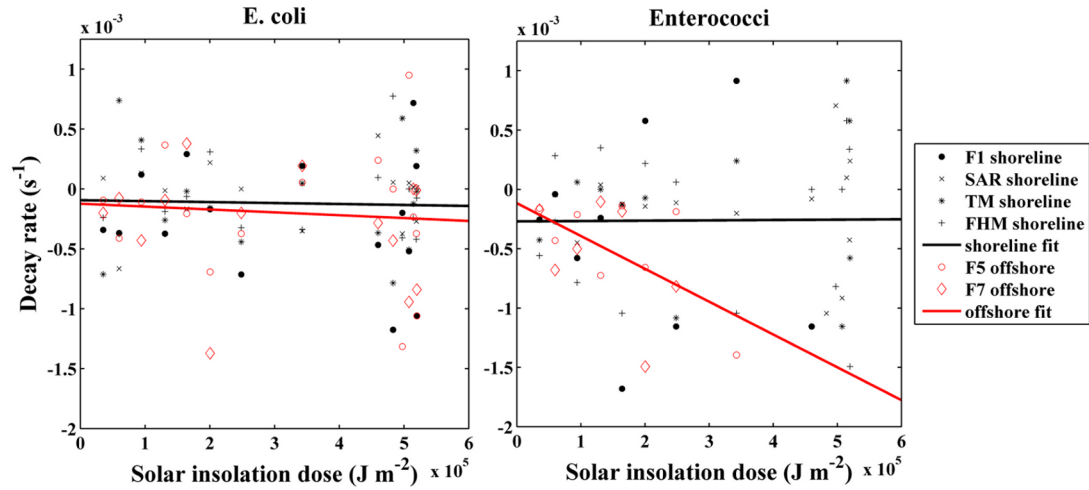
\*: mortality ranges are only applicable for models where mortality is not constant in time (ADI, ADSI, & ADGI)

a:  $m_0$  is the surfzone mortality parameter

b:  $m_I$  is the offshore mortality parameter

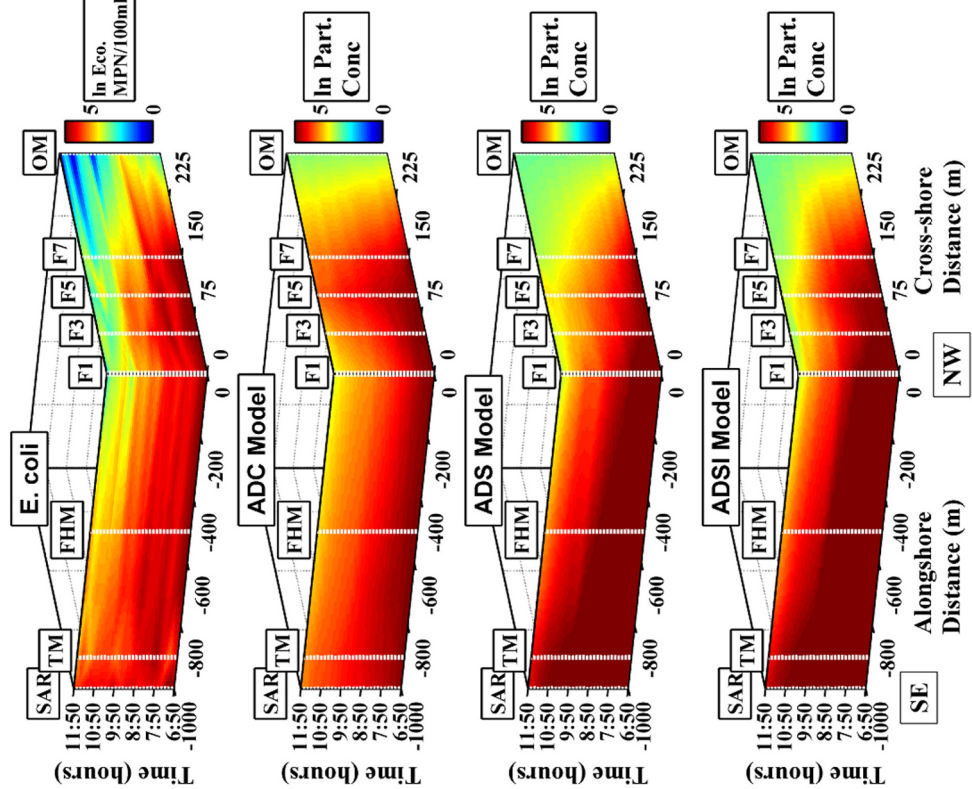
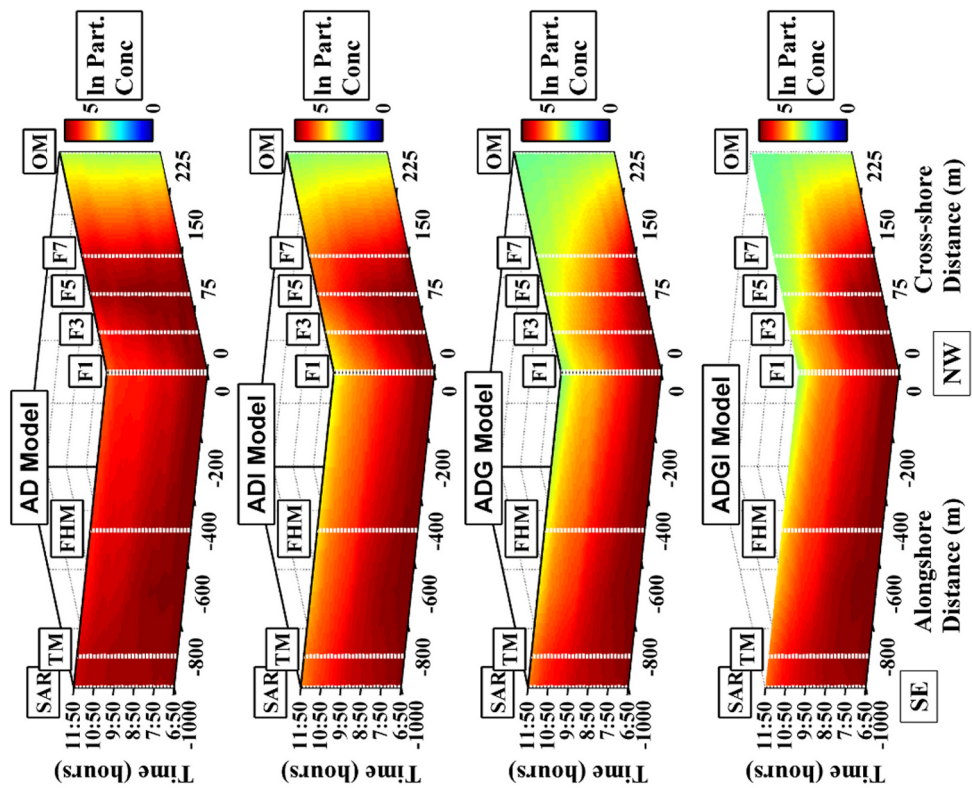


**Figure 3.1:** Species composition of onshore (SAR, TM, FHM, and F1) vs. offshore (F5 and F7) HB06 *Enterococcus* isolates. Note that the percentage of *E. faecium* exceeds that of *E. mundtii* at onshore, but not offshore, stations.



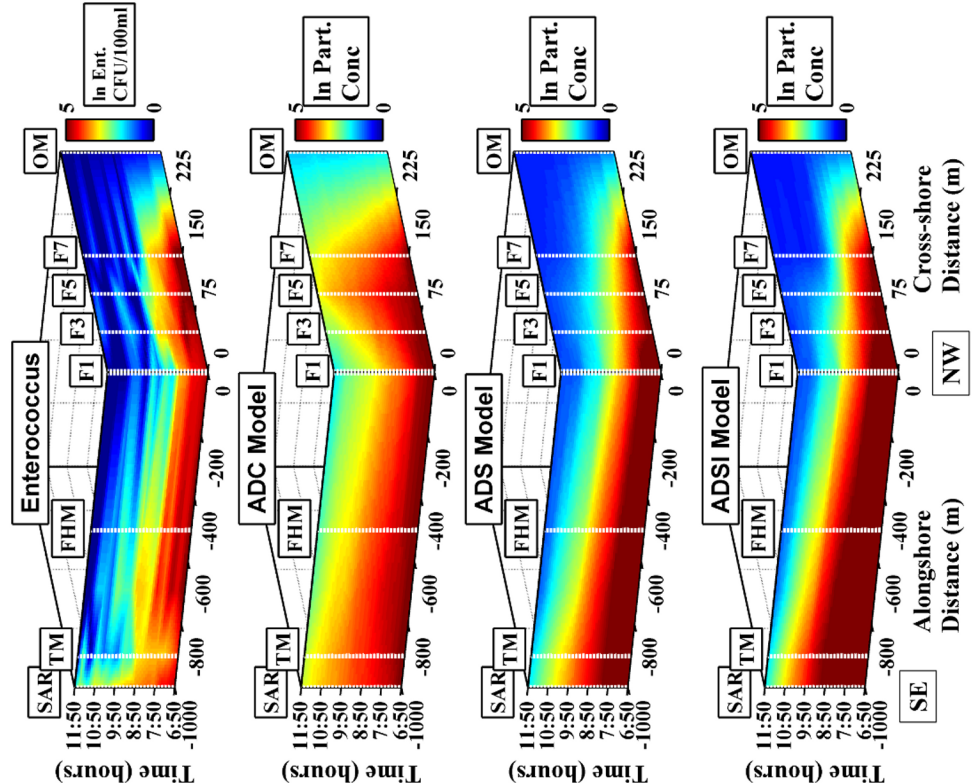
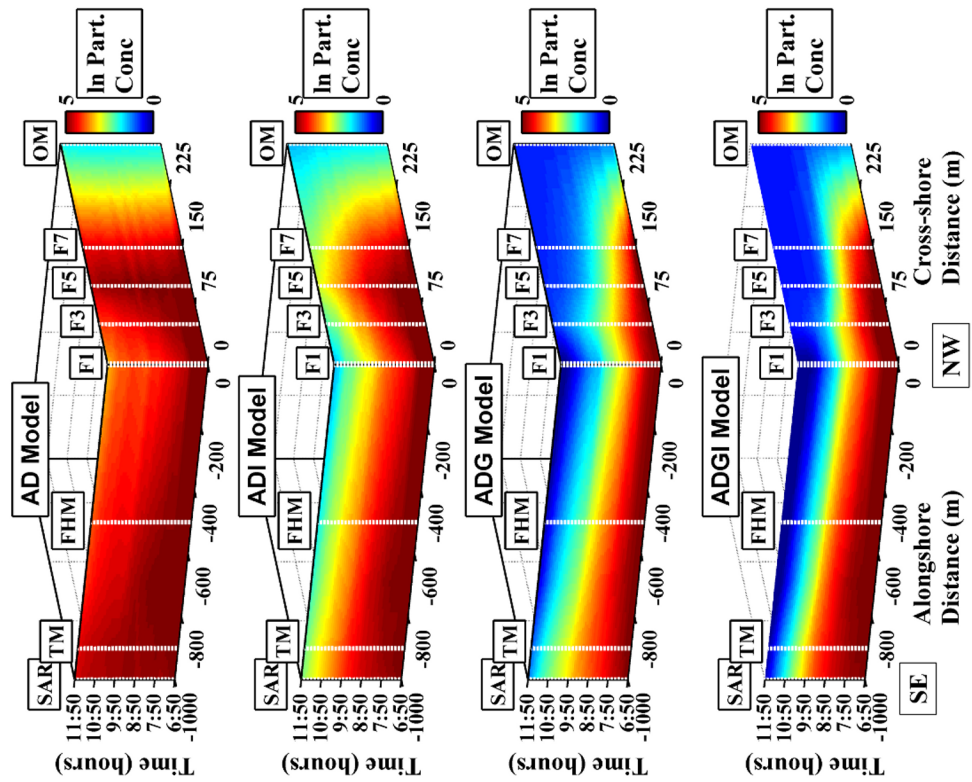
**Figure 3.2:** *E. coli* and *Enterococcus* decay rate vs. solar insolation dose averaged over shoreline (black) and offshore (red) locations. The lines are best-fit slopes. The regression skill ( $R^2 = 0.22$ ) is significant ( $p < 0.05$ ) for offshore *Enterococcus*, but not for *E. coli* or shoreline *Enterococcus*.

**Figure 3.3:** Contour plots of *E. coli* data, and best-fit model outputs as a function of cross-shore distance (m), alongshore distance (m), and time (hours). On the alongshore axis, the northernmost station (F1) is located at 0 m, with negative values indicating stations to the south. Color bar units are in natural log Most Probable Number (MPN) for *E. coli* data, and natural log of particle concentration for the mortality models. Note the over retention of *E. coli* particles at offshore stations with the AD, ADC, and ADI models.



**Figure 3.4:** Contour plots of *Enterococcus* data. Axes are the same as figure 3. Color bar units are in natural log Colony Forming Units (CFU) for *Enterococcus* data, and natural log of particle concentration for the mortality models. Note the over retention of *Enterococcus* particles at offshore stations with the AD, ADC, and ADI models.





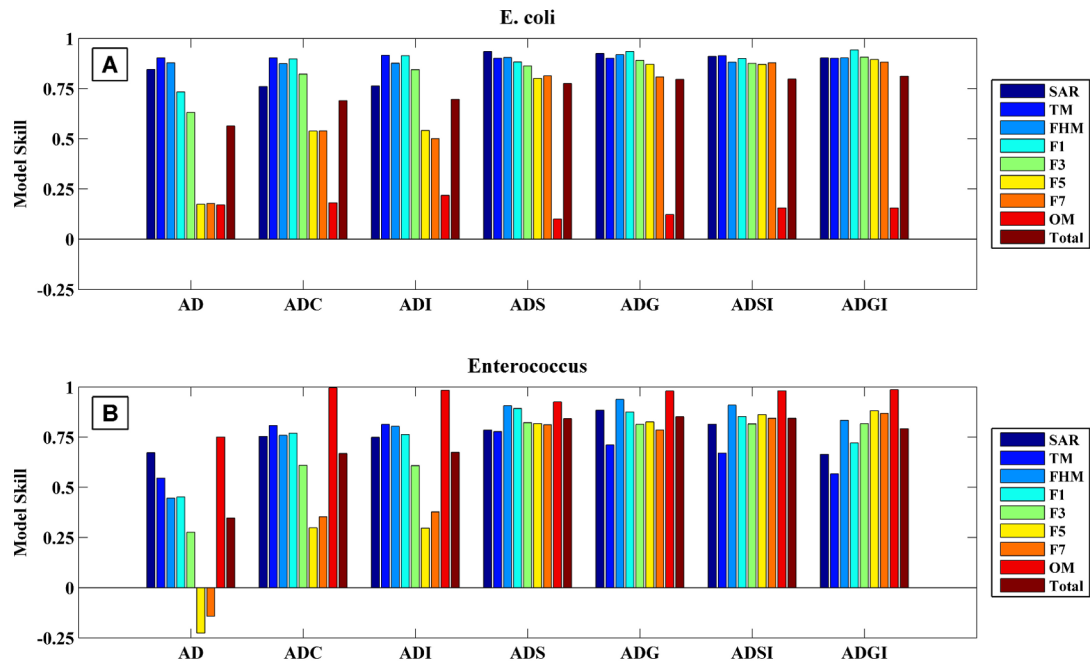


**Figure 3.5:** Station-specific and total skill for best-fit *E.coli* (A) and *Enterococcus* (B) models, where total skill refers to a bulk estimate calculated across all sampling stations. All mortality models improve model skill relative to the AD model at each sampling station, for both FIB groups. Model skill is highest for the models allowing for cross-shore variable FIB mortality (ADS, ADG, ADSI, and ADGI).

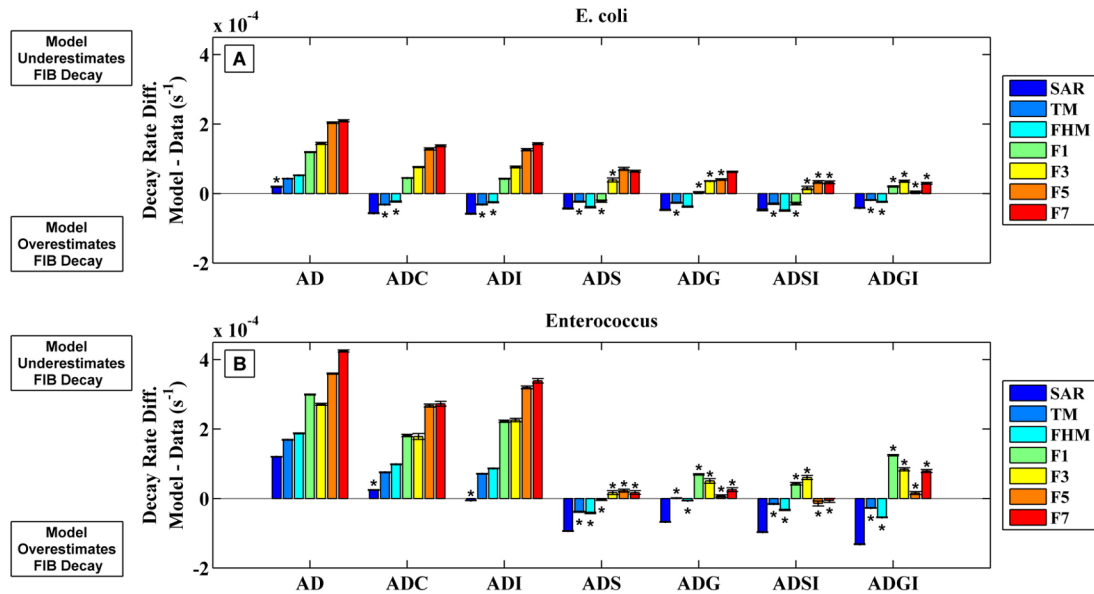
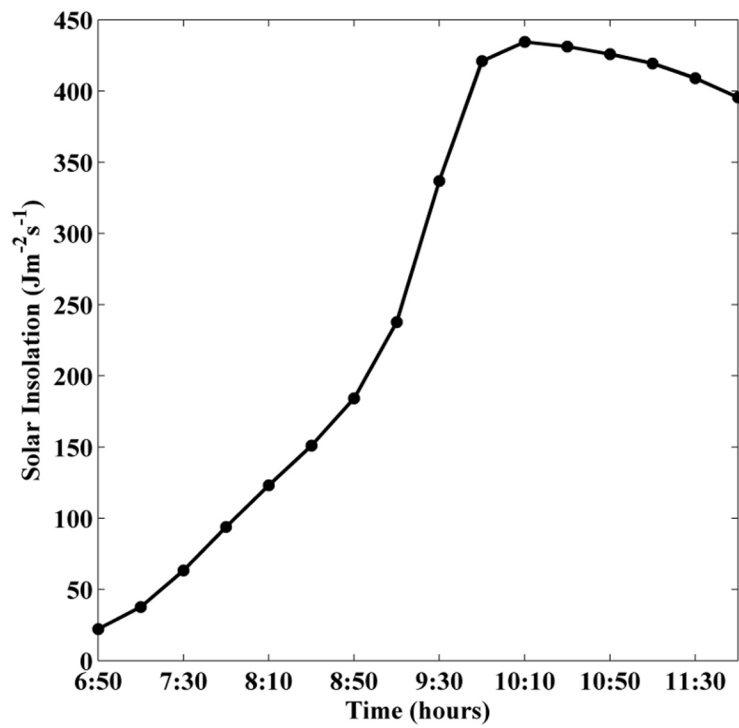
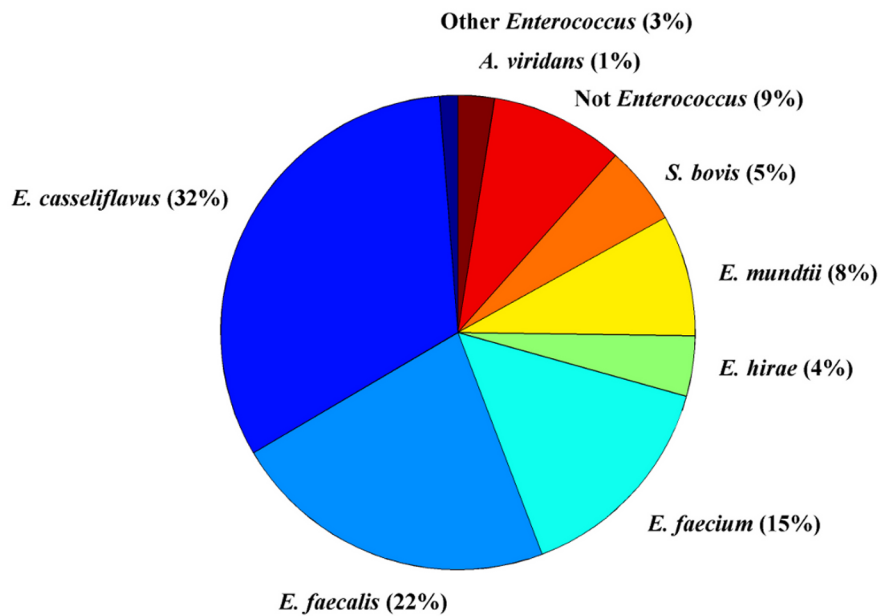


**Figure 3.6:** Decay rate differences (model – data) at each sampling station, for each best-fit model: **(A)** *E. coli* and **(B)** *Enterococcus*. An asterisk indicates decay rate differences that are not significantly different from zero ( $p < 0.05$ ).

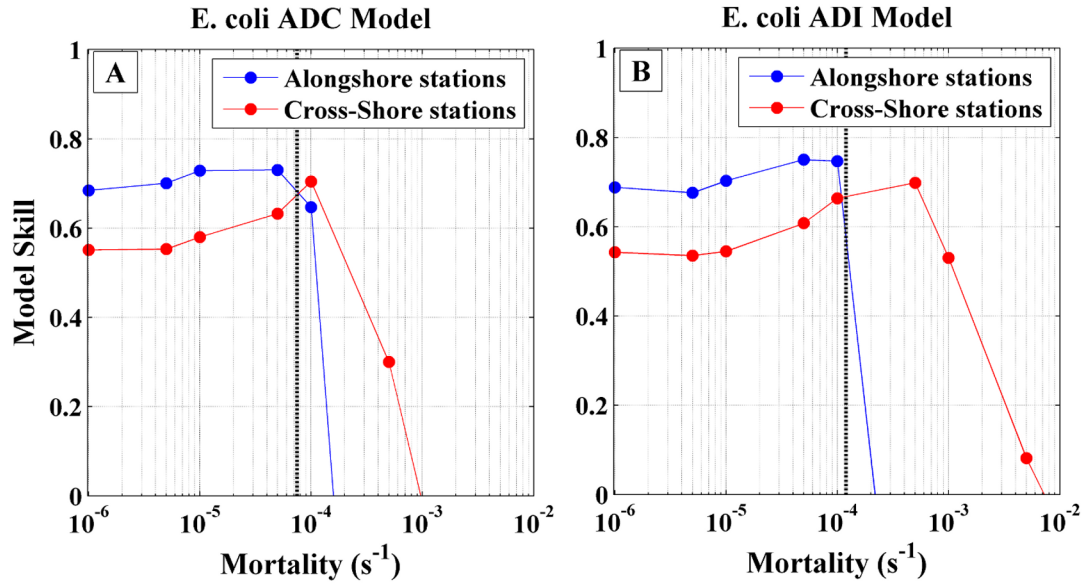
## Appendix 3.1: Supplementary Figures



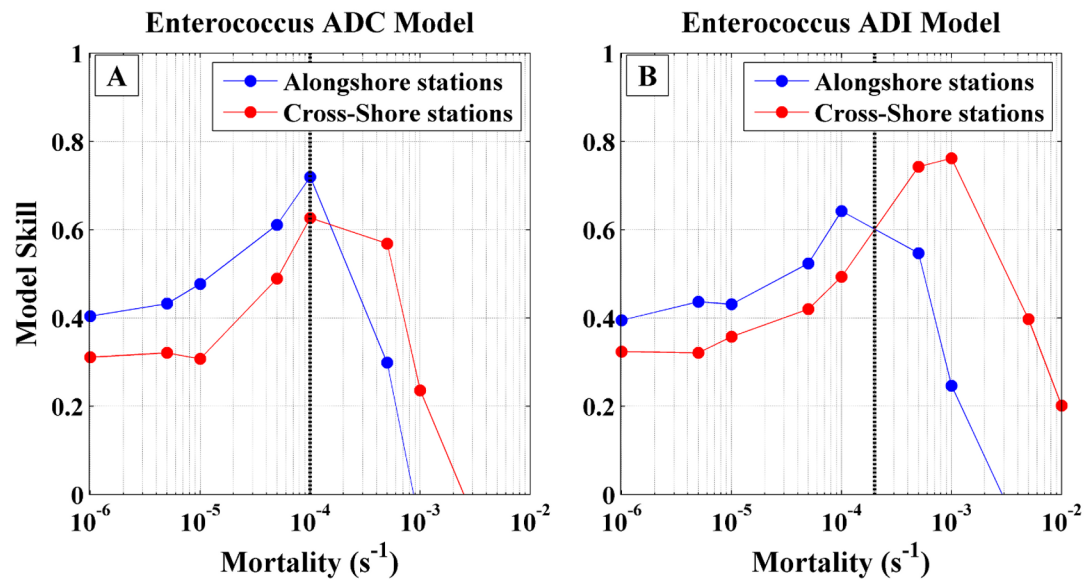
**SI Figure 3.1:** Solar insolation ( $y$ -axis) verses time ( $x$ -axis) measured on October 16<sup>th</sup>, 2006, at Huntington Beach, CA.



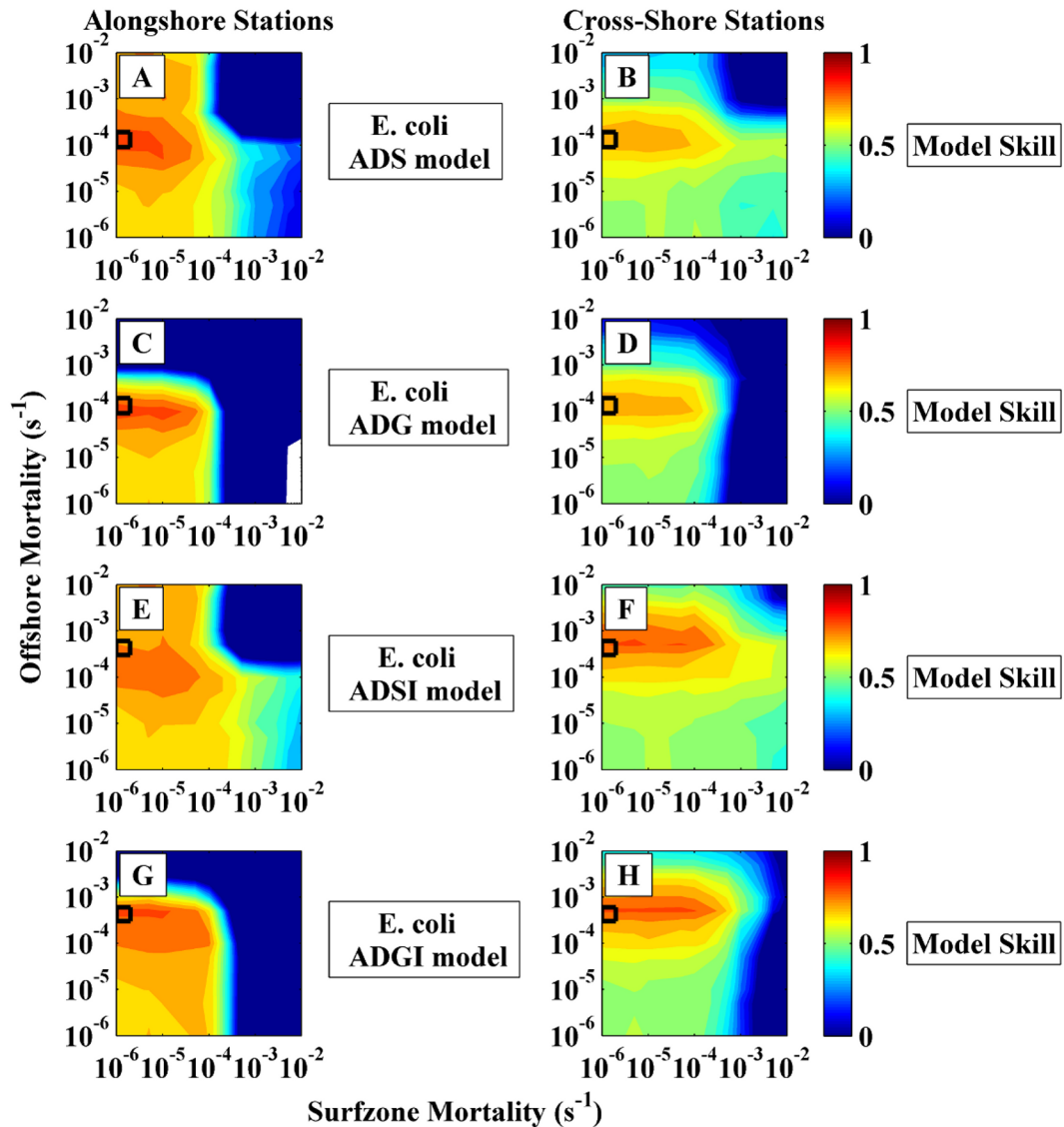
**SI Figure 3.2:** Pie chart of *Enterococcus* species composition. Chart is a composite of water samples from all stations. 242 colonies were examined in total. Note the dominance of the plant associated *E. casseliflavus* alongside the high percentages of *E. faecalis* and *E. faecium*.



**SI Figure 3.3:** Sensitivity analysis for one-parameter *E. coli* mortality models: (A) the ADC model (constant mortality) and (B) the ADI model (mortality is temporally dependent on the magnitude of solar insolation). Mortality parameter value ( $s^{-1}$ ) is on the x-axis and model skill for both alongshore (blue) and cross-shore (red) stations is on the y-axis. The best-fit mortality parameter for each model is identified by a dashed black line.

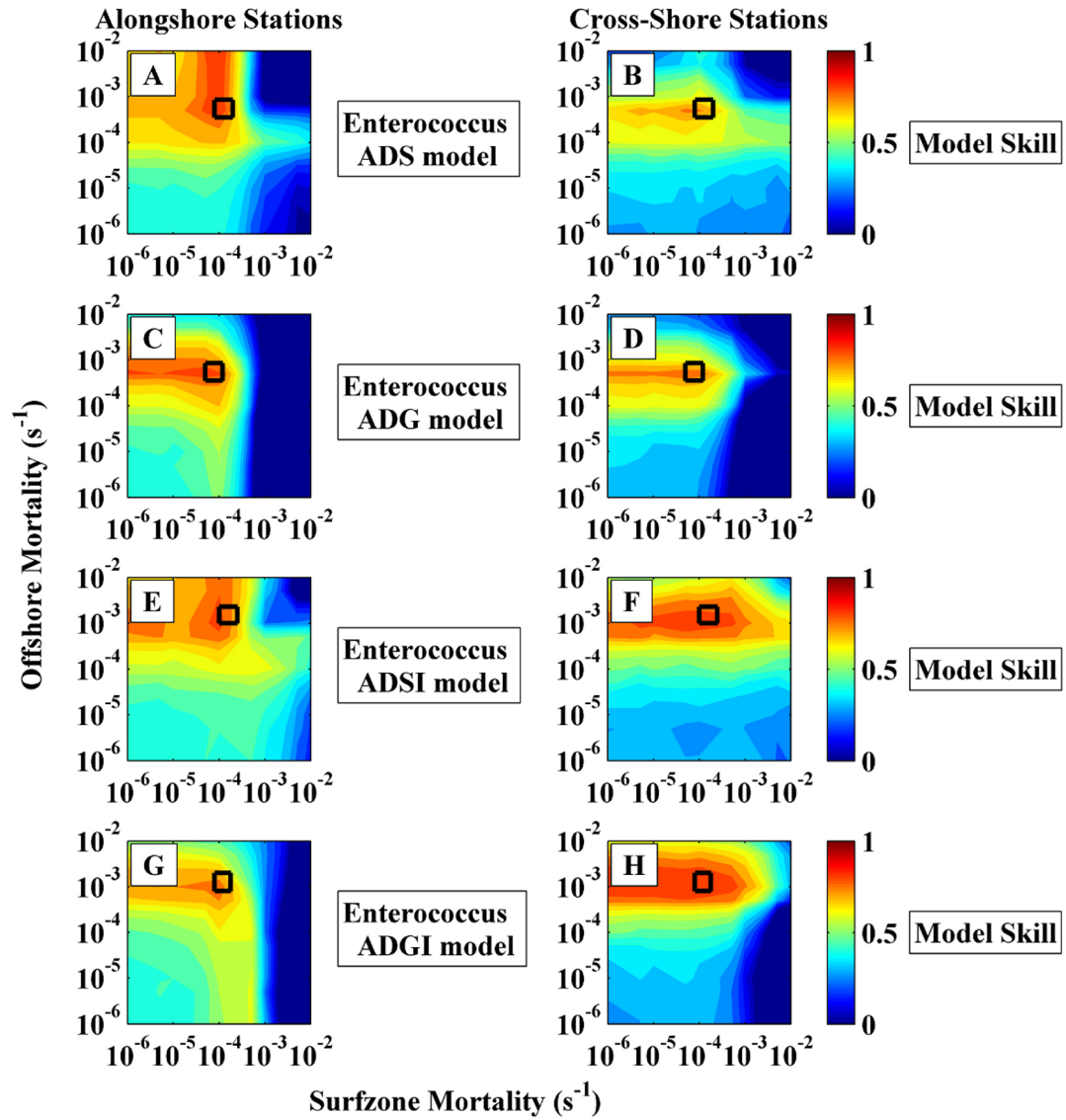


**SI Figure 3.4:** Same as SI figure 3, but for one-parameter *Enterococcus* mortality models.



**SI Figure 3.5:** Sensitivity analysis for two-parameter *E. coli* mortality models. The  $x$ -axis is  $m_o$ , the surfzone mortality parameter ( $s^{-1}$ ) and the  $y$ -axis is  $m_o$ , the offshore mortality parameter ( $s^{-1}$ ). Color is the model skill (see equation 2) evaluated at alongshore stations (A, C, E and G), or cross-shore stations (B, D, F, and H), respectively. The best-fit parameter pair for each mortality model is marked by a black box. Note that the surfzone mortality parameter is not well constrained for any of the two-parameter mortality models, while the offshore mortality parameter is highly constrained.





**SI Figure 3.6:** Same as SI figure 5, but for two-parameter *Enterococcus* mortality models.

## CHAPTER 4.

### THE EFFECTS OF THE BLOOM FORMING DINOFLAGELLATE *LINGULODINIUM POLYEDRUM* ON THE MORTALITY OF *ENTEROCOCCUS* *FAECIUM* IN SEAWATER: MORTALITY RATES, WATER QUALITY IMPACTS, AND MONITORING IMPLICATIONS

#### **Abstract**

Phytoplankton blooms have been shown to impact the growth, mortality, and nutrient uptake kinetics of natural bacterial assemblages. The effects of phytoplankton on allochthonous bacterial pollutants and fecal indicators, however, are not well understood. This study evaluates the impacts of bloom concentrations of the dinoflagellate *Lingulodinium polyedrum* on the survivorship of the fecal indicator *Enterococcus faecium*. Seawater microcosm experiments indicate that *L. polyedrum* can halve *Enterococcus* mortality rates in the absence of solar radiation. Observed *Enterococcus* decay was significantly biphasic, and poorly described by a simple exponential model. When evaluated in a physical context (using an individual based model including alongshore advection and horizontal diffusion), the enhanced FIB survivorship conferred by phytoplankton was shown to increase the spatial extent and intensity of a simulated FIB plume: early morning FIB concentrations were ~21% higher in models where FIB mortality was a function of phytoplankton concentration. This study also evaluated the utility of direct correlation analyses for detecting modeled relationships between phytoplankton and tidally-released FIB using two possible field sampling regimens (once-per-day and once-per-tide). Modeled

relationships between FIB and phytoplankton were inaccurately classified 25 – 67% of the time using once-per-day sampling methods. A tidal sampling scheme was found to increase our ability to detect modeled relationships, although classification was still inaccurate 0-42% of the time.

### **Introduction**

The growth and mortality of fecal indicator bacteria (FIB) in the surfzone are functions of complex environmental forcings. To date, research regarding FIB survivorship has been dominated by studies of physical factors such as solar radiation, temperature, pH, and salinity (Curtis et al., 1992; Solic and Krustulovick., 2002; Sinton et al., 2002; Ki et al., 2007; Boehm et al., 2009). Less attention has been paid to the effects of nearshore biotic assemblages on indicator bacteria, with the majority of work focusing on protistan grazing (Gonzalez et al., 1990; Hartke et al., 2002; Boehm et al., 2005; Surbeck et al., 2010). Because phytoplankton form dense, patchy blooms that periodically dominate surfzone marine communities where indicator bacteria are monitored, they may occasionally have a disproportionate effect on the coastal ecology of FIB (Billen and Fontigny, 1987; Hsieh et al., 2007). The Southern California bloom-forming dinoflagellate *Lingulodinium polyedrum*, can form particularly dense blooms in nearshore waters, with concentrations exceeding  $10^6$  cells  $L^{-1}$  (Kudela and Cochlan, 2000). Blooms of this organism have been observed at beaches with chronically poor bacteriological water quality (like Huntington Beach), making *L. polyedrum* an ideal candidate for exploring the effects of marine phytoplankton on the survivorship of fecal indicators (Omand et al., 2011).

Fecal indicator bacteria are sensitive to levels of environmental oxygen, light, toxins, dissolved organic matter (DOM), and pH, all factors regulated by phytoplankton (Curtis et al., 1992; Mykkestad, 1995; Ogino et al., 1997; Davies-Colley et al., 1999; Mourino-Perez et al., 2003; Jeong et al., 2004). High concentrations of FIB have been observed associated with benthic *Chladophera* mats, suggesting that algal matter may facilitate FIB accumulation and/or growth in lake environments (Whitman et al., 2003; Byappanahalli et al., 2003). In drinking water distribution systems fecal coliform levels have been observed to spike during the final stages of phytoplankton blooms, implying that planktonic algae may enhance FIB concentrations in a comparable fashion to algal mats (Lake et al., 2001).

Phytoplankton, however, may have inhibitory as well as facilitative effects on FIB. Microcosm experiments have shown that *E. coli* mortality is enhanced in the presence of the green algae *Chlorella* (Davis and Gloyna, 1970). This mortality is presumed to be caused by the production of the toxin chlorellin, though this has not been confirmed (Davis and Gloyna, 1970). In addition, phytoplankton leakage or lysis can release photosensitive humic material into the environment, which can react with sunlight and oxygen to form reactive oxygen species (ROS) (Anesio et al., 2005; Clark et al., 2008). These ROS may be important contributors to FIB oxidative stress, and thus mortality, in marine and freshwater systems (Davies-Colley et al., 1999; Muela et al., 2002; Clark et al., 2008; Clark et al., 2010).

Here we address the role of phytoplankton in regulating concentrations of FIB in seawater, thereby narrowing an important ecological gap in our understanding of FIB survivorship. Despite the presence of a comprehensive literature linking

phytoplankton exudates (including nutrients (Lignell, 1990; Baines and Pace, 1991; Moruino-Perez et al., 2003), ROS (Kim et al., 1999; Muela et al., 2002) and antimicrobial compounds (Casamatta and Wickstrom, 2000)) to growth or mortality of bacteria, the idea that phytoplankton might affect FIB survivorship has been met with severe criticism by funding agencies. The following are select quotations from reviewers regarding a FIB-phytoplankton interactions proposal submitted to the Coastal Environmental Quality Initiative Program in 2008;

“Phytoplankton are not likely to have significant effect on FIB”

“Interesting problem, not sure whether this actually would have an application in the future.”

“There is no observation along Huntington Beach showing the link between phytoplankton and FIB”

The manuscript below responds directly to these comments and will show 1) that the bloom-forming dinoflagellate *Lingulodinium polyedrum* can increase the survivorship of *Enterococcus* in seawater, 2) that this increased survivorship has the potential to increase both the spatial and temporal footprint of a FIB pulse at Huntington Beach, and 3) that the lack of direct correlation between phytoplankton and FIB at Huntington Beach (or other beaches) should not be taken to imply a lack of biotic effect. We show that it is difficult in practice to detect correlations between phytoplankton and FIB in

marine systems using a typical 1-per-day sampling regimen, given the complex source dynamics of fecal indicators.

## Methods

### ***FIB-Phytoplankton Microcosm Experiments:***

#### *Batch Cultures:*

Microcosm experiments were used to evaluate the effects of the bloom-forming dinoflagellate *Lingulodinium polyedrum* on rates of FIB growth or mortality in seawater. The axenic strain of *L. polyedrum* CCMP 1932 was used for all experiments. Batch cultures were grown in f/4 medium with 4X vitamin stock (Guillard, 1975), at 16°C. Cultures were grown on a 12:12 light:dark cycle using cool-white fluorescent tubes (160  $\mu\text{mol photon m}^{-2} \text{s}^{-1}$ ). Algal growth was monitored via direct cell counts using triplicate 1 ml aliquots in a Sedgewick-Rafter chamber. Cultures were ready for use when bloom conditions (cell concentrations of  $\sim 10^3 \text{ ml}^{-1}$ ) were reached.

The fecal indicator chosen for our microcosm experiments was *Enterococcus faecium* (ATCC strain 19434). *Enterococcus* is the preferred indicator of fecal pollution in marine waters (EPA, 2000), and *E. faecium* is one of the dominant *Enterococcus* species isolated from human feces (Sinton et al., 1993). *E. faecium* was cultured from frozen stock in brain heart infusion broth (BHIB). Initial cultures were grown at 35°C in a shaking water bath for 24 hours, and then subcultured (10  $\mu\text{l}$  aliquots) into cuvettes containing 3 ml of fresh BHIB. These new cultures were incubated (as described above), and their optical density (OD) was monitored every 20

minutes using a LKB ultraspec 2 (600 nm wavelength). When an OD of  $\sim 0.345$  was reached cells were harvested via centrifugation, washed three times in 0.2  $\mu\text{m}$  filtered seawater, and resuspended in 27 ml of f/4 media with 4X vitamin stock (the same media used for our phytoplankton cultures). At OD 0.345, cultures were consistently in exponential phase.

#### Microcosm Design:

Microcosm experiments were performed in 150 ml Pyrex flasks, in the dark, at 16°C. Seventy microcosms were prepared, 35 of which contained 50 ml of cultured *L. polyedrum* ( $10^3 \text{ ml}^{-1}$ ) (LP treatment). The remaining 35 contained 50 ml of sterile f/4 media and no phytoplankton (NP treatment). Twenty-seven flasks from each treatment (LP and NP) were inoculated with 1  $\mu\text{l}$  aliquots of the *Enterococcus* suspensions described above. The remainder were left as nonenterococcal controls. Replicate flasks (2-5 per treatment) and controls (1 per treatment) were removed at 0, 3, 6, 9, 12, 24, 48, and 72 hours, respectively, for enumeration of *L. polyedrum* and *E. faecium*. For phytoplankton enumeration 5 ml aliquots were fixed in buffered formalin (final concentration of 2% by volume) and counted using a Sedgewick-Rafter chamber (as above). For *Enterococcus*, 10 ml aliquots were pipetted into 90 ml of Milli-Q water (Millipore), and enumerated using the defined substrate test Enterolert (IDEXX Laboratories, Inc.).

#### ***Model Evaluation: the effects of phytoplankton on a surfzone pollutant patch***

##### Model Structure:

To evaluate the potential impacts of phytoplankton on the extent and intensity of surfzone bacterial contamination, model simulations were performed using a modified version of the 2D individual based FIB model (AD model) described in (Rippy et al., submitted ms 1). The model was developed for Huntington Beach, California, and includes both alongshore advection,  $u(y,t)$  and horizontal diffusion ( $k_h$ ). Advection was forced using 20 minute averaged alongshore velocities from a cross-shore transect of Acoustic Doppler Velocimeters (ADV's). These measurements were collected as part of an intensive physical-biological field program at Huntington Beach in 2006 (HB06).

Diffusion of FIB was dependent on their cross-shore location,

$$\kappa_h = \kappa_0 + \left( \frac{\kappa_1 - \kappa_0}{2} \right) \left( 1 - \tanh \left( \frac{(y - y_0)}{y_{scale}} \right) \right) \quad (1)$$

where  $k_0$  is the background (offshore) diffusivity,  $k_1$  is the elevated surfzone diffusivity,  $y_0$  is the cross-shore midpoint of the transition between  $k_0$  and  $k_1$  (i.e., the offshore edge of the surfzone) and  $y_{scale}$  determines the width of this transition in the cross-shore. The  $k_0$ ,  $k_1$ ,  $y_0$ , and  $y_{scale}$  values used here are those that provided the best fit to FIB data collected at Huntington Beach in 2006:  $0.05 \text{ m}^2 \text{ s}^{-1}$ ,  $0.5 \text{ m}^2 \text{ s}^{-1}$ , 50 m and 5 m, respectively (Rippy et al., submitted ms. 1).

To evaluate the effects of phytoplankton on surfzone FIB concentrations, the AD model was modified to include FIB mortality. The mortality function was designed based on the results of the FIB-phytoplankton microcosm experiments



discussed above. Mortality was biphasic and evaluated separately for resistant ( $R$ ) and sensitive ( $S$ ) FIB fractions,

$$\frac{dC_R}{dt} = -k_R C_R \quad (2.1)$$

$$k_R = \begin{cases} k_{R(LP)} & \text{Phytoplankton are Present} \\ k_{R(NP)} & \text{Phytoplankton are Absent} \end{cases} \quad (2.2)$$

$$\frac{dC_s}{dt} = -k_s C_s \quad (2.3)$$

$$k_s = \begin{cases} k_{s(LP)} & \text{Phytoplankton are Present} \\ k_{s(NP)} & \text{Phytoplankton are Absent} \end{cases} \quad (2.4)$$

$$C_{tot} = aC_R + (1-a)C_s \quad (2.5)$$

where  $C_{tot}$  is the total FIB concentration,  $C_R$  is the concentration of resistant FIB,  $C_s$  is the concentration of sensitive FIB,  $t$  is time,  $a$  is the fraction of FIB that are resistant,  $k_R$  is the mortality rate of the resistant fraction, and  $k_s$  is the mortality rate of the sensitive fraction. The response to phytoplankton is binary: when phytoplankton are present FIB mortality rates are  $k_{R(LP)}$  and  $k_{s(LP)}$ ; when phytoplankton are absent the mortality rates are  $k_{R(NP)}$  and  $k_{s(NP)}$ .

Model Initialization:

All model runs were performed from 1850 on 9/15/06 until 0650 on 9/16/06. This time window was selected because it is close to the time frame of the original model (Rippy et al., submitted ms 1), and because it falls between two high tides, during dark conditions. A night-time window was optimal because our decay rate parameterizations come from microcosm experiments performed in the dark. Initiating the model with FIB on a high tide confers realism to the simulations because high tide is often associated with FIB release via over beach transport (Grant et al., 2001; Whitman et al., 2003; Zhu et al., 2011).

Simulations were initialized with 80,000 bacterial particles containing a concentration of FIB  $C_{tot}$ . Particles were released in a uniform grid extending 160 m offshore, and from 1.5 – 2 km north of the Santa Ana River in the alongshore. Our across-shore patch boundary was taken directly from Rippy *et al.*, (submitted ms 1-2). The alongshore boundary was selected based on the predominantly southward surfzone currents during our time window (Rippy et al., submitted ms 1; their Fig. 2). Placing our initial patch to the north allowed us to evaluate the spatial extent and intensity of the resultant southward pollutant plume under three different scenarios: no FIB mortality (AD model), FIB mortality in the absence of phytoplankton (AD\_NP model), and FIB mortality in the presence of phytoplankton (AD\_LP model).

***Direct Correlations: Detecting FIB-phytoplankton interactions in marine systems***

In many instances, data from state or county water quality monitoring programs constitute our longest continuous FIB timeseries (Boehm et al., 2002).

These programs typically collect water samples once per day (or less). In order to determine if low frequency timeseries data from these programs could be used to identify relationships between phytoplankton and FIB in coastal waters, we first simulated FIB timeseries using simple time-dependent models forced with Huntington Beach field data (chlorophyll *a* (Chla) and water depth). In these models FIB concentration was a function of source dynamics (tidal) and biphasic mortality (parameterized using data from our seawater microcosms). No physical transports were included. Four different mortality forms were evaluated: mortality as a function of phytoplankton concentration (LP), mortality independent of phytoplankton concentration (NP), mortality as a function of phytoplankton concentration and solar radiation (LP + L), and mortality as a function of solar radiation but independent of phytoplankton concentration (NP + L). It was assumed that the relationship between FIB and the Huntington Beach phytoplankton community (given as Chla) would be the same as measured for *Enterococcus* and *L. polyedrum* in our microcosm experiments.

FIB timeseries (generated using the models above) and Huntington Beach Chla data were subsampled once per day to mimic the sampling frequency of water quality monitoring programs. FIB-Chla correlations were calculated for each model and evaluated to determine if modeled relationships between FIB and phytoplankton could be accurately recovered (e.g. significant positive correlations between Chla and FIB for LP or LP + L models and non-significant correlations between Chla and FIB for NP or NP + L models). All timeseries were also subsampled according to tide height (ie once per tide). This allowed us to assess whether or not a sampling regimen

tracking FIB source dynamics (FIB release in all models was tidally forced) improved our ability to accurately detect modeled relationships between FIB and phytoplankton. The field data used in these analyses, the structure of the FIB models themselves, and the statistical assessment of our FIB-Chla correlations are all described in more detail below.

*Field Data:*

All field data used for our model simulations was collected from 9/16 - 10/16/06 as part of the HB06 field program mentioned above (described in more detail in Rippy et al., submitted ms 1). Water depth (a proxy for tide height) was measured using a pressure sensor located in ~ 4 m water depth. This data was used to force tidal release of FIB: a single 20 MPN / 100 ml FIB pulse was released on every high tide (Fig. 4.1a).

Chla concentration (a proxy for phytoplankton) was measured using two WET Lab ECO Triplet fluorometers, one at ~ 14 m water depth and one mounted on a wirewalker (Omand et al., 2011). Only the bottom 2 m of data from this latter instrument were used. The two datasets were merged and daily averaged Chl a concentrations were calculated (Omand et al., 2011). The average Chla concentration over all sampling days was also determined, and to define a bloom threshold (1.8  $\mu\text{M}$  Chla) (Fig 4.1b). This threshold resulted in 2 discrete bloom events (denoted bloom 1 and bloom 2), and one other small event that will not be discussed here. The first bloom was longer than the second bloom, lasting for a total of 6 days instead of 2 (Fig 4.1b). During both events FIB mortality was considered “affected” by phytoplankton

(equations 2.1-2.7 (LP) and 3.1-3.7 (LP + L)). All chlorophyll data was courtesy of Melissa Omand.

*FIB Timeseries Simulations:*

FIB mortality for the phytoplankton dependent (LP) scenario was governed by equations 2.1-2.5, with the binary phytoplankton response terms in 2.2 and 2.4 changed from presence/absence to above/below the HB06 bloom threshold. FIB mortality for the phytoplankton-independent (NP) scenario excluded the binary response terms in 2.2 and 2.4:  $k_R$  (2.1) was always  $k_{R(NP)}$  and  $k_s$  (2.1) was always  $k_{s(NP)}$ .

For the model scenarios including solar radiation (LP + L and NP + L), mortality was modeled as:

$$\frac{dC_R}{dt} = -M_R C_R \quad (3.1)$$

$$M_R = k_R + mI(t) \quad (3.2)$$

$$k_R = \begin{cases} k_{R(LP)} & \text{Phytoplankton above bloom threshold} \\ k_{R(NP)} & \text{Phytoplankton below bloom threshold} \end{cases} \quad (3.3)$$

$$\frac{dC_s}{dt} = -M_s C_s \quad (3.4)$$

$$M_s = k_s + mI(t) \quad (3.5)$$

$$k_s = \begin{cases} k_{s(LP)} & \text{Phytoplankton above bloom threshold} \\ k_{s(NP)} & \text{Phytoplankton below bloom threshold} \end{cases} \quad (3.6)$$

$$C_{tot} = aC_R + (1-a)C_s \quad (3.7)$$

where  $C_{tot}$  is the total FIB concentration,  $C_R$  is the concentration of resistant FIB,  $C_s$  is the concentration of sensitive FIB,  $t$  is time,  $a$  is the fraction of FIB that are resistant,  $M_R$  is the bulk mortality rate of the resistant fraction, and  $M_s$  is the bulk mortality rate of the sensitive fraction. Bulk mortality rates contain mortality terms that can be influenced by phytoplankton concentration ( $k_s$  and  $k_R$ ) and a solar dependent mortality term ( $mI(t)$ ). Here,  $I$  is solar radiation in  $\text{MJ m}^{-2} \text{h}^{-1}$ .  $I(t)$  was modeled using a sine wave with an amplitude corresponding to the maximum solar radiation value measured at Huntington Beach on 10/16/06 ( $16.2 \text{ MJ m}^{-2} \text{h}^{-1}$ , Rippey et al., submitted ms. 2). The sine wave period was 24 hours, corresponding to a 12 hour light-dark cycle. Sunrise was set at 0650. The parameter  $m$  ( $0.22 \text{ m}^2 \text{ MJ}^{-1}$ ) was selected from literature, giving a maximum solar mortality rate of  $\sim 0.001 \text{ s}^{-1}$  (Sinton et al., 1999; Sinton et al., 2002).

The binary phytoplankton response terms (3.3 and 3.6) were only included for the LP + L model scenario. In the NP + L simulations, these terms were excluded:  $k_R$  (3.2) was always  $k_{R(NP)}$  and  $k_s$  (3.5) was always  $k_{s(NP)}$ .

It is important to point out that our LP + L model assumes that the response of FIB to phytoplankton in sunlight is the same as the response in dark conditions. This

may not be true in practice, but, due to a lack of data supporting alternate relationship forms, we have chosen to model it as such here.

*FIB – Chlorophyll Correlation Coefficients:*

All correlations were evaluated using a Spearman's rank correlation test, which requires no assumptions of data normality. Bias corrected 95% confidence intervals for these correlations were determined using bootstrap methods: data were sampled with replacement 10,000 times, and Spearman's correlation coefficients (Rho) were estimated for each new data set. When  $Rho = 0$  was within our 95% confidence intervals, FIB and phytoplankton were not significantly correlated. When  $Rho = 0$  was below (above) our confidence intervals, FIB-phytoplankton correlations were significant and positive (negative).

## **Results and Discussion**

***Microcosm Experiments:***

*Biphasic decay:*

Concentrations of *Enterococcus faecium* were observed to decrease over time in all inoculated seawater microcosms (Fig. 4.2). *Enterococcus* was never detected in control microcosms. Mortality was biphasic, with initial mortality rates exceeding those at the end of the experiment (Fig. 4.2). This pattern was well described by the modification of Chick's law proposed by Frost and Streeter (1924)

$$C(t) = aC_0e^{(-k_R t)} + (1 - a)C_0e^{(-k_s t)} \quad (4)$$

where  $C_0$  is initial *Enterococcus* concentration,  $t$  is time,  $a$  is the fraction of *Enterococcus* that are resistant to decay,  $k_R$  is the mortality rate of the resistant fraction, and  $k_s$  is the mortality rate of the sensitive fraction. Biphasic mortality better approximated observed FIB data than simple exponential decay. Root mean square error for biphasic models was ~20% less than for exponential models (565.2 vs. 701 MPN 100 ml<sup>-1</sup> (NP); 701.2 vs. 861.8 MPN 100 ml<sup>-1</sup> (LP)) (Table 4.1). Furthermore, the corrected Akaike Information Criterion (AICc) for our biphasic models was ~ 10 IC units lower than for our exponential models, suggesting that biphasic decay significantly improves goodness of fit. (Note that this difference in AICc scores can be interpreted in terms of relative model likelihood. In this framework our reported  $\Delta$ AICc of 10 corresponds a ratio of biphasic model probability to exponential model probability (Akaike weight ratio) of 0.9964 : 0.0036. This indicates that a biphasic model is 278 times more likely to explain observed mortality than an exponential model; Burnham and Anderson, 2002) (Table 4.1).

To our knowledge this is the first time that biphasic decay has been shown to significantly improve our ability to model *Enterococcus* mortality in dark seawater treatments. Yamahara et al., (2012), Bae and Wuertz (2012), and Maraccini et al., (2012) all found that simple exponential decay was sufficient to depict *Enterococcus* mortality in both sand and seawater. Jeanneau et al., (2012), however, found that biphasic bacterial decay improved fits for *Enterococcus* (seawater and freshwater), *E.*



*coli* (freshwater), and *Bifidobacterium adolescentis* (freshwater), but these improvements were not significant. Similarly, Easton et al., (2005) observed biphasic decay for *Enterococcus*, *E. coli*, and total coliform bacteria, but only fits for *E. coli* and total coliforms were significant. Our results suggest that bacterial decay can be significantly biphasic for at least one species of *Enterococcus*. This has important water-quality implications because under biphasic decay FIB mortality rate decreases over time, resulting in greater environmental persistence than would be expected under simple exponential decay.

To date, several mechanisms for biphasic bacterial decay have been put forward: bacterial self-regulation via quorum sensing (resulting in density-dependent decay rates); rapid loss of culturable cells to a viable but not culturable (VBNC) state, followed by slow decay of the remaining population; the co occurrence of multiple FIB species or strains with different intrinsic mortality rates; and/or the co-occurrence of growing and dying subpopulations of FIB, resulting in temporally variable net mortality rates (Velz et al., 1984; Strauss, 1999; Easton et al., 2005; You et al., 2006; Hellweger et al., 2009; Rogers et al., 2011; Bucci et al., 2011). While our microcosm experiments were not designed to distinguish among these mechanisms, because they were performed using a single strain of *Enterococcus faecium*, we can state that the biphasic mortality we observed was not caused by the presence of multiple bacterial strains with different intrinsic mortality rates. To date, this study is one of only a handful to show biphasic decay in pure FIB cultures (Easton et al., 2005; Hellweger et al., 2009; Bucci et al., 2011). Further research is required to identify the mechanisms underlying this response.

Mortality of *Enterococci*: the effects of phytoplankton

In all microcosms with *L. polyedrum*, phytoplankton cell counts remained around  $10^3 \text{ ml}^{-1}$  for the duration of the experiment (SI Fig. 4.1). *Enterococcus* survivorship in treatments with phytoplankton was enhanced relative to treatments without phytoplankton (Fig. 4.2). This trend was not statistically significant at the  $p < 0.05$  level, as reflected by the slight overlap of the confidence intervals in Fig. 4.2. It could, however, be environmentally significant, as mortality rates for both the sensitive and resistant fractions were halved in the presence of phytoplankton, with no overlap in the standard error bounds of rates for the sensitive fraction (Table 4.1).

The observed increases in FIB survivorship for microcosms with phytoplankton relative to those without, suggests that antagonistic mechanisms, whereby phytoplankton negatively impact FIB, are not dominant during dark conditions. This is interesting given that *L. polyedrum* can exhibit mixotrophy, which could supplement nutritional requirements in the dark, when photosynthesis is not possible (Jeong et al., 2004; Jeong et al., 2005; Seong et al., 2006). Enhanced *Enterococcus* survivorship in microcosms with *L. polyedrum* could be due to dissolved organic matter (DOM) release. Algal exudates can contain high concentrations of carbohydrates, especially polysaccharides, which facilitate *Enterococcus* growth (Facklam and Collins, 1989; Mykkestad, 1995). Wolter (1982) showed that dinoflagellate blooms, in particular, result in high algal DOM uptake by marine bacteria. In light of the enhanced enterococcal survivorship observed in our seawater microcosms, this mechanism should be evaluated for fecal indicator bacteria.

It is important to point out here that, although *Enterococcus* mortality was reduced in dark microcosm treatments containing phytoplankton, the effects of phytoplankton on FIB mortality in light microcosm treatments remains unknown. Given that phytoplankton can release photosensitive organic matter that can react with oxygen and light to form antimicrobial compounds, it should not be assumed that the dominant mechanisms affecting FIB-phytoplankton interactions in the dark will be the same as those in the light. Further research is required to evaluate FIB-phytoplankton interactions in the context of solar radiation.

Although the tendency to describe FIB mortality using simple exponential decay makes it difficult to directly compare mortality rates from our experiments to those from others, our rate estimates were typically consistent with rates from the literature. In our experiments, mortality rates in the absence of phytoplankton were  $0.33 \text{ h}^{-1}$  (sensitive fraction) and  $0.019 \text{ h}^{-1}$  (resistant fraction), and mortality rates in the presence of phytoplankton were  $0.17 \text{ h}^{-1}$  (sensitive fraction) and  $0.008 \text{ h}^{-1}$  (resistant fraction) (Table 4.1). With the exception of our sensitive FIB fraction in the absence of phytoplankton, these rates fell within the reported bounds for *Enterococcus* dark mortality in seawater ( $0.005 - 0.18 \text{ h}^{-1}$ ) (Sinton et al., 1999; Sinton et al., 2002; Maraccini et al., 2012). Mortality rates for the sensitive FIB fraction (no phytoplankton) were slightly higher.

***The effects of phytoplankton on a surfzone pollutant patch:***

In the absence of mortality, a FIB patch initiated at 1850 in the Huntington Beach AD model, 1.5 – 2 km north of the Santa Ana River, was still detectable in the

surfzone 12 hours later (0650) (Fig. 4.3a). By 0650, FIB had been transported up to 1.5 km south of the initial bacterial patch. FIB concentrations in the resultant plume ranged from 7-122 MPN 100 ml<sup>-1</sup>, well below the release concentration (400 MPN 100 ml<sup>-1</sup>) (Fig. 4.3a). FIB levels exceeding the EPA 30 day geometric mean standard for *Enterococcus* (35 MPN 100 ml<sup>-1</sup>) were detectable up to 1.4 km south of the release location (Fig. 4.3a).

The inclusion of biphasic mortality in the AD model (parameterized using rates from our microcosm experiments) changed both the extent and intensity of the FIB plume observed at 0650. Biphasic mortality in the absence of phytoplankton (AD\_NP model) caused FIB to decline well below the EPA geometric mean standard for *Enterococcus* by 0650 (Fig. 4.3b). In this scenario, early morning waters were reasonably clean, and would not constitute a health risk to beach goers. In the presence of phytoplankton, FIB contamination patterns more closely approximated the AD model. At 0650, the geometric mean standard for *Enterococcus* was exceeded up to 740 m south of the initial FIB release, indicating poor water quality and health risk (Fig. 4.3c). On average, the presence of phytoplankton increased early morning FIB concentrations by 21% (Fig. 4.4).

These simulations demonstrate that the effects of phytoplankton on FIB contamination in marine systems can be significant, and are not masked by losses due to physical processes like advection and mixing. The presence or absence of phytoplankton can cause FIB concentrations to exceed, or drop below health risk standards, over 100's of meters of beachfront. This makes the effects of phytoplankton communities on nearshore FIB persistence worth exploring. This mechanism should

also be evaluated for specific human pathogens because some – particularly the bacteria – may respond to phytoplankton in a similar manner as FIB. Others, however, may not, resulting in a disconnect between indicator bacteria and human health risk in the nearshore that should be acknowledged.

***Detecting FIB-phytoplankton interactions using direct correlations:***

***Generated FIB timeseries***

When the only source of FIB loss is from biphasic dark mortality (rates estimated in microcosm experiments) FIB released to the surfzone at a tidal frequency will accumulate in the nearshore (Fig. 4.5a). This occurs because our experimentally determined rates are insufficient to reduce FIB levels to zero in  $\sim 12$  h. When a 20 MPN 100 ml<sup>-1</sup> FIB pulse is released every high tide it takes  $\sim 5$  d for FIB concentrations to stabilize about a mean (31 MPN 100 ml<sup>-1</sup>) (Fig 4.5a). For this reason, all of our simulation experiments included a 5 d spin-up phase that was never included in our direct correlation analyses.

When FIB were modeled as insensitive to phytoplankton and solar radiation dose (NP model), concentrations stabilized about the aforementioned mean (31 MPN 100 ml<sup>-1</sup>), and ranged from 46 MPN 100 ml<sup>-1</sup> (high tide) to 23 MPN 100 ml<sup>-1</sup> (just prior to the subsequent high tide) (Fig 4.5a). When FIB were modeled as sensitive to phytoplankton above a bloom threshold (LP model), however, FIB concentrations increased significantly during blooms, reaching a maximum on the last high tide of each bloom event (Fig 4.5a). Maximum concentration was a function of bloom duration. The FIB max during the first bloom ( $\sim 6$  d in duration) was 73 MPN 100 ml<sup>-1</sup>

<sup>1</sup>, and the FIB max during the second bloom (~2 d in duration) was 57 MPN 100 ml<sup>-1</sup> (Fig 4.5a). Following bloom events FIB concentrations relaxed back to non-bloom levels. Relaxation was biphasic, with FIB concentrations rebounding to within 5% of non-bloom levels ~6.8 and 4.9 days following termination of bloom events 1 and 2, respectfully (Fig 4.5a).

The inclusion of solar mortality in the NP model (NP + L) enhanced FIB loss during the day, decreasing the mean concentration of nearshore FIB from 31 MPN 100 ml<sup>-1</sup> to 12 MPN 100 ml<sup>-1</sup> (Fig. 4.5b). Clear diel cycling was seen, with the lowest FIB levels occurring just prior to high tide during the day (~2 MPN 100 ml<sup>-1</sup>). At night, FIB levels prior to high tide were higher (~8 MPN 100 ml<sup>-1</sup>) (Fig. 4.5b). When FIB were modeled as sensitive to both light and phytoplankton (LP + L), phytoplankton bloom events still led to increased FIB concentrations. This effect, however, was muted. At most, FIB concentrations during bloom events were 5 MPN 100 ml<sup>-1</sup> higher in the LP + L model than the NP + L model (a 41% increase) (Fig. 4.5b). In models without solar radiation, FIB concentrations during bloom events could be up to 29 MPN 100 ml<sup>-1</sup> higher in the LP + L model (a 94% increase) (Fig. 4.5a). The effects of blooms on FIB concentrations were also more ephemeral when FIB were solar sensitive, with FIB rebounding to pre-bloom levels in < 1 day for both bloom events.

*Direct Correlations: 1-per-day sampling:*

By sampling our Chl a and simulated FIB timeseries once per day, for each possible sampling hour, we generated 24 timeseries per FIB model that could be used to evaluate the correlation between FIB and phytoplankton. For the NP model, FIB-

Chl a correlations were not significant for the majority of sampling hours (67%), as would be expected given the lack of explicit relationship between FIB and phytoplankton in the formulation of the NP model (Fig. 4.6a, c). Notably, however, significant relationships were observed 34% of the time, purely by chance, with a fairly even split between negative and positive correlations (20 and 13%, respectively) (Fig. 4.6c).

FIB-Chla correlations in the LP model were always positively skewed relative to those from the NP model. This indicates that direct correlation analyses can detect the relationship between FIB and phytoplankton in the LP model, where bloom concentrations of phytoplankton enhance FIB persistence relative to background concentrations (Fig. 4.6b). Despite this positive skew, however, FIB-Chla correlations were only significant for 75% of sampling hours (Fig. 4.6b).

When solar insolation was included in models, the number of non-significant FIB - Chla relationships detected by direct correlation methods increased. This was most notable for the LP + L model, where FIB-Chla correlations went from being predominantly positive to predominantly non-significant (58%) upon including solar mortality (Fig. 4.6c - d). The positive skew in LP model correlations was still apparent, but less pronounced (Fig. 4.6b). These findings suggest that as systems become increasingly complex (e.g. additional sources of mortality are present), direct correlation analyses performed using 1-per-day samples become less reliable for detecting existing relationships between FIB and phytoplankton. It is notable that we see this trend even in simple models that exclude all physical transports and assume a single, cyclical FIB source with a constant release magnitude. This does not bode well

for our ability to use data from water quality monitoring programs to detect relationships between FIB and marine communities in complex systems like the surfzone. Below we evaluate the ability of tidally driven sampling (once per tide) to improve accurate detection of FIB-phytoplankton relationships using direct correlation methods.

*Direct Correlations: tidal sampling:*

For our once per tide sampling regimen, Chla and simulated FIB timeseries were sampled on high tide, and every hour post high tide, for a total of 11 hours. This resulted in 12 timeseries per FIB model that could be used to evaluate the correlation between FIB and phytoplankton. For the NP model, 92% of correlations between FIB and Chla were not significant: when no relationship was modeled, none was detected (Fig. 4.7c). For the LP model, FIB and Chl a were always significantly positively correlated, indicating that the modeled relationship between FIB and phytoplankton was accurately identified 100% of the time (Fig. 4.7a, c). This suggests that tidally driven sampling improves our ability to detect the relationship between FIB and phytoplankton in the LP model relative to daily sampling (tidal: 100% accuracy vs. daily: 75% accuracy) (Fig. 4.6c; Fig. 4.7c). This is not surprising, given the tidal forcing of modeled FIB.

When solar mortality was included in our models, tidal sampling became less powerful for reliably detecting underlying relationships between phytoplankton and FIB. This was likely due to the diel frequency of the solar signal. FIB-Chla correlations in our LP + L model were still positive 58% of the time, however, an



improvement over 33% of the time using daily sampling methods (Fig. 4.6d; 4.7d). This suggests that a tidal sampling regime has the potential to improve our ability to resolve FIB extra-enteric relationships in marine systems where FIB sources and transports are tidally driven. Notably, increased system complexity (especially the inclusion of sources or removal mechanisms that occur at different dominant frequencies; e.g. solar radiation or rainfall) may act to reduce the benefits of a tidal sampling regime relative to a diurnal one.

It is important to note that, although tidal sampling improved our ability to accurately detect FIB-phytoplankton relationships via direct correlation analysis, our results were still incorrect up to 42% of the time (Fig. 4.7d). This suggests that alternate methods are required in order to detect relationships between FIB and marine community constituents – like phytoplankton – with any confidence. Increased sample frequency and/or spatial resolution of sampling may enhance our ability to detect extra-enteric FIB relationships in marine systems. It is likely, however, that direct field measurements of FIB growth or mortality rates will prove necessary to resolve these relationships, as only rate measurements can inform us about the dynamics underlying changing concentrations of FIB.

### **Summary and Conclusions**

The results of this study show that phytoplankton can increase the survivorship (decrease mortality rates) of the fecal indicator *Enterococcus* in marine systems. These effects can significantly enhance the spatial extent and intensity of pollution events in the surfzone, but may prove difficult detect using water quality monitoring

data collected with a 1-per-day sampling regimen. Enhanced FIB persistence during bloom conditions may explain the ear, eye, and skin infections reported by beachgoers who swim/surf/dive/etc in marine waters during nontoxic phytoplankton blooms. Horner *et al.* (2010), linked a clinical case of bilateral mastoiditis (severe middle ear infection) to high bacterial loads (fecal coliforms, *Enterococcus*, and *Pseudomonas aeruginosa*, among others) and a red-tide bloom in Monterey, California. The results of our study provide experimental evidence that phytoplankton can enhance the survivorship of fecal bacteria in the manner surmised by Honner *et al.* (2010). Further work is required to identify the mechanism underlying this relationship, and to evaluate the effects of phytoplankton on FIB survivorship under varying environmental conditions.

In addition to the need to characterize FIB-phytoplankton relationships more completely, our study suggests that further evaluation of the manner in which we use field data to detect this sort of relationship is warranted. When bacterial sources release FIB at a higher frequency than data is collected, aliasing occurs. In our model simulations where FIB-Chla correlations were evaluated for tidally forced FIB sampled once-per-day, aliasing resulted in inaccurate classification of modeled FIB-phytoplankton relationships 25-67% of the time. A tidal sampling scheme increased our ability to detect relationships between FIB and phytoplankton, with fewer modeled relationships classified inaccurately (0-42%). 42% inaccuracy is still high, however, suggesting that alternative methods for evaluating these relationships are required. A more powerful approach may involve the direct measurement of FIB mortality rates *in situ*.

### Acknowledgements

This work was supported by CA SeaGrant and the California Department of Boating and Waterways. Special thanks to Xavier Mayali for providing axenic cultures of *Lingulodinium polyedrum* and Melissa Omand for her Huntington Beach chlorophyll *a* timeseries. I also wish to thank volunteers and staff from the Integrative Oceanography Division (B. Woodward, B. Boyd, D. Clark, K. Smith, D. Darnell, I. Nagy, J. Leichter, M. Omand, M. Okihiro, M. Yates, M. McKenna, S. Henderson, D. Michrokowski). Their data collection during the Huntington Beach field program (HB06) provided measurements necessary for the construction of the individual based model used in this manuscript to assess FIB-phytoplankton interactions in a realistic physical context. Chapter 4, in part, is being prepared for submission to Environmental Science & Technology, 2012, Rippey, M. A.; Franks, P. J. S., ACS Publications, 2012. The dissertation author was the primary investigator and author of this paper.

### Literature Cited

- Anesio, A. M.; Graneli, W.; Aiken, G. R.; Kieber, D. J.; Mopper, K. 2005. Effect of humic substance photodegradation on bacterial growth and respiration in lake water. *Applied and Environmental Microbiology*. 71, 6267-6275.
- Bae, S.; Wuertz, S. 2011. Survival of host-associated Bacteroidales cells and their relationship with *Enterococcus spp.*, *Campylobacter jejuni*, *Salmonella enterica* serovar Typhimurium, and adenovirus in freshwater microcosms as measured by propidium monoazide-quantitative PCR. *Applied and Environmental Microbiology*. 78: 922-932.
- Baines, S. B.; Pace, M. L. 1991. The production of dissolved organic matter by phytoplankton and its importance to bacteria: patterns across marine and freshwater systems. *Limnology and Oceanography*. 36, 1078-1090.
- Billen, G.; Fontigny, A. 1987. Dynamics of a Phaeocystis-dominated spring bloom in Belgian coastal waters. II. Bacterioplankton dynamics. *Marine Ecology Progress Series*. 37: 249-257.
- Boehm, A. B.; Grant, S. B.; Kin, J. H.; Mowbray, S. L.; McGee, C. D.; Clark, C. D.; Foley, D. M.; Wellman, D. E. 2002. Decadal and shorter period variability of surf zone water quality at Huntington Beach, California. *Environmental Science and Technology*. 36: 3885-3892.
- Boehm, A. B.; Keymer, D. P.; Shellenbarger, G. G. 2005. An analytical model of enterococci inactivation, grazing, and transport in the surfzone of a marine beach. *Water Research*. 39, 3565-3578.
- Boehm, A.; Yamahara, K.; Love, D. C.; Peterson, B. M.; McNeill, K.; Nelson, K. L. 2009. Covariation and photoinactivation of traditional and novel indicator organisms and human viruses at a sewage impacted marine beach. *Environmental Science and Technology*. 43, 8046-8052.
- Bucci, V.; Vulić, M.; Ruan, X.; Hellweger, F. L. 2011. Population dynamics of *Escherichia coli* in surface water. *JAWRA Journal of the American Water Resources Association*. 47: 611-619.
- Burnham, K. P.; Anderson, D. R. 2002. Model selection and inference: a practical information-theoretic approach, second edition. Springer-Verlag, New York.
- Byappanahalli, M. N.; Shively, D. A.; Nevers, M. B.; Sadowsky, M. J.; Whitman, R. L. 2003. Growth and survival of *Escherichia coli* and enterococci populations in the macro-alga, *Cladophora* (Chlorophyta). *FEMS Microbiology Ecology*.

46, 203-211.

- Casamatta, D. A.; Wickstrom, C. E. 2000. Sensitivity of two disjunct bacterioplankton communities to exudates from the cyanobacterium *Microcystis aeruginosa* Kutzing. *Microbial Ecology*. 40: 64-73.
- Clark, C.; De Bruyn, W. J.; Hirsch, C. M.; Aiona, P. 2010. Diel cycles of hydrogen peroxide in marine bathing waters in Southern California, USA: *In situ* surf zone measurements. *Marine Pollution Bulletin*. 60: 2284–2288.
- Clark, C.; De Bruyn, W. J.; Jakubowski, S. D., Grant. S. B. 2008. Hydrogen peroxide production in marine bathing waters: Implications for fecal indicator bacteria mortality. *Marine Pollution Bulletin*. 56: 397–401.
- Curtis, T. P.; Mara, D. D.; Silva, S. A. 1992. Influence of pH, oxygen and humic substances on ability of sunlight to damage fecal coliforms in waste stabilization pond water. *Applied and Environmental Microbiology*. 58: 1335-1343.
- Davies-Colley, R. J.; Donnison, A. M.; Speed, D. J.; Ross, C. M.; Nagels, J. W. 1999. Inactivation of faecal indicator microorganisms in waste stabilization ponds: interactions of environmental factors with sunlight. *Water Research*. 5, 1220-1230.
- Davis, E. M.; Gloyna, E. F. 1970. Bactericidal effects of algae on organisms. F. W. P. C. A., Tech. Rept.
- Easton, J. H., J. J. Gauther, M. M. Lalor, and R. E. Pitt. 2005. Die-off of pathogenic *E. coli* O157:H7 in sewage contaminated waters. *Journal of the American Water Resources Association*. 41:1187–1193.
- Facklam, R. R.; Collins, M. D. Identification of *Enterococcus* species isolated from human infections by a conventional test scheme. *Journal of Clinical Microbiology*. 4: 731-734.
- Frost, W. H.; Streeter, H. W. 1924. A study of the pollution and natural purification of the Ohio River. II: Report on surveys and laboratory studies. *Public Health Bulletin No. 143*, U.S. Public Health Service, Washington, D.C.
- Gonzalez, J. M.; Sherr, E. B.; Sherr, B. F. 1990. Size-selective grazing on bacteria by natural assemblages of estuarine flagellates and ciliates. *Applied and Environmental Microbiology*, 56: 583-589.
- Grant, S. B.; Sanders, B. F.; Boehm, A. B.; Redman, J. A.; Kim, J. H.; Mrse, R. D.; Chu, A. K.; Gouldin, M.; McGee, C. D.; Gardiner, N. A.; Jones, B. H.;

- Svejkovsky, J.; Leipzig, G. V.; Brown, A. 2001. Generation of enterococci bacteria in a coastal saltwater marsh and its impact on surf zone water quality. *Environmental Science and Technology*. 35, 2407-2416.
- Guillard, R. R. L. 1975. Culture of phytoplankton for feeding marine invertebrates. In Smith, W. L. & Chanley, M. H. [Eds.] *Culture of Marine Invertebrate Animals*. Plenum Press, New York, pp. 26–60.
- Hartke, A.; Lemarinier, S.; Pichereau, V.; Auffray, Y. 2002. Survival of *Enterococcus faecalis* in seawater microcosms is limited in the presence of bacterivorous zooflagellates. *Current Microbiology* 44, 329-335.
- Hellweger, F. L.; Bucci, V.; Litman, M. R.; Gu, A. Z.; Onnis-Hayden, A. 2009. Biphasic decay kinetics of fecal bacteria in surface water not a density effect. *Journal of Environmental Engineering*. 135: 372-376.
- Honner, S.; Kudela, R. M.; Handler, E. 2010. Bilateral mastoiditis from red tide exposure. *Journal of Emergency Medicine*. in press.
- Hsieh, J. L.; Fries, S.; Noble, R. T. 2007. *Vibrio* and phytoplankton dynamics during the summer of 2004 in a eutrophying estuary. *Ecological Applications* 17: 102–109.
- Jeanneau, L.; Solecki, O.; Wery, N.; Jarde, E.; Gourmelon, M.; Communal, P. Y.; Jadas-Hecart, A.; Caprais, M. P.; Grunau, G.; Pourcher, A, M. 2012. Relative decay of fecal indicator bacteria and human-associated markers: a microcosm study simulating wastewater input into seawater and freshwater. *Environmental Science and Technology*. 46: 2375-2382.
- Jeong, H. J.; Yoo, Y. D.; Kin, J. S.; Kin, T. H.; Kin, J. H.; Kang, N. S.; Yih, W. 2004. Mixotrophy in the phototrophic harmful alga *Cochlodinium polykrikoides* (Dinophyceae): Prey species, the effects of prey concentration, and grazing impact. *Journal of Eukaryotic Microbiology*. 51:563-569.
- Jeong, H. J.; Yoo, Y. D.; Park, J. Y.; Song, J. Y.; Kim, S. T.; Lee, S. H.; Kim, K. Y.; Yih, W. H. 2005. Feeding by the phototrophic red-tide algal predators: five species newly revealed and six species previously known to be mixotrophic. *Aquatic Microbial Ecology*. 40:133–150
- Ki, S. J.; Ensari, S.; Kim, J. H. 2007. Solar and tidal modulations of fecal indicator bacteria in coastal waters at Huntington Beach, California. *Environmental Management*. 39, 867-875.
- Kim, C. S.; Lee, S. G.; Lee, C. K.; Kim, H. G.; Jung, J. 1999. Reactive oxygen species as causative agents in the ichthyotoxicity of the red tide dinoflagellate

*Cochlodinium polykrikoides* *J. Plankton Res.* 21: 2105-2115.

- Kudela, R. M.; Cochlan, W. P. 2000. Nitrogen and carbon uptake kinetics and the influence of irradiance for a red tide bloom off southern California. *Aquatic Microbial Ecology*. 21: 31-47.
- Lake, R.,; Driver, S.; Ewington, S. 2001. The role of algae in causing coliform problems within the distribution system, p 153. Proceedings of the Second World Water Congress. International Water Association, Berlin, Germany.
- Lignell, R. 1990. Excretion of organic carbon by phytoplankton: its relation to algal biomass, primary productivity and bacterial secondary productivity in the Baltic Sea. *Marine Ecology Progress Series*. 68: 85-99.
- Maraccini, P. A.; Ferguson, D. M.; Boehm, A. B. 2012. Diurnal variation in *Enterococcus* species composition in polluted ocean water and a potential role for the enterococcal carotenoid in protection against photoinactivation. *Applied and Environmental Microbiology*. 78: 305-310.
- Mourino-Perez, R. R.; Worden, A. Z.; Azam, F. 2003. Growth of vibrio cholerae O1 in red tide waters off California. *Applied and Environmental Microbiology*. 69, 6923-6931.
- Muela, A.; Garcia-Bringas, J. M.; Seco, C.; Arana, I.; Barcina, I. 2002. Participation of oxygen and the role of exogenous and endogenous sensitizers in the photoinactivation of *Escherichia coli* by photosynthetically active radiation, UV-A and UV-B. *Microbial Ecology*. 44, 354-364.
- Myklestad, S. M. 1995. Release of extracellular products by phytoplankton with special emphasis on polysaccharides. *Science of The Total Environment*. 165: 155-164.
- Ogino, H.; Kumagai, M.; Yasumoto, T. 1997. Toxicologic evaluation of yessotoxin. *Natural Toxins*. 5: 255-259.
- Omand, M. M.; Leichter, J. J.; Franks, P. J. S.; Guza, R. T.; Lucas, A. J.; Feddersen, F. 2011. Physical and biological processes underlying the sudden surface appearance of a red tide in the nearshore. *Limnology and Oceanography*. 56, 787-801.
- Rogers, S. W.; Donnelly, M.; Peed, L.; Kelty, C. A.; Mondal, S.; Zhong, Z.; Shanks, O. C. 2011. Decay of bacterial pathogens, fecal indicators, and real-time quantitative PCR genetic markers in manure-amended soils. *Applied and Environmental Microbiology*. 77: 4839-4848.

- Seong, K. A.; Jeong, H. J.; Kim, S.; Kim, G. H.; Kang, J. H. 2006. Bacterivory by co-occurring red-tide algae, heterotrophic nanoflagellates and ciliates. *Marine Ecology Progress Series*. 322: 85-97.
- Sinton, L. W.; Donnison, A. M.; Hastie, C. M. 1993b. Faecal streptococci as faecal pollution indicators: a review. Part II: Sanitary Significance, Survival and Use. *New Zealand Journal of Marine and Freshwater Research*. 27: 117-137.
- Sinton, L. W.; Finlay, R. K.; Lynch, P. A. 1999. Sunlight inactivation of fecal bacteriophages and bacteria in sewage-polluted seawater. *Applied and Environmental Microbiology*. 65, 3605-3613.
- Sinton, L. W.; Hall, C. H.; Lynch, P. A.; Davies-Colley, R. J. 2002. Sunlight inactivation of fecal indicator bacteria and bacteriophages from waste stabilization pond effluent in fresh and saline waters. *Applied and Environmental Microbiology* 68, 1122-1131.
- Solic, M.; Krstulovic, N. 1992. Separate and combined effects of solar radiation, temperature, salinity, and pH in the survival of fecal coliforms in seawater. *Marine Pollution Bulletin*. 24, 411-416.
- Surbeck, C. Q.; Jiang, S. C. Grant, S. B. 2010. Ecological control of fecal indicator bacteria in an urban stream. *Environmental Science and Technology* 44, 631-637.
- Strauss, E. 1999. A symphony of bacterial voices. *Science*. 284: 1302–1304.
- Velz, C. J. 1984. Applied stream sanitation, 2nd ed. John Wiley & Sons, Inc., New York, NY.
- Whitman, R. L.; Shively, D. A.; Pawlick, H.; Nevers, M. B.; Byappanahalli, M. N. 2003. Occurrence of *Escherichia coli* and enterococci in *Cladophora* (Chlorophyta) in nearshore water and beach sand of Lake Michigan. *Applied and Environmental Microbiology*. 69: 4714-4719.
- Wolter, K. 1982. Bacterial incorporation of organic substances released by natural phytoplankton populations. *Marine Ecology Progress Series*. 7: 287-295.
- Yamahara, K. M.; Sassoubre, L. M.; Goodwin, K. D.; Boehm, A. B. 2012. Occurrence and persistence of bacterial pathogens and indicator organisms in beach sand along the California coast. *Applied and Environmental Microbiology*. 78: 1733-1745.
- You, Y.; Rankin, S. C.; Aceto, H. W.; Benson, C. E.; Toth, J. D.; Dou, Z. 2006.



Survival of *Salmonella enterica* serovar Newport in manure and manure-amended soils. *Applied and Environmental Microbiology*. 72: 5777–5783.

Zhu, X.; Wang, J. D.; Solo-Gabriele, H. M.; Fleming, L. E. 2011. A water quality modeling study of non-point sources at recreational marine beaches. *Water Research*. 45: 2985-2995.

**Table 4.1:** A comparison of first-order exponential and biphasic decay models for enterococci (w & w/o phytoplankton)

Treatment	Model Form	Model Parameters				RMSE (MPN 100 ml <sup>-1</sup> )	AICc
		$C_0$ (MPN 100 ml <sup>-1</sup> )	$a$	$k_s$ (h <sup>-1</sup> )	$k_R$ (h <sup>-1</sup> )		
<i>L. polyedrum</i>	exponential	5498.63 (± 346.6)	--	-0.0780 (± 0.0123)	--	861.8	430.22
	biphasic	5671.05 (± 496.19)	0.3491 (± 0.1763)	-0.1753 (± 0.0592)	-0.0082 (± 0.0109)	686.6	419.92*
No plankton	exponential	5220.77 (± 295.6)	--	-0.1307 (± 0.0155)	--	701.0	435.43
	biphasic	5461.29 (± 452.08)	0.3205 (± 0.0941)	-0.3237 (± 0.0802)	-0.0196 (± 0.0122)	553.3	424.17*

\* biphasic models perform better than exponential models (AICc biphasic < AICc exp + 2 IC units)

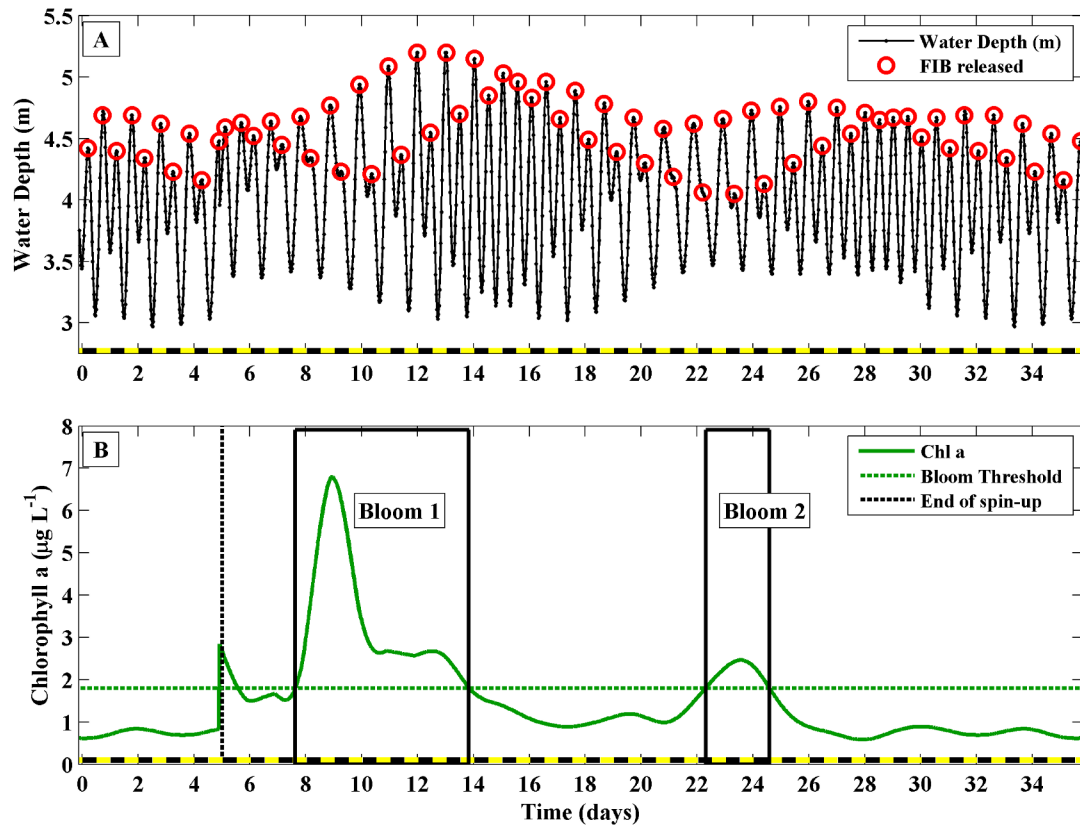


**Figure 4.1:** **A)** Observed water depth (m) and **B)** chlorophyll a (Chl a) concentration ( $\mu\text{g L}^{-1}$ ) at Huntington Beach, California, in fall 2006. Time (days) is on the  $x$ -axis for both plots. A yellow (day) and black (night) dashed colored line is used to depict day-night cycles. In **A)** red dots mark high tide, which was used to force FIB release events in our NP, LP, NP + L and LP + L models. In **B)** a green dashed line indicates the bloom threshold used to force a binary response to phytoplankton concentration in our LP and LP + L models. The bloom threshold was exceeded 3 times, although one was minor. The two larger events (bloom 1 and 2) are marked with black boxes. All models were run for 5 days to allow them to stabilize. The end of this spin-up phase is marked by a black dashed line.

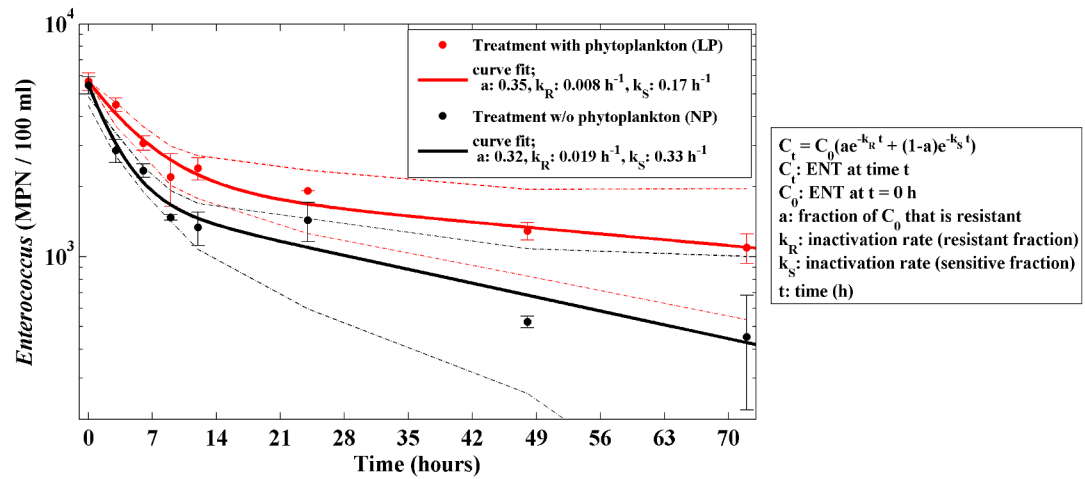


**Figure 4.2:** Biphasic mortality of *Enterococcus faecium* in seawater microcosm treatments with (red) or without (black) the phytoplankter *Lingulodinium polyedrum*. Curve fits and mortality rates were estimated using the equation in the box to the right. 95% confidence intervals for fits are shown using dashed lines.

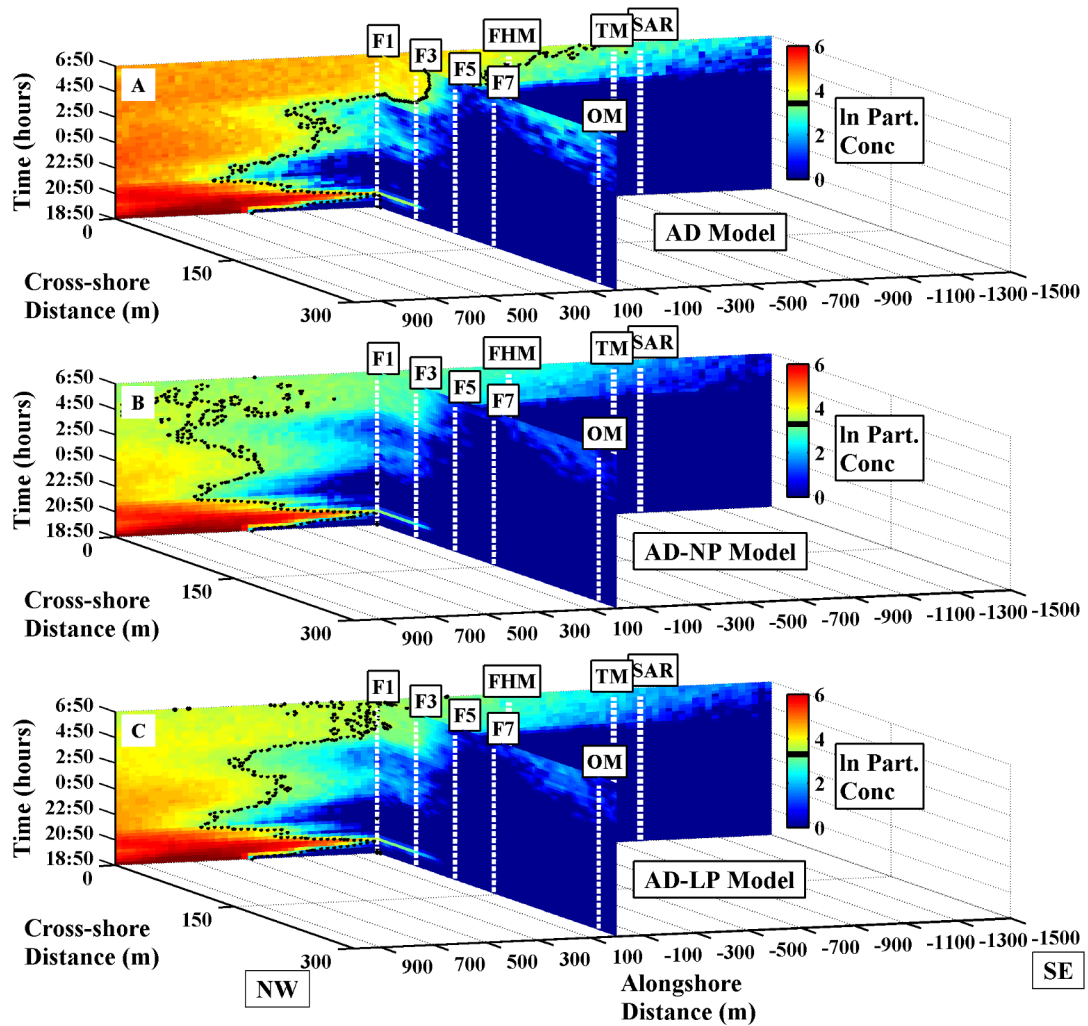


**Figure 4.3:** Along and cross-shore transport of FIB particles at Huntington Beach, under three model scenarios: **A)** shows the AD (advection + diffusion) model, **B)** shows the AD\_NP (advection + diffusion + no phytoplankton) model, and **C)** shows the AD\_LP (advection + diffusion + *L. poyedrum*) model. All plots are oriented with alongshore distance (m) on the long axis. Distance is relative to the alongshore location of the cross-shore transect at 0 m (F1, F3, F5, F7, OM). Negative alongshore values are to the south of the transect (FHM, TM, and SAR), and positive alongshore values are to the north of the transect. Cross-shore distance (m) is on the short axis, with F1 at the shoreline and OM ~ 300 m offshore. Time (h) is on the vertical axis, increasing upwards. The colorbar is natural log of FIB particle concentration ( $\ln$  MPN  $100\text{ ml}^{-1}$ ). In all models FIB particles were released at 1850 (high tide), between 500 and 1000 m in the alongshore. Black dots mark the along and cross-shore progression of the 35 MPN  $100\text{ ml}^{-1}$  EPA geometric mean standard for *Enterococcus*.

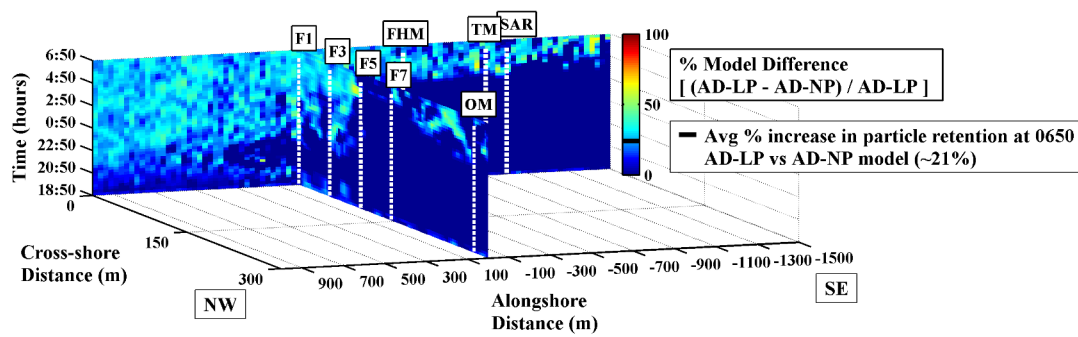


**Figure 4.4:** Plot of percent difference in particle retention between the AD\_LP model (with phytoplankton) and the AD\_NP model (without phytoplankton). Plot orientation is the same as in Fig. 4.3. The colorbar is percent model difference. This statistic is calculated by taking the difference between particle concentration in the AD\_LP and AD\_NP models, and normalizing by the AD\_LP model. At 0650, the average percent increase in FIB particle retention for the AD\_LP model was 21% (black line on colorbar).

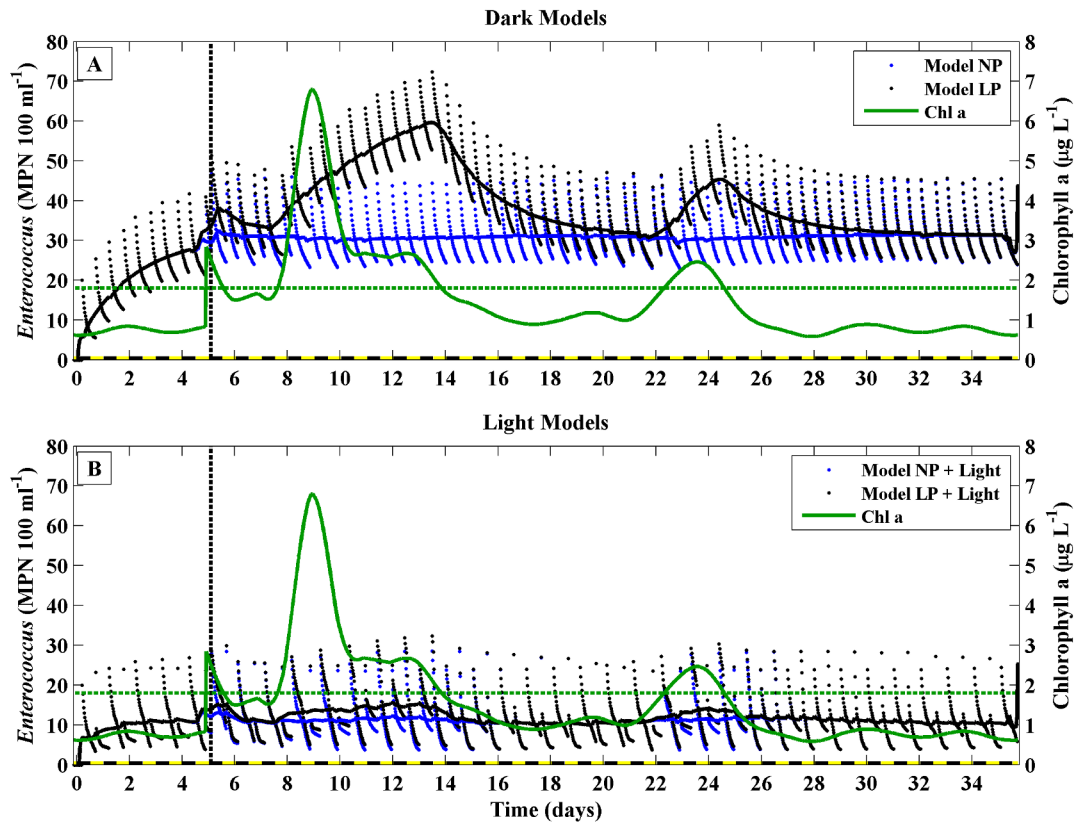
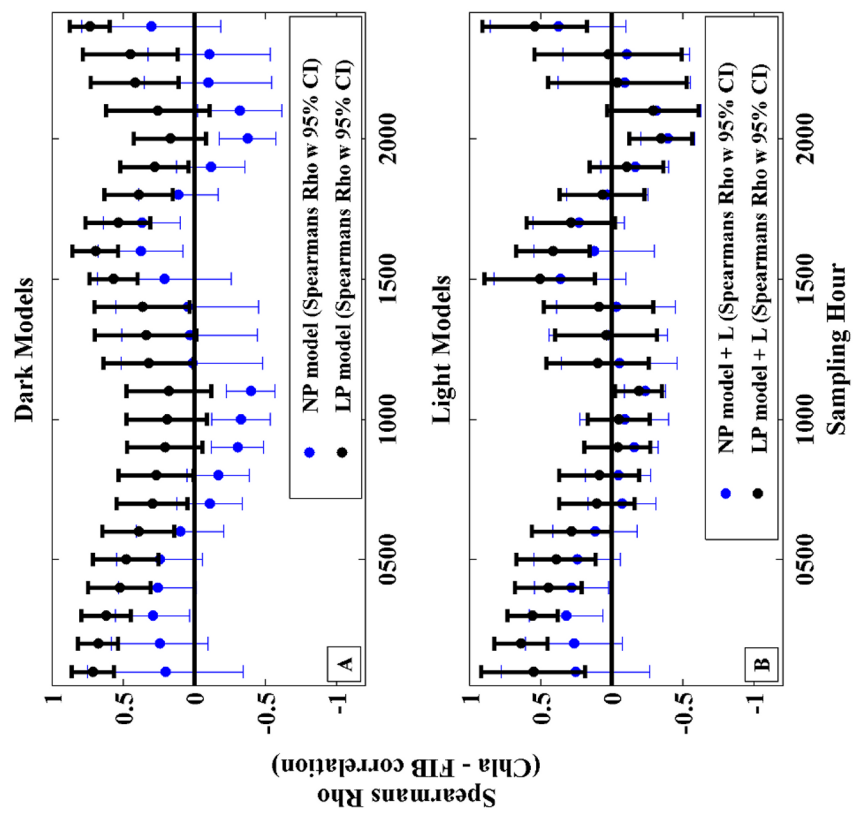
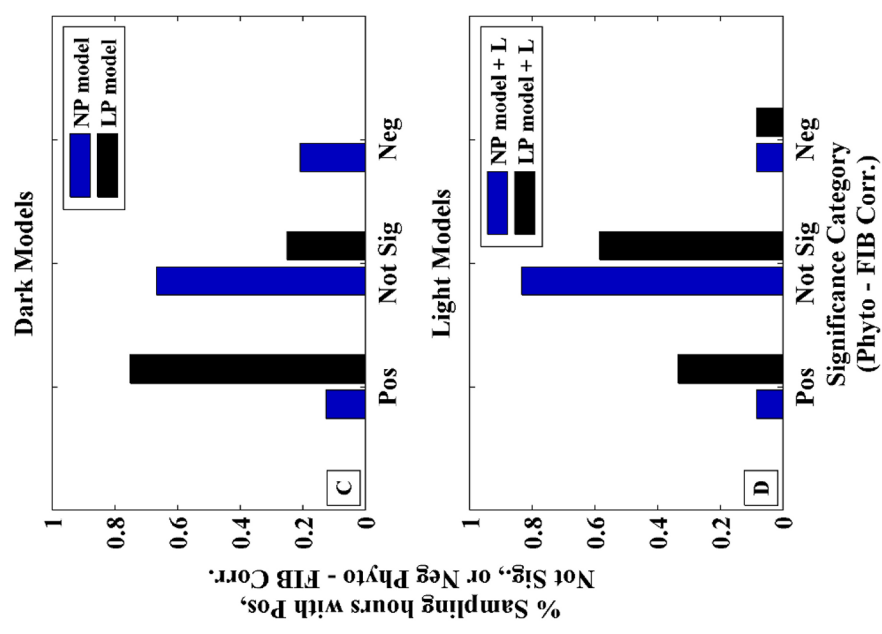


**Figure 4.5:** Timeseries of modeled *Enterococcus* and Huntington Beach chlorophyll a concentrations. For both plots time (days) is on the  $x$ -axis, chlorophyll a concentration ( $\mu\text{g L}^{-1}$ ) is on the right  $y$ -axis, and *Enterococcus* concentration (MPN 100  $\text{ml}^{-1}$ ) is on the left  $y$ -axis. A yellow (day) and black (night) dashed colored line depicts day-night cycles. The dashed green line is the phytoplankton bloom threshold, and the dashed black line marks the end of our model spin-up phase. *Enterococcus* data generated from models where mortality was (LP and LP + L) or was not (NP and NP + L) a function of phytoplankton concentration are shown with black and blue dots, respectively. Daily average *Enterococcus* concentrations are shown using solid lines of the corresponding color. Results from dark models (NP and LP), with no solar FIB mortality, are shown in **A**). Results from light models (NP + L and LP + L), where mortality was a function of solar radiation, are shown in **B**).

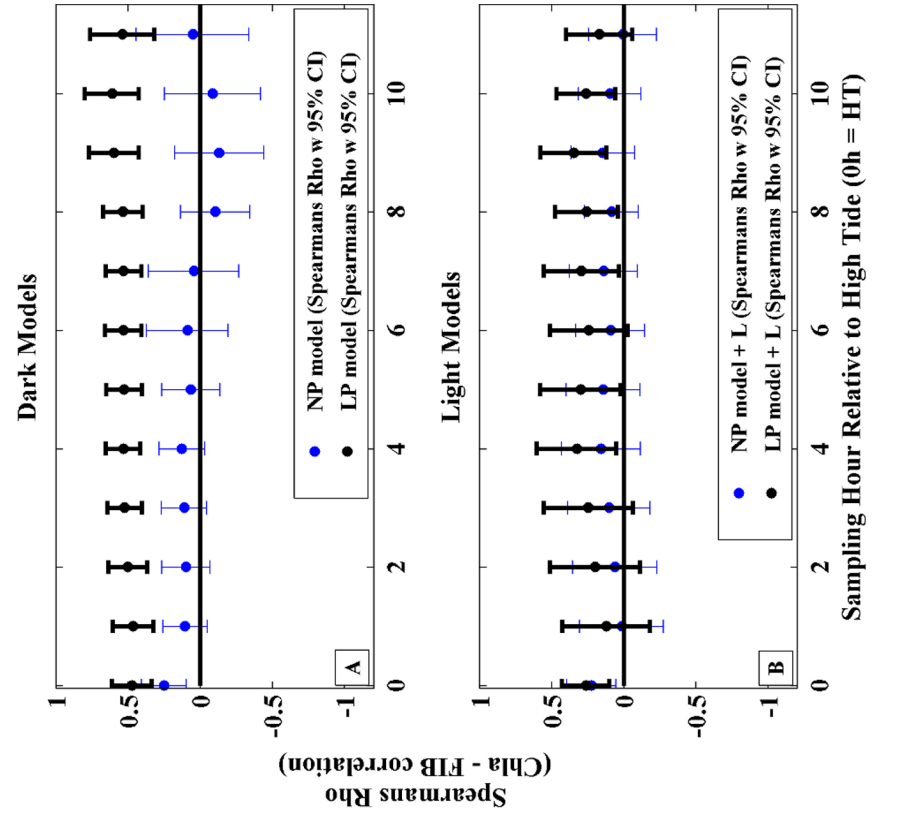
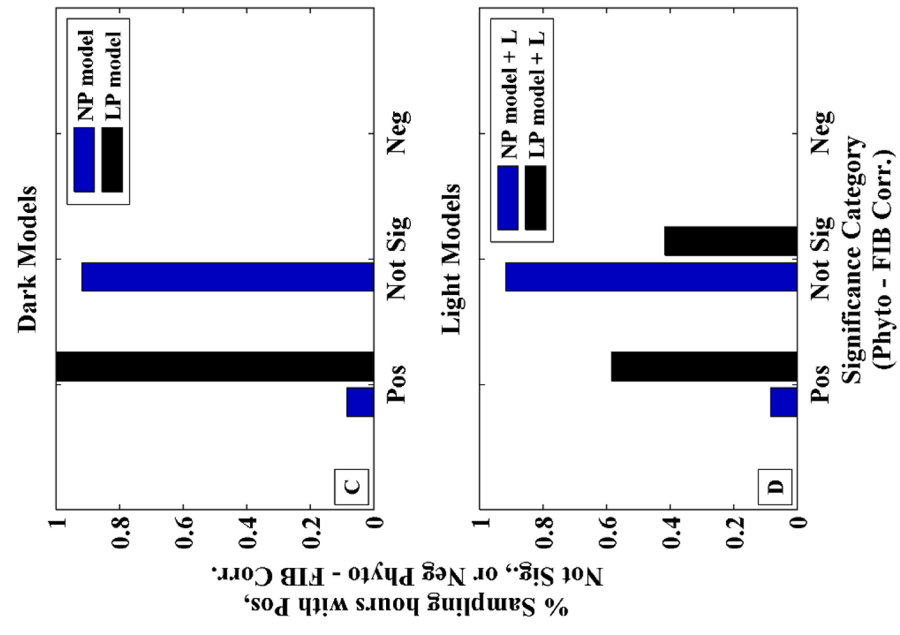
**Figure 4.6: A & B)** *Enterococcus* – chlorophyll a correlation coefficients (Spearman's Rho) evaluated at all possible sampling hours. Sampling hour is on the *x*-axis, with 0100 (the first timepoint) corresponding to samples at 1 am, and 2400 (the last timepoint) to midnight samples. All estimates of Spearman's Rho are shown with 95% confidence intervals. Correlation coefficients for models where FIB mortality was a function of phytoplankton concentration (LP and LP + L) are shown in black. Models where FIB and phytoplankton concentrations are independent (NP and NP + L) are shown in blue. **C & D)** Bar graphs showing the percent of sampling hours with positive, negative or non-significant correlations between *Enterococcus* and chlorophyll a. Significance category (positive, negative or non-significant) is on the *x*-axis, and the percent of sampling hours that fall within each category is on the *y*-axis. The color scheme is identical to **A** and **B**. Models where FIB were solar sensitive are on the bottom (**B & D**). Dark models are on the top (**A & C**).



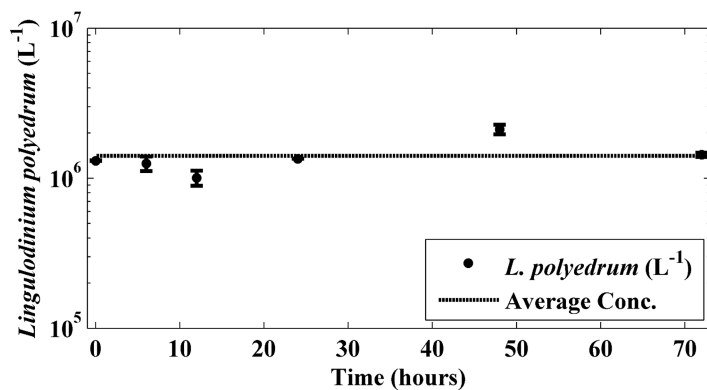


Spearman's Rho (Chla - FIB correlation)

**Figure 4.7: A & B)** *Enterococcus* – chlorophyll a correlation coefficients (Spearman's Rho) evaluated at high tide, and every hour following high tide, for a total of 11 hours. The  $x$ -axis is sampling hour relative to high tide which occurs at  $t = 0$  h). Otherwise, plot orientation and color is identical to Fig. 4.6. **C and D)** Bar graphs showing the percent of (tidal) sampling hours with positive, negative, or non-significant correlations between *Enterococcus* and chlorophyll a. Plot orientation and color is also identical to Fig. 4.6.



## Appendix 4.1: Supplementary Figures



**SI Figure 4.1:** Timeseries of *Lingulodinium polyedrum* concentration in experimental microcosms containing phytoplankton. Time (h) is on the *x*-axis, and *L. polyedrum* concentration (cells ml<sup>-1</sup>) is on the *y*-axis. Error bars are standard error from replicate seawater microcosms. The average concentration of *L. polyedrum* averaged over the experiment duration (72 h) is marked by a dashed black line.

## CHAPTER 5.

### BEACH NOURISHMENT IMPACTS ON BACTERIOLOGICAL WATER QUALITY AND PHYTOPLANKTON BLOOM DYNAMICS

#### **Abstract**

In 2009 the Sediment Fate and Transport Study performed a beach nourishment with fine-grained sediments ( $< 63 \mu\text{m}$ ) at Border Field State Beach (BFSB), near California's San Diego-Mexico border. The study was designed to monitor the fate and transport of this material in the nearshore/surfzone as well as its effects on local bacteriological water quality, phytoplankton communities, benthic, and epibenthic fauna. Here we examine the bacteriological water quality and phytoplankton component of the study. We found that nourishment material had no obvious affect on phytoplankton patchiness or bloom formation at BFSB, and that phytoplankton were most strongly correlated with nitrate, tide height, and alongshore current direction ( $p < 0.05$ ). In contrast, nourishment sediments were found to be a clear source of the fecal indicator *Enterococcus*; Spearman's rank correlations between fines and enterococci were highly significant ( $p < 0.01$ ), and generalized linear model analysis identified fine sediments as the single best predictor of enterococci during our study. Although high concentrations of enterococci were released into the surfzone with nourishment sediments, the residence time of these fecal indicators was short ( $\sim 23$  h). By combining microcosm experiments and field sampling, we were able to determine that these short residence times were driven by a combination of rapid FIB inactivation immediately post placement (e-folding rate of  $\sim 5.5 \times 10^{-2} \text{ s}^{-1}$ ) and

physical dilution/mixing.

### **Introduction**

Fine-grained sediments (<63  $\mu\text{m}$  in size) are natural constituents of nearshore waters along the coast of California. In the greater San Diego area, episodic river inputs are the dominant source of fine sediments, discharging  $\sim 0.40 \text{ Mt y}^{-1}$  (Farnsworth and Warrick, 2007). In these flows, fine material may dominate the suspended sediment load ( $\sim 77\%$  in the Tijuana river), making fines an important contributor to local marsh and beach sediments (Farnsworth and Warrick, 2007).

Despite the natural contribution of fines to Southern California's beaches, all material used for opportunistic beach nourishments must be < 20% fines (silt and clay) unless 1) the grain size distribution matches that of the proposed placement site or 2) it meets chemical/biological contamination criteria and is unlikely to negatively impact natural resources in the area (U.S CFR 404b). These regulations are intended to ensure that sediment placements do not deleteriously affect water quality, ecosystem function, circulation, salinity gradients, or aquatic organisms. Our understanding of the effects fine sediments have on these processes, however, is limited, making the potential impacts of a nourishment with fine material difficult to predict. Here we present results from “The Sediment Fate and Transport Study”, exploring the effects of a beach nourishment composed of > 20% fines on concentrations of fecal indicator bacteria (water quality) and phytoplankton (aquatic organisms) at Border Fields State Beach (BFSB), California. The study was part of a larger field campaign that also monitored the fate and transport of fines in the surfzone/nearshore and their effects on

local benthic and epibenthic fauna.

This study chose to evaluate the impacts of fine sediments on phytoplankton and fecal indicator bacteria because the rapid growth/mortality rates of these organisms in coastal waters makes them ideal for monitoring short-term responses to episodic events like sediment placements (Sinton et al., 2002; Calbet and Landry, 2004; Yamahara et al., 2009). Nuisance phytoplankton blooms have been closely linked to inorganic nutrient inputs from natural and/or anthropogenic sources (Pennock and Sharp, 1994; Xu et al., 2008; Cloern and Jassby, 2010). These inorganics (especially phosphate) often exhibit elevated concentrations in the fine fraction of sediments due to the attraction of cations ( $\text{Ca}^{2+}$ , and  $\text{Fe}^{3+}$ ) to negatively charged clay particles (Andrieux-Loyer and Aminot, 2001). These cations reversibly bind nutrients, forming a reservoir of complex nutrient salts that are readily converted to bioavailable forms in seawater (Aminot and Andrieux-Loyer, 1996). For this reason a beach nourishment with fine sediments might be expected to induce phytoplankton blooms by providing episodic inputs of the inorganic nutrients required for growth.

Fine-grained sediments have also been shown to harbor high concentrations of fecal indicator bacteria (FIB) (Evanson and Ambrose, 2006; Guber et al., 2007). FIB are non-pathogenic enteric bacteria that are used to track bacterial pathogens in coastal systems due to their high concentrations in human and animal waste (Sinton et al., 1993a). FIB are strongly associated with infection (ear, eye, and skin) and gastrointestinal illness in humans (flu-like symptoms including fever, vomiting, and diarrhea) (Cabelli et al., 1982, Pruss et al., 1998; Turbow et al., 2003). Disease incidence tends to be higher for people engaging in recreational activities that involve

full seawater immersion (swimmers and surfers) or “sand contact activities” (digging or being buried in sand) (Henrickson et al., 2001; Heaney et al., 2009). Because concentrations of FIB in sediment can exceed those reported in coastal waters by 10-100 fold (Yamahara et al., 2007; Halliday and Gast, 2011), and FIB attachment to fine-grained material may exceed attachment to coarser particles (Jeng et al., 2005; Guber et al., 2007), a fine-sediment beach nourishment has the potential to pose a significant health risk to beach goers.

## **Methods**

### ***Field Site Description:***

Border Field State Beach (BFSB) is an ~ 2.4 km stretch of Southern California beachfront, with its southern edge at the San Diego-Mexico border. This beach is backed by the Tijuana Estuary, which receives large volumes of sediment and water from the Tijuana River watershed (Callaway and Zedler, 2004; Wallace et al., 2005; Farnsworth and Warrick, 2007). This watershed covers approximately 4,450 km<sup>2</sup> in both Mexico and California (Ojeda-Revah et al., 2008; Elwany, 2011). During the rainy season, watershed discharge to BFSB often contains elevated levels of fecal indicator bacteria (total coliforms, enterococci and *E. coli*), viruses (hepatitis A and adenoviruses), heavy metals, and sediment (Gersberg et al., 2000; Jiang et al., 2001; Gersberg et al., 2004; Brooks et al., 2005; Gersberg et al., 2006; Farnsworth and Warrick, 2007). Habitat loss due sediment discharge in the estuary prompted the construction of the Goat Canyon Retention Basin in 2005 (Elwany, 2011). This basin traps more than 40,000 cubic yards of sediment annually, and yet is still insufficient to



capture the sediment loads expected during an above average rainfall event (Elwany, 2011; Warrick et al., 2012).

***Beach Nourishment:***

35,000 cubic yards of sediment was placed on BFSB between 9/21 and 10/2/09. Sediments were pre-screened in 2008 for chemical and biological hazards, and declared safe for placement. The sediments used for the nourishment contained 26-46% fines (grain size <63 mm). In the BFSB surfzone, concentrations of suspended fines were typically low ( $\sim 0.01 \text{ g L}^{-1}$  or less), making fines a good tracer for nourishment material. All sediments were dredged from the Goat Canyon Retention Basin in the Tijuana River Estuary, and sieved to remove trash and large debris. Sediments were trucked to the beach and placed according to the schedule in SI Table 5.1. All sediment was placed at station HT (Fig. 5.1), below the high tide line.

***Biological Monitoring Program:***

***Sample Collection***

From 9/21 - 10/13/09, concentrations of suspended fine sediments, sands, the FIB enterococci, nutrients (phosphate, nitrate, nitrite, ammonia, and silicate) and chlorophyll a (Chla), a proxy for phytoplankton, were monitored in surfzone waters at BFSB and Imperial Beach (directly to the north of BFSB). All water samples were collected between 0430 and 0530 in knee-deep water. Samples were taken at eight alongshore stations spanning  $\sim 3.3 \text{ km}$ ; BF, S1, HT, M, N1, N2, TJR, and F1 (Fig. 5.1).

F1 was the only station located at Imperial Beach itself, and was situated ~ 600 m south of the Imperial Beach pier. Daily samples were collected at three of eight stations (HT, TJR, and F1), and analyzed for all constituents. The five additional stations (BF, S1, M, N1, and N2) were sampled every other day for all variables except Chla. Pressure sensors, temperature loggers, and Acoustic Doppler velocimeters (ADVs) were deployed at station F1 and five additional stations in the cross-shore; F2, F3, VS, F5 and F6 (Fig. 5.1). Measurements from these six locations were used to estimate tide height, temperature, and alongshore current speed/direction during our study. These physical measurements were courtesy of the Imperial Beach 2009 project (IB09, R.T. Guza and F. Feddersen, SIO, PIs).

### Sample Analyses

Water samples were analyzed for enterococci within 2 hours of collection using IDEXX Enterolert. To quantify Chla concentrations, samples were filtered onto triplicate GF/F filters and pigments were extracted with 90% acetone, for 24 hours, in the freezer. Extracted samples were quantified on a Turner Designs T700 fluorometer. The Chla concentrations calculated here can be thought of as “raw” concentrations, as the phaeophytin signal was not removed.

Water samples for nutrient analyses were frozen within 2 hours of collection and shipped to MSI Analytical Laboratories. Concentrations of dissolved silicate, phosphate, nitrite, nitrate + nitrite, and ammonium were enumerated using flow injection analysis. Water samples for the analysis of fine sediment and sand concentrations were refrigerated, and shipped via overnight mail to the USGS PCMSC

Sediment Laboratory in Menlo Park, California. To determine suspended-sediment concentration, samples were wet sieved through a 63 $\mu$ m sieve. This separated them into sand (> 63  $\mu$ m) and fine (< 63  $\mu$ m) fractions, which were dried and weighed.

***Enterococci in Nourishment Sediments:***

Samples of sediment from nourishment material were collected on 9/25/09 and 10/1/09. Three separate placements were sampled between 0700 and 0730 on each sampling day, resulting in a total of six samples. To enumerate enterococci, 10g of sediment per sample was suspended in 100ml of MQ water. The mixture was shaken by hand for two minutes to dislodge bacteria, and allowed to settle for one minute. The supernatant was collected and analyzed for enterococci using IDEXX Enterolert.

To test for false *Enterococcus* positives in our Enterolert assays, ten positive and ten negative Enterolert wells were biochemically screened. The back of the quantitray was disinfected with 70% alcohol and medium was withdrawn from each well using sterile syringes. The medium was plated on brain heart infusion agar (1 plate per Enterolert well) and allowed to grow for 48 hours (35°C). 1-3 isolates were picked from each plate exhibiting growth and subjected to the following seven biochemical tests: a gram stain, a catalase test, disk tests for pyrrolidonyl aminopeptidase (PYR) and lucine arylamidase (LAP) (Remel, Inc., Lenexa, KS, USA), growth in brain heart infusion broth at 45°C and with 6.5% NaCl (35°C), and hydrolysis of esculatin in the presence of 40% bile salts (35°C). All isolates that were gram positive, catalase negative, PYR and LAP positive, hydrolyzed esculatin, and grew at both 45°C and in the presence of 6.5% NaCl, were identified as *Enterococcus*

(American Society for Microbiology 2003).

### ***Water Quality Assessment: Correlations and Predictive Statistical Models***

Two methods were used to identify parameters for predicting enterococci or Chla at BFSB. First, direct correlations between all measured parameters (tide height, temperature, alongshore velocity, fines, sands and nutrients) were assessed. Because data distributions were non-normal, correlation was evaluated using Spearman's rank (rho). The significance of these correlations was determined using bootstrap methods; data were sampled with replacement 100,000 times, and rho was estimated for each new data set. 95% bias-corrected bootstrap confidence intervals (CI's) were calculated. When rho of 0 fell outside those 95% CI's, correlations were determined to be significant ( $p \leq 0.05$ ).

Generalized linear models (GLM's) were also used to identify significant predictors of enterococci or Chla during our study. GLM's are multiple linear regression models that allow for response variables with non-normal distributions. Chla measurements were modeled as a gamma distribution with a log-link, as in Vargas *et al.*, (2009). Concentrations of enterococci were modeled as presence/absence data using a binomial GLM with a logit link. Presence was defined as  $\geq 10$  MPN 100 ml<sup>-1</sup>, and absence as  $< 10$  MPN 100 ml<sup>-1</sup> of seawater.

Because alongshore velocity and temperature were only measured at one sampling station, and this sampling station (F1) was separated from other stations by both a river outlet and a bend in the coast (Fig. 5.1), these parameters were excluded from GLM analyses. All combinations of the remaining parameters (fine sediments,

sands, nitrate, nitrite, ammonium, silicate, phosphate and tide height) were explored. Second-order interaction terms were also evaluated. Functional marginality was invoked so that no model could contain second-order interaction terms without also containing both main effect variables (Nelder, 2000). All models were parameterized using maximum likelihood estimation. Best-fit models were identified using the Bayesian Information Criterion (BIC), which is a more consistent selection criteria than AIC (De Luna and Skouras, 2003; Yang, 2005). All GLM analyses were performed in R using the statistical routine *glmulti* (Calacagno and de Mazancourt, 2010).

#### ***Surfzone Residence Time of Enterococcus:***

On four separate dates surfzone concentrations of enterococci were monitored at HT station every 30 minutes for 4 h. Sampling occurred on 9/26, 9/27, 9/29, and 10/1. The time ( $\Delta t$ ) between the midpoint of each sampling event and the most recent nourishment was calculated for all dates. We refer to this  $\Delta t$  as time-since-placement. All sampling events occurred either during or after placements containing  $\geq 2,240$  CYs of sediment. Concentrations of enterococci (averaged over each sampling event) were evaluated with respect to time-since-placement, to determine rough residence times for nourishment-associated enterococci in the surfzone. Surfzone residence times reflect losses due to physical transport and bacterial inactivation (mortality + loss due to induction of a viable but not cultural state). Microcosm experiments, discussed below, were used to quantify the inactivation component directly.

### ***Enterococcus Inactivation: Microcosm Experiments***

Inactivation rates of nourishment-associated enterococci were evaluated in the surfzone on 10/1/09 using field deployable seawater microcosms. Microcosm experiments eliminate physical dilution of bacteria, which can be a dominant source of loss in the surfzone (Boehm 2003; Boehm et al., 2005; Rippy et al., submitted m.s. 1). All microcosms were mounted on a floating platform (DrEMP; Drifting *Enterococcus* Mortality Platform), moored in the surfzone, shoreward of breaking waves.

#### *Microcosm Platform: DrEMP*

DrEMP is a floating frame that maintains 22, 250 ml microcosms in ~1 m water depth (SI Fig. 5.1). All microcosms were constructed from fused silica, which allows the penetration of potentially bactericidal UV wavelengths in addition to the visible spectrum (Bell et al., 1993; Davies-Cooley et al., 1994). Half the microcosms were left uncovered and the remainder were enclosed in black plastic to eliminate light penetration. This allowed us to evaluate the contribution of solar radiation to inactivation rates of nourishment-associated enterococci. DrEMP was equipped with a PAR sensor to quantify solar radiation during our experiments (Alec Electronics MDS-MKV/L, 360-690 nm) (JFE Advantech Co., Ltd). Similar sensors were deployed on additional dates (10/3/09 - 10/30/09) when no nourishment took place to evaluate surfzone solar penetration in the absence of the sediment plume.

#### *Microcosm Sample Collection:*

On 10/1/09 sediment placement began at 0700 and continued until 1700. At

0735, a 5 L surfzone sample containing suspended nourishment sediments and seawater was collected, shaken, and distributed into the 22 silica microcosms on the DrEMP platform. DrEMP was deployed by 0755, and the first samples (1 light and 1 dark microcosm) were removed and placed on ice at 0800. Subsequent pairs of samples were taken every 30 minutes for five hours. All samples were analyzed for concentrations of enterococci within six hours of collection, using IDEXX Enterolert.

### **Results and Discussion:**

#### ***Physical Environment:***

In fall 2009, the cross-shore averaged (16 – 140 m cross-shore) alongshore current in our sampling domain was predominantly northward, reflecting south swell conditions. At two times during our study, however, (9/30 - 10/1/09 and 10/4 - 10/5/09) alongshore flows were southward, reflecting west to northwest swell (Fig. 5.2a). Some southward flow was also observed at the beginning of the study (9/21 – 9/23/09), when alongshore currents were found to change direction in phase with the tide (Fig. 5.2a, c). Maximum southern alongshore velocities were  $\sim 0.25 \text{ ms}^{-1}$  and maximum northern alongshore velocities were  $\sim 0.39 \text{ ms}^{-1}$  (Fig. 5.2a). Two thirds of the sediment placements performed during our study took place when alongshore currents were to the north, suggesting that these sediments (and any associated contaminants) were transported northward towards Imperial Beach proper.

During the study period, cross-shore averaged water temperature exhibited strong diel cycling, and an overall trend towards lower temperatures. Averaged over all stations and times, water temperature was  $\sim 18^\circ\text{C}$  (max:  $21^\circ\text{C}$  and min:  $16.2^\circ\text{C}$ ).

Most sediment placements occurred during the warmer half of the study, prior to 9/29/09 (Fig. 5.2b). Placements occurred both on neap and spring tides (Fig. 5.2c).

### ***Water Quality Assessment: Phytoplankton***

#### *Spatio-temporal Patterns in Chla:*

Surfzone concentrations of Chla ranged from 2-10 mM during our study. High concentration Chla peaks, correlated in the alongshore, were observed three times during this study (Fig. 5.3a). An additional peak was also observed at the Tijuana River outlet near the end of the study (Fig. 5.3a). Alongshore-parallel bands of Chla are common in the nearshore and can be caused by a variety of processes including vertical mixing of subsurface phytoplankton blooms via internal wave breaking (Omand et al., 2011), alongshore transport/mixing of localized blooms by wind and wave driven currents (Tester et al., 1991; McPhee-Shaw et al., 2011), and point/non-point source release of nutrients coupled with mixing and alongshore transport (Hewson et al., 2001; Cembella et al., 2005). We evaluated the association between alongshore transport, nutrients, tides, and phytoplankton at BFSB using both direct correlation analyses and GLM's.

#### *Parameter Correlations:*

Chla concentrations were significantly, and inversely, correlated with surfzone nitrate concentrations and tide height ( $p < 0.01$ ) (Fig. 5.3; SI Table 5.2). Chla was also correlated with alongshore water velocity: low Chla levels (2-4  $\mu\text{M}$ ) were observed during strong northward flows ( $>0.2 \text{ ms}^{-1}$ ), and high Chla levels (4-10  $\mu\text{M}$ ) during



southward or weak northward ( $<0.2 \text{ ms}^{-1}$ ) flows ( $p < 0.05$ ) (Fig. 5.3; SI Table 5.2).

Chla was not correlated with fine sediments from the beach nourishment or any of the four additional inorganic nutrients measured (silicate, phosphate, nitrite, or ammonium) (SI Table 5.2). This implies that the BFSB nourishment did not impact surfzone water quality by stimulating nuisance phytoplankton blooms.

The lack of observed correlation between nourishment sediments and Chla may reflect the nutrient composition of the nourishment material. During our study, nourishment sediments were well correlated with concentrations of phosphate, but not nitrogen (nitrate, nitrite or ammonium) (Fig. 5.3; SI Table 5.2). The nitrogen to phosphorous ratio (N:P) in surfzone waters at BFSB was always below 16 (the Redfield ratio), suggesting nitrogen (not phosphorous) limitation of phytoplankton growth (Redfield, 1934; Redfield, 1958; Smith, 2006) (SI Fig. 5.2). Thus, nourishment sediments would not be expected to fuel phytoplankton blooms because they are rich in a non-limiting nutrient (phosphate).

It may be that the phytoplankton dynamics we observed at BFSB reflect physical transport of bloom waters rather than individual bloom events. The inverse relationship detected between nitrate and Chla at BFSB is consistent with nitrate uptake by phytoplankton in a given water mass (Koike et al., 1982; Smith et al., 1995; Rocha et al., 2009). In light of the association between Chla and physical processes (alongshore current direction & tide height) at BFSB, this relationship may point to episodic physical transport of phytoplankton-rich/nutrient-poor waters into and out of the surfzone as the primary mechanism driving the phytoplankton patterns we observed.

Generalized Linear Model Analyses:

Our GLM analyses identified both tide height and nitrate as important parameters for predicting Chla concentrations at BFSB (note that alongshore currents were excluded from these analyses). In total, two best-fit predictive models for Chla concentrations were identified. Both models included nitrate and tide height, and one model included an additional nitrate - tide height (N:TH) interaction term (SI Table 5.3). All model parameters were significant at the  $p < 0.01$  level except the N:TH interaction term, which was only marginally significant ( $p < 0.1$ ) (SI Table 5.3). Percent deviance explained (%DE) was calculated for both best-fit models as a measure of goodness-of-fit (Dobson, 1999). Note that %DE is equivalent to  $R^2$  for normally distributed data. The %DE for both of our best-fit Chla models (over the entire sampling domain) was ~35%. Notably, the model including the N:TH interaction term had a slightly higher %DE (SI Table 5.3).

Model performance was found to be spatially variable, with lower model-data fits for northern stations (TJR and F1) than southern stations (HT) (avg %DE TJR and F1: ~33.08; avg %DE HT: 44.89) (Fig. 5.4). The spatial variability in the predictive success of our best-fit GLM's may suggest that the processes underlying phytoplankton patchiness at BFSB vary alongshore. Northern and southern alongshore stations are separated by a river outlet/sand bar system and a bend in the coastline that could result in different local dynamics affecting phytoplankton (Fig. 5.4). Because predictive statistical models include no dynamics, and assume spatially homogeneous correlations between parameters, their performance is likely to vary

spatially, as was observed here in the alongshore.

### ***Water Quality Assessment: Enterococcus***

#### *Spatio-temporal Patterns:*

Surfzone concentrations of *Enterococcus* ranged from 0-257 MPN 100 ml<sup>-1</sup> during our study. FIB contamination was highest at the nourishment site HT; all measured concentrations of enterococci > 32 MPN 100 ml<sup>-1</sup> occurred at this sampling station (Fig 5.5a). The majority of the FIB signal at BFSB occurred during the first half of the study, with concentrations dropping to near zero levels after 10/2/09 (Fig 5.5a). Two pulses of FIB were observed. The first contained higher concentrations of *Enterococcus* and occurred from 9/22/09 – 9/26/09. The second, weaker, pulse occurred from 9/20/09 – 10/1/09 (Fig 5.5a).

*Enterococcus* concentrations at BFSB (especially the Tijuana River {TJR}) were lower than expected given the contaminant levels typically reported during winter months (Brooks et al., 2005). This suggests that during low-flow conditions TJR is not a major source of FIB contamination to neighboring beaches. Low summer/fall FIB levels at TJR may imply that the estuary does a good job of filtering and removing FIB from the system following winter rains. Alternatively, it is possible that FIB contamination remains in the river/estuary during summer/fall, but that contaminant loads are sediment associated, requiring storm events and resuspension for FIB exceedences to be observed.

#### *Parameter Correlations:*

*Enterococcus* concentrations were significantly and positively correlated with fine sediment, silicate, and phosphate concentrations during our study ( $p < 0.05$ ) (Fig 5.5; SI Table 5.2). Correlations were not observed between *Enterococcus* and tide height, alongshore current direction, or water temperature, all of which have been associated with FIB contamination at other California beaches (SI Table 5.2) (Grant et al., 2001; Boehm et al., 2002; Boehm et al., 2004; Kim et al., 2004; Wong et al., 2012). Similarly, *Enterococcus* was not correlated with any of the three parameters most strongly associated with phytoplankton concentrations (nitrate, tide height, or alongshore current direction), implying that the dynamics underlying patterns in phytoplankton and FIB at BFSB were different (SI Table 5.2).

The variable most strongly correlated with enterococci at BFSB was fine sediments; both exhibited high concentrations at the beach nourishment site (HT), both were elevated for the nourishment duration (the first half of the study), and both occurred in two pulses, the second of which was weaker than the first (Fig. 5.5 a-b). This two-pulse pattern may have resulted from the sediment placement schedule for the beach nourishment. No sediments were placed from 9/26 – 9/27/09, resulting in a lack of surfzone fines and FIB on 9/27/09 and 9/28/09 (prior to placement). When sediment placement recommenced the amount of material deposited was reduced (14,000 CYs vs. 21,000 CYs) (SI Table 5.1). This reduction was coincident with lower measured concentrations of surfzone fines and *Enterococcus*. This clearly suggests that the elevated levels of surfzone *Enterococcus* observed during our study were linked to fine sediment resuspension from the beach nourishment.

Like *Enterococcus* and suspended fine sediments, concentrations of the

inorganic nutrients silicate and phosphate were intensified at the nourishment site and had a clear first pulse (Fig. 5.5). No obvious second pulse was observed for either inorganic nutrient, however, and concentrations of both remained high at the end of the study instead of decreasing (Fig. 5.5). The coincidence of the initial nutrient pulse with fine sediment suggests that these nutrients (like enterococci) may have been associated with the beach nourishment itself. The high nutrient concentrations during the second half of our study, however, do not mirror suspended sediment patterns. These elevated concentrations may reflect additional processes like upwelling or nutrient transport from offshore, as they were correlated with an overall decrease in surfzone water temperature (Wong et al., 2012) (SI Fig. 5.3). Notably, these high nutrient concentrations may also be associated with tidal flow from the Tijuana River, as the majority of nutrients examined had hot-spots near the river outlet (Fig. 5.5; SI Fig. 5.3).

Generalized Linear Model Analyses:

Our GLM analyses indicate that fine sediments were the single most important parameter for predicting the presence/absence of *Enterococcus* at BFSB ( $p < 0.01$ ) (SI Table 5.4). The inclusion of additional parameters such as silicate or phosphate did not significantly improve model-data fits. This said, the %DE explained by our best-fit GLM was only 9.72, indicating poor overall model performance (SI Table 5.4). This poor performance reflects extreme spatial variability in model predictive capacity. At the nourishment site the %DE explained by our GLM was 45.04 (Fig. 5.4). At stations distant from the nourishment site (TJR: 380 m and F1: 2000 m), the

%DE explained was 4.22 and 1.89, respectively (Fig. 5.4). It may be that over time and with distance from the nourishment, fine sediments dissociate from *Enterococcus* due to differences in surfzone removal rates, resulting in variable dose relationships between fines and FIB. This could explain the decreased predictive performance for our fine sediment GLM at stations increasingly distant from HT.

An alternate explanation for the poor performance of our GLM at stations beyond HT is that contamination events at these distant locations were driven by episodic processes uncorrelated with fines. GLM's, by design, only incorporate variables that significantly increase the predictive power of a model. This may reduce their efficacy in predicting FIB contamination at beaches with point-sources of bacterial pollution (like our beach nourishment), which can swamp the signal from low-frequency, patchy, or ephemeral contamination events (however severe). This problem might be circumvented for management purposes by developing multiple models for beaches dominated by point sources: one for the point source location, and one excluding it, allowing lower-frequency contamination events to be resolved.

### ***Sediment Enterococcus Levels:***

The results of our direct correlation and GLM analyses for *Enterococcus* suggest that nourishment sediments are a FIB source and should contain high concentrations of bacteria. This inference was confirmed by direct examination, which revealed sediment *Enterococcus* loads ranging from 117-51,486 MPN 100 g<sup>-1</sup> of sediments (Fig. 5.6). Our maximum measured FIB concentrations are on the high end of those observed at other temperate beaches in California (Yamahara et al., 2007).

Concentrations of *Enterococcus* were found to vary both with placement day and among placements within a day (Fig. 5.6). This suggests that surfzone FIB loading due to the suspension of nourishment sediments should be variable, reflecting the patchy concentrations of FIB found in those sediments. This could have contributed to the low overall performance of our best-fit GLM for *Enterococcus*, as the relationship between the predictor variable (fines) and the response variable (*Enterococcus*) was inherently unstable.

Biochemical analyses of bacteria from the Enterolert assay of our 10/1/09 sediment sample did not reveal any false *Enterococcus* positives. 60% of negative Enterolert wells exhibited no bacterial growth on brain heart infusion agar. The remaining 40% that did exhibit growth were found to contain gram-negative bacteria, not enterococci (SI Table 5.5). Of our positive Enterolert wells, 20% were found to contain nonenterococcal isolates (SI Table 5.5). This 20% false positive rate is higher than rates reported by the EPA (US EPA, 2000), but is consistent with rates found by Ferguson *et al.* (2005). The high false positive rates observed in this study suggest that some caution is warranted when using Enterolert to enumerate enterococci in sediments. Genetic methods like QPCR may provide a reliable, more specific, alternative (Noble and Weisberg., 2005; Wade et al., 2006).

### ***Surfzone Residence Time: Enterococcus***

Elevated concentrations of *Enterococcus* were observed at station HT during the sediment placement on 10/1/09. The 4 h average FIB level was 141 MPN 100 ml<sup>-1</sup>, above the EPA single-sample standard for enterococci (104 MPN 100 ml<sup>-1</sup>). Twenty-

three hours post placement, enterococci were almost undetectable in the surfzone (average of 1 MPN 100 ml<sup>-1</sup>) (Fig. 5.7). FIB decay was well described by an exponential with a decay rate of 0.24 h<sup>-1</sup> (6.7 x 10<sup>-5</sup> s<sup>-1</sup>) (Fig. 5.7). FIB levels dropped below EPA single-sample standards in ~1.3 h, and below geometric mean standards (35 MPN 100 ml<sup>-1</sup>) in ~5.8 h (Fig. 5.7). The short residence time of FIB in the surfzone following sediment placement suggests that the local water quality effects of nourishment sediments are ephemeral. FIB residence time is likely to reflect both physical transport of enterococci out of the system and biological inactivation (Boehm et al., 2005; Rippey et al., submitted ms 1-2). If physical transport is the dominant source of removal, then the rapid FIB loss we measured at BFSB cannot be equated with ephemeral health risk because the pollutant plume is likely to impact beaches north or south of the nourishment location. If, however, inactivation is the dominant source of removal, then our short residence times do imply that health risk associated with Goat Canyon sediments is short lived. The contribution of inactivation to surfzone *Enterococcus* loss at BFSB is evaluated below.

### ***Enterococcus Inactivation: Microcosm Experiments***

Our microcosm experiments showed rapid inactivation of nourishment-associated *Enterococcus* in surfzone waters during the first 0.5 h of sampling. Following these initial declines, *Enterococcus* concentrations were relatively stable for the remaining 4.5 h (Fig. 5.8a). These declines were well explained by an asymptotic exponential model of the form:



$$C(t) = C_0 a + C_0 (1 - a) e^{-k_s t} \quad (1)$$

where  $t$  is time,  $C(t)$  is the concentration of *Enterococcus* at time  $t$ ,  $C_0$  is the starting concentration of *Enterococcus*,  $a$  is the fraction of *Enterococcus* that are resistant to inactivation, and  $k_s$  is the inactivation rate of the sensitive fraction.

FIB inactivation in dark microcosm treatments was not significantly different from light treatments, suggesting that solar radiation was not a major contributor to *Enterococcus* inactivation in these experiments ( $p < 0.05$ ) (Fig. 5.8a). Surfzone solar insolation levels were low on average ( $67.54 \mu\text{Ein m}^{-2} \text{s}^{-1}$ ), despite it being a sunny day (avg. insolation in air:  $1842.99 \mu\text{Ein m}^{-2} \text{s}^{-1}$ ) (Fig. 5.8b). On days with similar light intensities (but no nourishment plume) average surfzone insolation was over an order of magnitude higher ( $1031.75 \mu\text{Ein m}^{-2} \text{s}^{-1}$ ) (Fig. 5.8b). This suggests that our microcosms were shaded by the sediment plume itself, implying that, in addition to being a source of enterococci to the surfzone, nourishment sediments may provide FIB with solar protection. This could affect the intensity of FIB contamination in sediment plumes transported to nearby beaches, as solar radiation can be a dominant source of FIB mortality (Sinton et al., 2002; Boehm et al., 2009; Zhu et al., 2011).

Despite the apparent solar protection provided by nourishment sediments, it appears that ~61 % of nourishment-associated enterococci undergo rapid inactivation in surfzone waters ( $k_s = -4.8 \times 10^{-2} \text{s}^{-1} - -8.4 \times 10^{-2} \text{s}^{-1}$ ) (Fig. 5.8a); the remainder were resistant to inactivation (Fig. 5.8a). The inactivation rates of our sensitive fraction were markedly higher than those typically observed for enterococci, which range from

( $10^{-6}$  -  $10^{-3}$  s<sup>-1</sup>) (Sinton et al., 2002, Boehm et al., 2005; Maraccini et al., 2012). These elevated rates could reflect sensitivity to any number of environmental variables including temperature, pH, salinity, etc (Rozen and Belkin, 2001). The sensitive fraction could consist of a single *Enterococcus* species (or species group) with higher than average seawater inactivation rates (Easton et al., 2005; Maraccini et al., 2012). Alternatively, it is possible that this sensitive fraction was composed of previously damaged and/or stressed cells, explaining their rapid decay.

Our microcosm experiments suggest that FIB inactivation was temporally variable, with initial rates of loss enhanced relative to subsequent rates. This pattern implies that initial rates of surfzone FIB loss may be much faster than estimated using the exponential fit in our residence-time analysis (discussed above) ( $\sim 5.5 \times 10^{-2}$  s<sup>-1</sup> vs.  $6.4 \times 10^{-5}$  s<sup>-1</sup>) (Fig. 5.7; Fig. 5.8a). The results of this analysis are still informative, however, as they reveal declining *Enterococcus* concentrations 8-23 hours following sediment placement (Fig. 5.7) *Enterococcus* concentrations stabilized rapidly in our microcosm experiments, making it likely that these additional losses are due to physical transport and dilution (Fig. 5.8a). Taken together, our residence-time and microcosm studies suggest that both inactivation and dilution contribute to surfzone FIB loss at BFSB. Specifically, sensitive FIB ( $\sim 61\%$  of the population) appear to be inactivated within 1 hour, with subsequent losses driven by physics. This suggests that the majority of nourishment-associated FIB will be inactivated before they can be transported to other beaches.

In this study we have shown that beach nourishments with estuarine sediments have the potential to impact water quality at Southern California beaches.

Nourishment sediments had no obvious affect on phytoplankton patchiness or bloom formation at BFSB, but were identified (using direct correlations and GLM's) as a clear source of the fecal indicator *Enterococcus*. Although high concentrations of enterococci were released into the surfzone with nourishment sediments, the residence time of these indicators was short (~23 h). By combining microcosm experiments with field sampling, we were able to determine that these short residence times were driven by a combination of rapid FIB inactivation immediately post placement, and physical dilution/mixing. From a management perspective our findings show that 1) nourishment sediments can impact bacteriological water quality, and 2) the effects of these impacts are short term. This said, FIB are only indicators of fecal pollution, not pathogens. To truly understand the health risk implications of this sort of beach nourishment, it would be necessary to carefully screen Goat Canyon sediments for human pathogens and evaluate the seawater inactivation rates of those pathogens to see how they compare with the rates measured here for enterococci.

### **Acknowledgements**

This work was supported by the California Department of Boating and Waterways, NSF, ONR, CA SeaGrant, the California Coastal Conservancy, and NOAA. Special thanks to volunteers and staff from the Integrative Oceanography Division (B. Woodward, B. Boyd, D. Clark, K. Smith, D. Darnell, R. Grenzeback, A. Gale, M. Omand, M. Okihiro, M. Yates, A. Doria, M. Cape, B. Carter, T. Hall, B. Neal, and the entire Guza clan) for their assistance in data collection. I also wish to thank the USGS PCMSC sediment laboratory for their analysis of sediment

concentrations during this experiment. Chapter 5, in part, is being prepared for submission to *Environmental Science & Technology*, 2012, Rippey, M. A.; Warrick, J. A.; Franks, P. J. S.; Feddersen, F.; Guza, R. T., ACS Publications, 2012. The dissertation author was the primary investigator and author of this paper.

### Literature Cited

- Aminot, A.; Andrieux-Loyer, F. 1996. Concept and determination of exchangeable phosphate in aquatic sediments. *Water Research*. 30: 2805–2811.
- Andrieux-Loyer, F.; Aminot, A. 2001. Phosphorus forms related to sediment grain size and geochemical characteristics in French coastal areas. *Estuarine, Coastal, and Shelf Science*. 52: 617-629.
- Bell, R. G.; Davies-Colley, R. J.; Nagels, J. W. 1993. *In-situ* technique for faecal bacteria inactivation studies. In Proceedings of the 11<sup>th</sup> Australian Conference on Coastal and Ocean Engineering, Townsville. National Conference Publication 93/4. The Institution of Engineers, Canberra, Australia.
- Boehm, A. B.; Grant, S. B.; Kin, J. H.; Mowbray, S. L.; McGee, C. D.; Clark, C. D.; Foley, D. M.; Wellman, D. E. 2002a. Decadal and shorter period variability of surf zone water quality at Huntington Beach, California. *Environmental Science and Technology*. 36: 3885-3892.
- Boehm, A. B. 2003. Model of microbial transport and inactivation in the surfzone and application to field measurements of total coliform in northern Orange County, California. *Environmental Science and Technology*. 37, 5511-5517.
- Boehm, A. B.; Keymer, D. P.; Shellenbarger, G. G. 2005. An analytical model of enterococci inactivation, grazing, and transport in the surfzone of a marine beach. *Water Research*. 39, 3565-3578.
- Boehm, A. B.; Lluch-Cota, D. B.; Davis, K. A.; Winant, C. D.; Monismith, S. G. 2004. Covariation of coastal water temperature and microbial pollution at interannual to tidal periods. *Geophysical Research Letters*. 31: L06309 5PP.
- Boehm, A. B.; Yamahara, K.; Love, D. C.; Peterson, B. M.; McNeill, K.; Nelson, K. L. 2009. Covariation and photoinactivation of traditional and novel indicator organisms and human viruses at a sewage impacted marine beach. *Environmental Science and Technology*. 43, 8046-8052.
- Brooks, H. A.; Gersberg, R. M.; Dahr, A. K. Detection and quantification of hepatitis A virus in seawater via real time RT:PCR. *Journal of Virological Methods*. 127: 109-118.
- Cabelli, V. J.; Dufour, A. P.; McCabe, L. J.; Levin, M. A. 1982. Swimming-associated gastroenteritis and water quality. *American Journal of Epidemiology*. 115: 606-616.

- Calacagno, V.; de Mazancourt, C. 2010. glmulti: An R package for easy automated model selection with (Generalized) Linear Models. *Journal of Statistical Software*. 34: 1-29.
- Calbet, A.; Landry, M. R. 2004. Phytoplankton growth, microzooplankton grazing and carbon cycling in marine systems. *Limnology and Oceanography*. 49: 51-57.
- Callaway, J. C.; Zedler, J.B. 2004. Restoration of urban salt marshes: lessons from Southern California. *Urban Ecosystems*. 7: 107-124.
- Cambella, A. D.; Ibarra, D. A.; Diogene, J.; Dahl, E. 2005. Harmful algal blooms and their assessment in fjords and coastal embayments. *Oceanography*. 18: 158-171.
- Cloern, J. E.; Jassby, A. D. 2010. Patterns and scales of phytoplankton variability in estuarine-coastal ecosystems. *Estuaries and Coasts*. 33: 230-241.
- Davies-Colley, R. J.; Bell, R. G; Donnison, A. M. 1994. Sunlight inactivation of enterococci and fecal coliforms in sewage effluent diluted in seawater. *Applied and Environmental Microbiology*. 60: 2049-2058.
- De Luna, X. Skouras, K. 2003. Choosing a model selection strategy. *Scandinavian Journal of Statistics*. 30: 113-128.
- Dobson A. 1999. An Introduction to Generalized Linear Models. Chapman & Hall /CRC, London.
- Easton, J. H., J. J. Gauther, M. M. Lalor, and R. E. Pitt. 2005. Die-off of pathogenic *E. coli* O157:H7 in sewage contaminated waters. *Journal of the American Water Resources Association*. 41:1187-1193.
- Elwany M. H. S. 2011. Characteristics, restoration, and enhancement of Southern California lagoons. In: Roberts, T.M., Rosati, J.D., and Wang, P. (eds.), *Proceedings, Symposium to Honor Dr. Nicholas C. Kraus*, Journal of Coastal Research, Special Issue, No. 59, pp. 246-255. West Palm Beach (Florida), ISSN 0749-0208.
- Evanson, M.; Ambrose, R. F. 2006. Sources and growth dynamics of fecal indicator bacteria in a coastal wetland system and potential impacts to adjacent waters. *Water Research*. 40: 475-486.
- Farnsworth. K. L.; Warrick, J. A. 2007. Sources, dispersal, and fate of fine sediment supplied to coastal California. Scientific Investigations Report. U.S. Geological Survey. no. 2007-5254. 77PP.

- Ferguson, D. M.; Moore, D. F.; Getrich, M. A.; Zhouandai, M. H. 2005. Enumeration and speciation of enterococci found in marine and intertidal sediments and coastal water in Southern California. *Journal of Applied Microbiology*. 99, 598–608.
- Gersberg RM, Brown C, Zambrano V, Worthington K, Weis D. Quality of urban runoff in the Tijuana River watershed. In: Westerhoff P, editor. US-Mexican Border Environment: water issues along the US-Mexican border, SCERP Monograph Series, No. 2. San Diego, CA: San Diego State University Press, 2000. p. 31–45.
- Gersberg, R. M; Daft, D.; Yorkey, D. 2004. Temporal pattern of toxicity in runoff from the Tijuana River Watershed. *Water Research*. 38: 559-568.
- Gersberg, R. M.; Rose, M. A.; Robles-Sikisaka, R.; Dahr, A. K. 2006. Quantitative detection of hepatitis a virus and enteroviruses near the United States-Mexico border and correlation with levels of fecal indicator bacteria. *Applied and Environmental Microbiology*. 72: 7438-7444.
- Grant, S. B.; Sanders, B. F.; Boehm, A. B.; Redman, J. A.; Kim, J. H.; Mrse, R. D.; Chu, A. K.; Gouldin, M.; McGee, C. D.; Gardiner, N. A.; Jones, B. H.; Svejksky, J.; Leipzig, G. V.; Brown, A. 2001. Generation of enterococci bacteria in a coastal saltwater marsh and its impact on surf zone water quality. *Environmental Science and Technology*. 35, 2407-2416.
- Guber, A. K.; Pachepsky, Y. A.; Shelton, D. R.; Yu, O. 2007. Effect of bovine manure on fecal coliform attachment to soil and soil particles of different sizes. *Applied and Environmental Microbiology*. 10: 3363-3370.
- Halliday, E.; Gast, R. J.; 2011. Bacteria in beach sands: an emerging challenge in protecting coastal water quality and bather health. *Environmental Science and Technology*. 45, 370-379.
- Heaney, C. D.; Sams, E.; Wing, S.; Marshall, S.; Brenner, K.; Dufour, A. P.; Wade, T. J. Contact with beach sand among beachgoers and risk of illness. *American Journal of Epidemiology*. 2009, 170, 165-172.
- Henrickson, S. E.; Wong, T.; Allen, P.; Ford, T.; Epstein, P. R. Marine Swimming-Related Illness: Implications for Monitoring and Environmental Policy. *Environmental Health Perspectives*. 2001, 109, 645-650.
- Hewson, I.; O'neil, J. M.; Aball, E. 2001. A low-latitude bloom of the surf-zone diatom, *Anaulus australis* (Centrales, Bacillariophyta) on the coast of Southern

- Queensland (Australia). *Journal of Plankton Research*. 23: 1233-1236.
- Jeng, H. C.; England, A. J.; Bradford, H. B. 2005. Indicator organisms associated with stormwater suspended particles and estuarine sediment. *Journal of Environmental Science and Health, Part A: Toxic/Hazardous Substances and Environmental Engineering*. 40: 779-791.
- Jiang, S.; Noble, R.; Chu, W. 2001. Human adenoviruses and coliphages in urban runoff-impacted coastal waters of Southern California. *Applied and Environmental Microbiology*. 179-184.
- Kim, J. H.; Grant, S. B.; McGee, C. D.; Sanders, B. F.; and Largier, J. L. 2004. Locating sources of surf zone pollution: a mass budget analysis of fecal indicator bacteria at Huntington Beach, California. *Environmental Science and Technology*. 38: 2626-2636.
- Koike, I.; Furuya, K.; Otake, H.; Nakai, T.; Menoto, T.; Hattori, A. 1982. Horizontal distributions of surface chlorophyll a and nitrogenous nutrients near Bering Strait and Unimak Pass. *Deep Sea Research Part A. Oceanographic Research Papers*. 29: 149-155.
- Maraccini, P. A.; Ferguson, D. M.; Boehm, A. B. 2012. Diurnal variation in *Enterococcus* species composition in polluted ocean water and a potential role for the enterococcal carotenoid in protection against photoinactivation. *Applied and Environmental Microbiology*. 78: 305-310.
- McPhee-Shaw, E. E.; Nielsen, R. J.; Largier, J. L.; Menge, B. A. 2005. Nearshore Chlorophyll-a events and wave-driven transport. *Geophysical Research Letters*. 38: L02604 5PP.
- Nelder, J. A. 2000. Functional marginality and response-surface fitting. *Journal of Applied Statistics*. 27: 109-112.
- Noble, R. T.; Weisberg, S. B. 2005. A review of technologies for rapid detection of bacteria in recreational waters. *Journal of Water and Health*. 3: 381-392.
- Ojeda-Revah, L.; Bocco, G.; Ezcurra, E.; Espejel, I. 2008. Land-cover/use transitions in the binational Tijuana River watershed during a period of rapid industrialization. *Applied Vegetation Science*. 11: 107-116.
- Omand, M. M.; Leichter, J. J.; Franks, P. J. S.; Guza, R. T.; Lucas, A. J.; Feddersen, F. 2011. Physical and biological processes underlying the sudden surface appearance of a red tide in the nearshore. *Limnology and Oceanography*. 56: 787-801.



- Pennock, J. R.; Sharp, J. H. 1994. Temporal alternation between light- and nutrient-limitation of phytoplankton production in a coastal plain estuary. *Marine Ecology Progress Series*. 111: 275-288.
- Pruss, A. 1998. Review of epidemiological studies on health effects from exposure to recreational water. *International Journal of Epidemiology*. 27: 1-7.
- Redfield, A. C. 1958. The biological control of chemical factors in the environment. *American Scientist*. 46: 205-222.
- Redfield, A. C. 1934. On the proportions of organic derivatives in sea water and their relation to the composition of plankton, p. 176- 192. In James Livingstone Memorial Volume. Univ. of Liver-pool.
- Rocha, R. R.; Thomaz, S. M.; Carvalho, P.; Gomez, L. C. 2009. Modeling chlorophyll a and dissolved oxygen concentration in tropical floodplain lakes (Parana River Brazil). *Brazil Journal of Biology*. 69: 491-500.
- Rozen, Y.; Belkin, S. 2001. Survival of enteric bacteria in seawater. *FEMS Microbiology Reviews*, 25: 513-529.
- Sinton, L. W.; Donnison, A. M.; Hastie, C. M. 1993a. Faecal streptococci as faecal pollution indicators: a review. Part 1: Taxonomy and Enumeration. *New Zealand Journal of Marine and Freshwater Research*. 27, 101-115.
- Sinton, L. W.; Hall, C. H.; Lynch, P. A.; Davies-Colley, R. J. 2002. Sunlight inactivation of fecal indicator bacteria and bacteriophages from waste stabilization pond effluent in fresh and saline waters. *Applied and Environmental Microbiology* 68, 1122-1131.
- Smith, V. H. 2006. Response of estuarine and coastal marine phytoplankton to nitrogen and phosphorus enrichment. *Limnology and Oceanography*. 51: 337-384
- Smith, W. O. J.; Walsh, I. D.; Booth, B. C.; Deming, J. W. 1995. Particulate matter and phytoplankton and bacterial biomass distributions in the North East water Polynya during summer 1992. *Journal of Geophysical Research*. 100: C34341-C34356.
- Tester, P. A.; Stumpf, R. P; Vukovich, F. M.; Fowler, P. R.; Turner, J. T. 1991. An expatriate red tide bloom: transports, distribution, and persistence. *Limnology and Oceanography*. 36: 1053-1061.
- Turbow, D. J.; Osgood, N. D.; Jiang, S. C. 2003. Evaluation of recreational health risk in coastal waters based on *Enterococcus* densities and bathing patterns.

- Environmental Medicine*. 111: 598-603.
- U.S. Code of Federal Regulations 2003b. Title 40, Ch. 1, part 230 – section 404b. Guidelines for specification of disposal sites for dredged or fill material.
- USEPA. 2000. Improved enumeration methods for the recreational water quality indicators: enterococci & *Escherichia coli*. EPA/821/R-97/004. U.S. Environmental Protection Agency, Office of Science and Technology.
- Vargas, M; Brown, C. W.; Sapiano, M. R. P. 2009. Phenology of marine phytoplankton from satellite ocean color measurements. *Geophysical Research Letters*. 36: L01608 5PP.
- Wade, T. J.; Calderon, R. L.; Sams, E.; Beach, M.; Brenner, K. P.; Williams, A. H.; Dufour, A. P. 2006. Rapidly measured indicators of recreational water quality are predictive of swimming-associated gastrointestinal illness. *Environmental Health Perspectives*. 114: 24-8.
- Wallace, K. J.; Callaway, J. C.; Zedler, J. B. 2005. Evolution of tidal creek networks in a high sedimentation environment: a 5-year experiment at Tijuana Estuary, California. *Estuaries and Coasts*. 28: 795-811.
- Warrick, J.A.; Rosenberger, K.; Lam, A.; Ferreira, J.; Miller, I. M.; Rippy, M.; Svejksky, J.; Mustain, N. 2012. Observations of coastal sediment dynamics of the Tijuana Estuary Fine Sediment Fate and Transport Demonstration Project, Imperial Beach, California, U.S. Geological Survey Open-File Report 2012-1083, 29 p and data files. (Available at <http://pubs.usgs.gov/of/2012/1083/>.)
- Wong, S. H. C.; Santoro, A. E.; Nidzieko, N. J.; Hench, J. L.; Boehm, A. B. 2012. Coupled physical, chemical, and microbiological measurements suggest a connection between internal waves and surf zone water quality in the Southern California Bight. *Continental Shelf Research*. 34: 64-78.
- Xu, J.; Ho, A. Y. T.; Yin, K.; Yuan, X.; Anderson, D. M.; Lee, J. H. W.; Harrison, P. J. 2008. Temporal and spatial variations in nutrient stoichiometry and regulation of phytoplankton biomass in Hong Kong waters: Influence of the Pearl River outflow and sewage inputs. *Marine Pollution Bulletin*. 54: 335-348.
- Yamahara, K. M.; Layton, B. A.; Santoro, A. E.; Boehm, A. B. 2007. Beach sands along the California coast are diffuse sources of fecal bacteria to coastal waters. *Environmental Science and Technology*. 41: 4515- 4521.
- Yamahara, K. M.; Walters, S. P.; Boehm, A. B. 2009. Growth of enterococci in unaltered, unseeded beach sands subjected to tidal wetting. *Applied and*

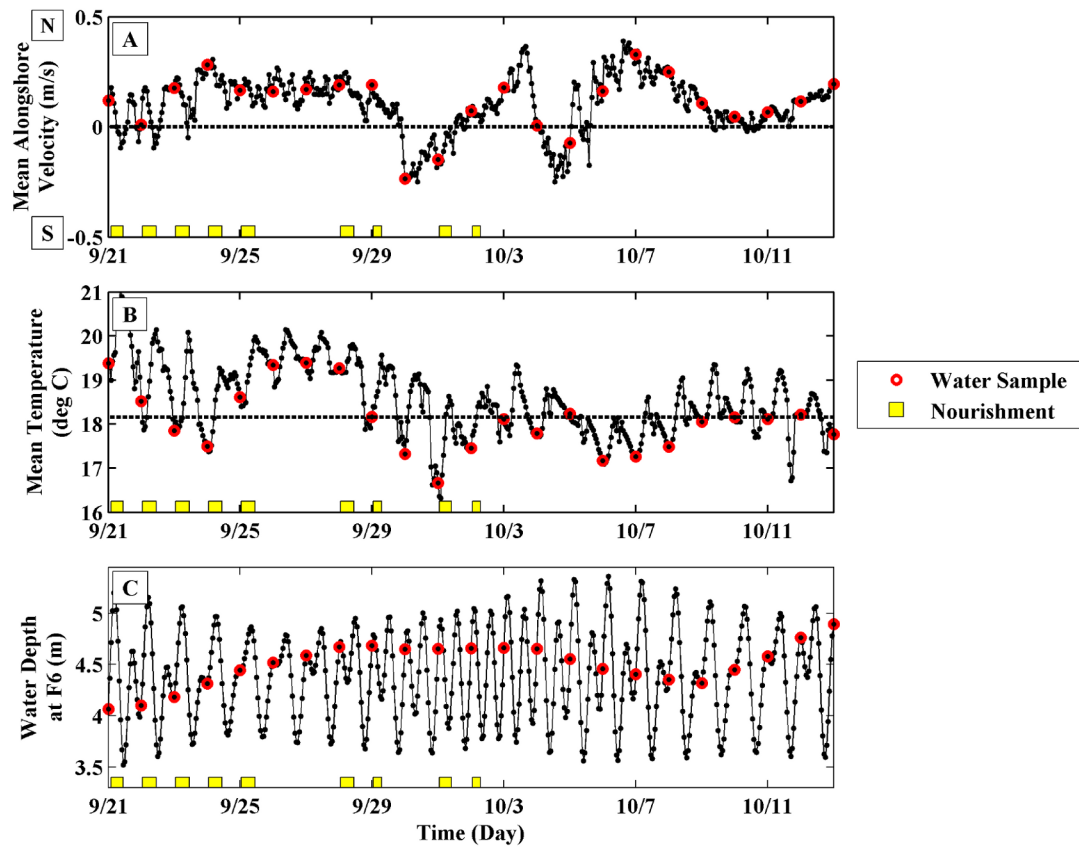
*Environmental Microbiology*. 75: 1517-1524.

Yang, Y. 2005. Can the strengths of AIC and BIC be shared? A conflict between model identification and regression estimation. *Biometrika*. 92: 937-950.

Zhu, X.; Wang, J. D.; Solo-Gabriele, H. M.; Fleming, L. E. 2011. A water quality modeling study of non-point sources at recreational marine beaches. *Water Research*. 45: 2985-2995.

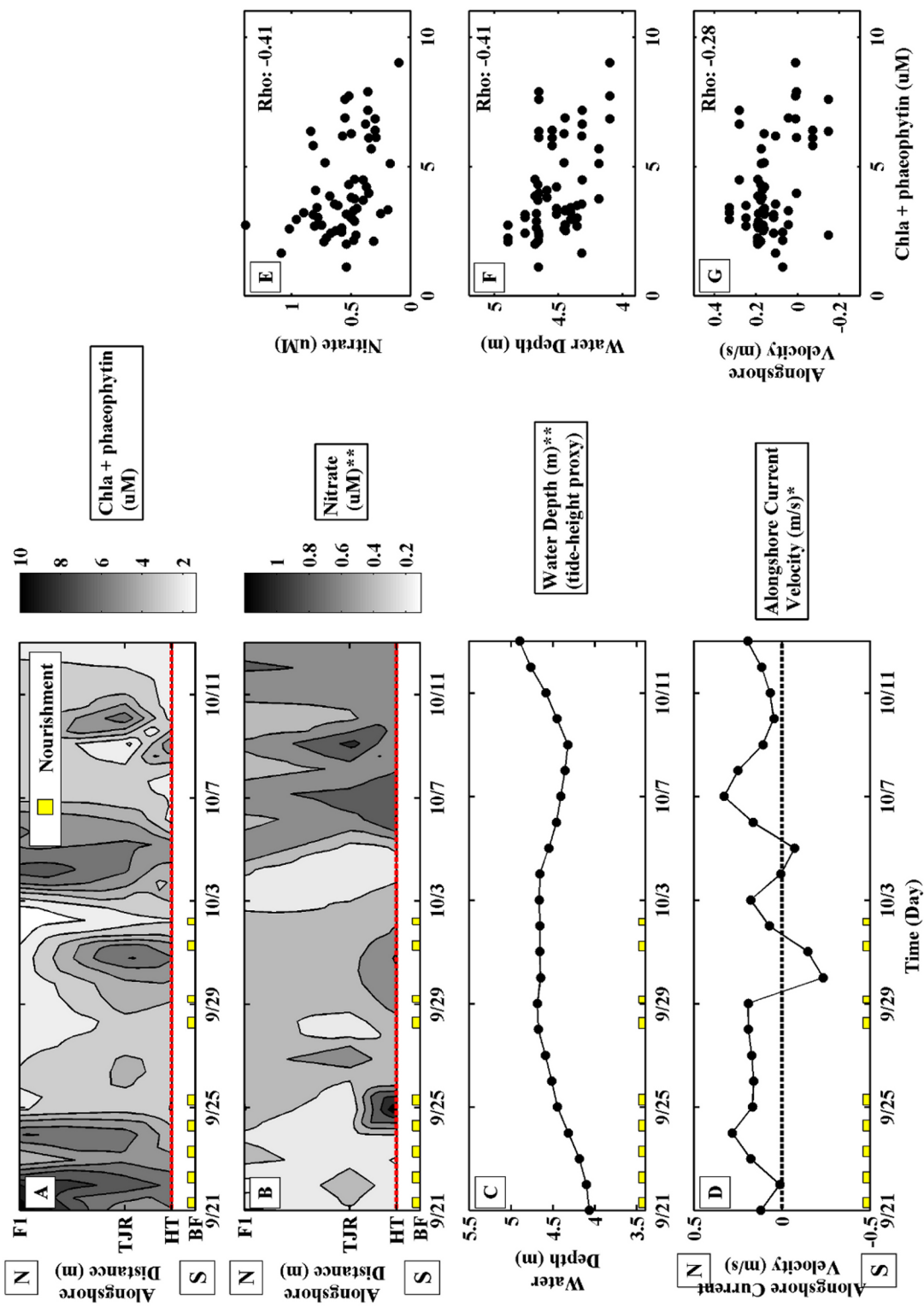


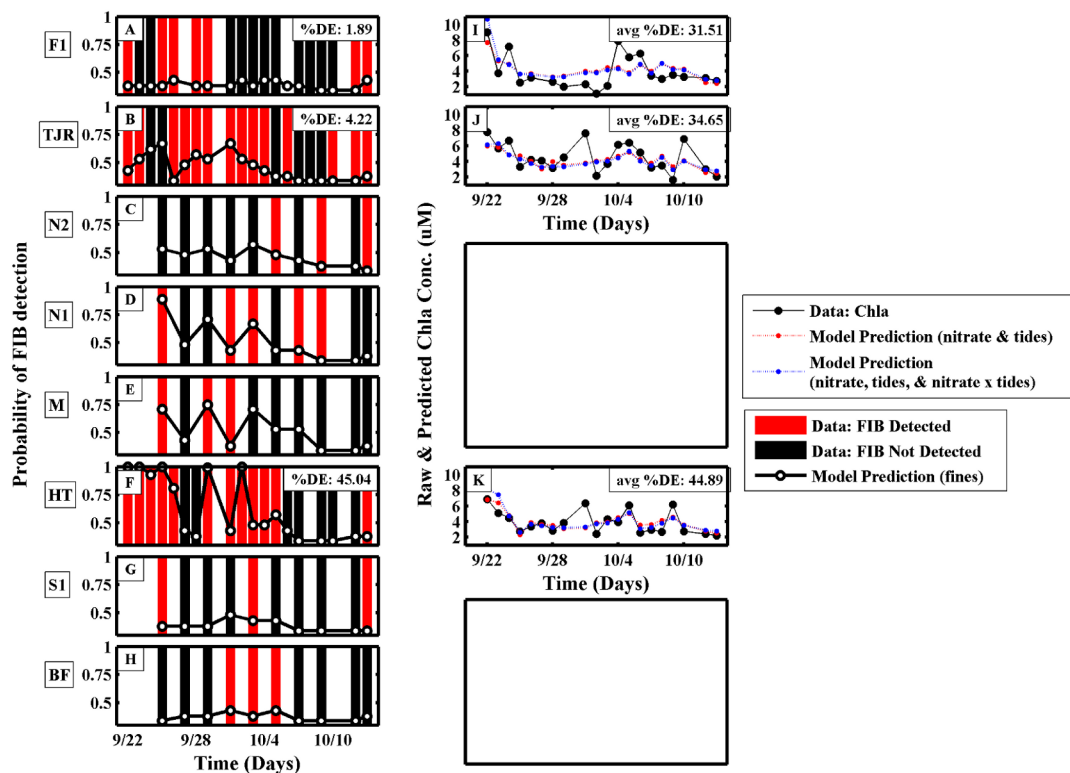
**Figure 5.1:** Schematic of field sampling at Boarder Fields State Beach. Samples were taken along a 3.3 km alongshore transect (dashed red line). Sample locations are labeled with white boxes. *Enterococcus*, nitrate, nitrite, ammonium, phosphate, silicate, sands, and fines were monitored at all stations. Chlorophyll concentrations were monitored at TJR, HT, and BF. Tide height, alongshore current direction and temperature were measured at F1 and at five additional locations spanning 130 m in the cross-shore (solid red line). Sediments for the beach nourishment came from the Goat Canyon Retention Basin (white dashed box).



**Figure 5.2:** 130 m cross-shore averaged (A) alongshore currents and (B) temperature. (C) Mean water depth (a proxy for tide height) measured ~130 m offshore (at F6) versus time (days) from 9/21/09 – 10/13/09. Red circles mark when water samples were collected, and yellow boxes mark nourishment events.

**Figure 5.3:** Concentrations of **(A)** chlorophyll ( $\mu\text{M}$ ) and all parameters significantly correlated with chlorophyll at the  $p < 0.05$  (\*) or  $p < 0.01$  (\*\*) level; **(B)** nitrate ( $\mu\text{M}$ ), **(C)** water depth (m), and **(D)** cross-shore averaged alongshore current velocity ( $\text{ms}^{-1}$ ). The  $x$ -axis for **A-D** is time (days). The  $y$ -axis is alongshore distance (m) (**A-B**) or parameter magnitude (**C-D**). A red dashed line marks the beach nourishment location (HT) (**A-B**), and yellow boxes indicate individual nourishment events. Subplots **(E-G)** show direct correlations between chlorophyll ( $x$ -axis) and **(E)** nitrate, **(F)** water depth, or **(G)** alongshore velocity ( $y$ -axis). Spearman's correlation coefficients ( $\rho$ ) are shown in the upper right hand corner of each correlation plot.

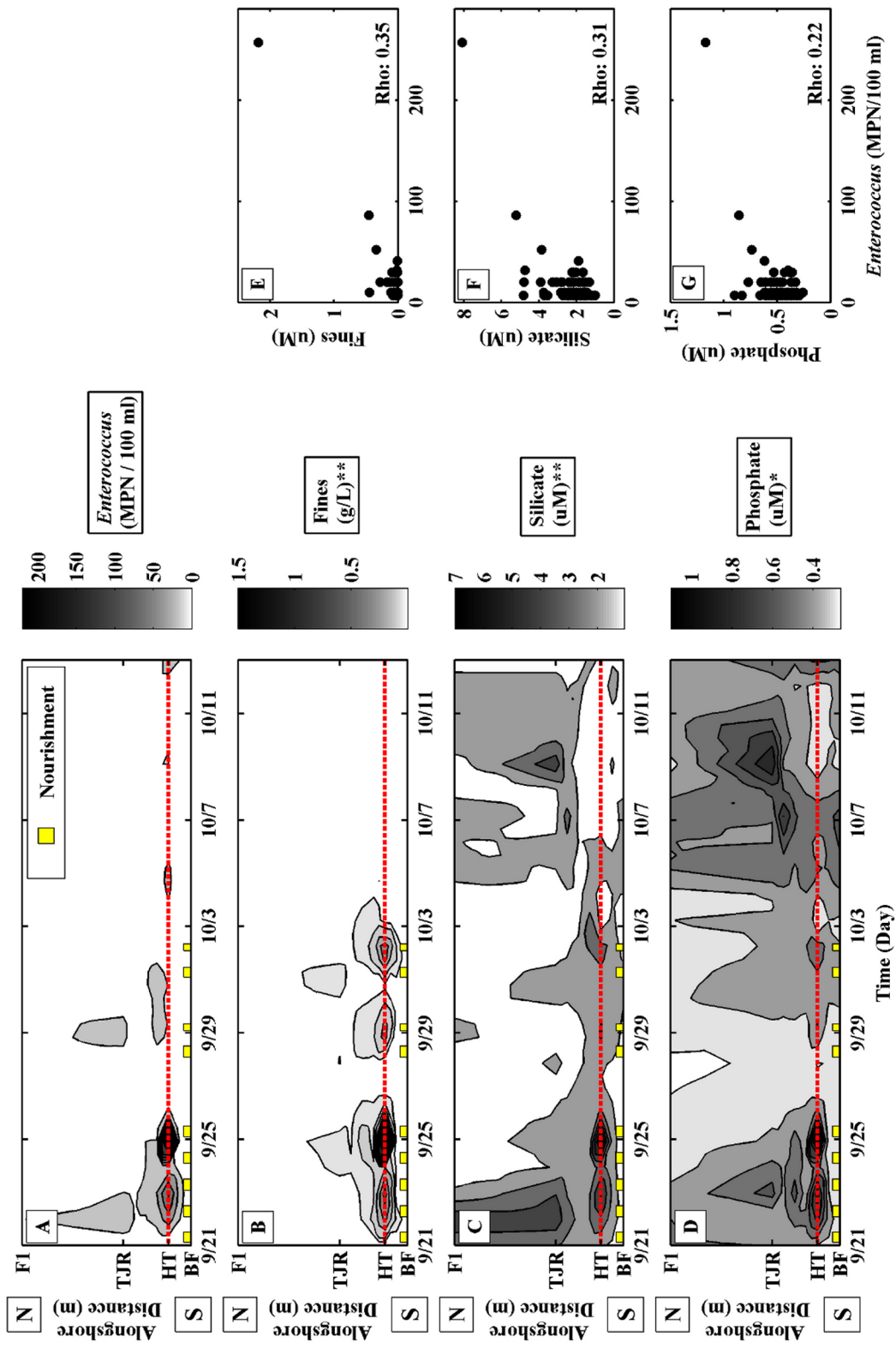




**Figure 5.4:** (A-H) Best-fit GLM output for *Enterococcus* (fines only) compared with presence/absence data. The  $x$ -axis is time (days) and the  $y$ -axis is the probability of bacterial detection using the fine sediment GLM. Model predictions are shown as white circles, and *Enterococcus* data is shown as colored bars; presence (red bar) and absence (black bar). (I-K) Best-fit GLM outputs for chlorophyll (red or blue) compared with chlorophyll data (black). The  $x$ -axis is time (days) and the  $y$ -axis is the actual or predicted chlorophyll concentration ( $\mu\text{M}$ ). The nitrate + tides model is shown in red, and the nitrate + tides + interaction term model is shown in blue. All plots (A-K) are organized by sampling station, with the northernmost station at the top (F1) and the southernmost station at bottom (BF for enterococci and HT for chlorophyll) (see Fig. 1). For both enterococci and chlorophyll, best-fit GLM's were spatially variable. The percent deviance explained (see upper right hand corner of A, B, F, I, J, and K) was highest at HT station. This pattern was most pronounced for enterococci.



**Figure 5.5:** Concentrations of (A) *Enterococcus* (MPN 100 ml<sup>-1</sup>) and all parameters significantly correlated with *Enterococcus* at the  $p < 0.05$  (\*) or  $p < 0.01$  (\*\*) level; (B) fine sediment (gL<sup>-1</sup>), (C) silicate (μM), and (D) phosphate (μM). The  $x$ -axis for A-D is time (days). The  $y$ -axis is alongshore distance (m). All color bars are log concentration. A red dashed line marks the beach nourishment location (HT) and yellow boxes indicate individual nourishment events. Subplots (E-G) show direct correlations between *Enterococcus* ( $x$ -axis) and (E) fine sediment, (F) silicate or (G) phosphate ( $y$ -axis). Spearman's correlation coefficients (Rho) are shown in the lower right hand corner of each correlation plot.



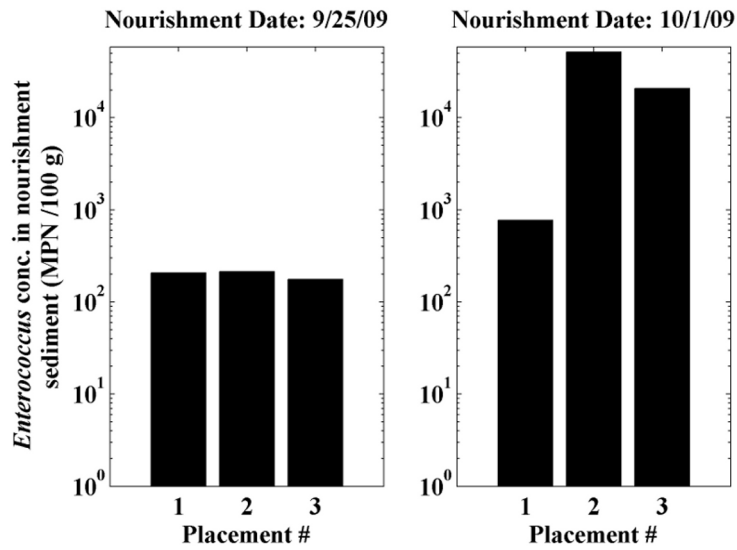


**Figure 5.6:** *Enterococcus* concentrations in beach nourishment sediments from six different placements spanning two nourishment dates; 9/25/09 and 10/1/09. The x-axis is the placement number (1:3) on each day, and the y-axis is *Enterococcus* concentration (MPN 100g<sup>-1</sup>).

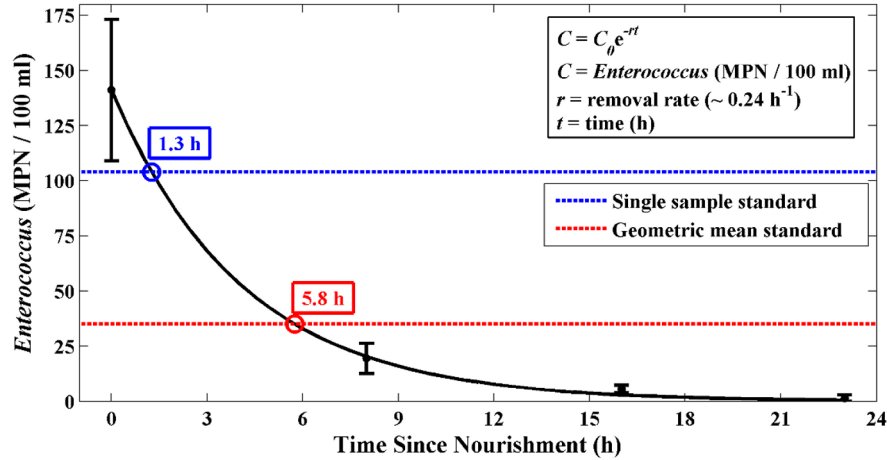


**Figure 5.7:** Surfzone residence time of enterococci at HT sampling station (black line). Four -hour-averaged *Enterococcus* concentrations (MPN 100 ml<sup>-1</sup>) are on the y-axis. Temporal averages are shown to avoid over or underestimating bacterial retention due to patchy *Enterococcus* concentrations. Time since the last nourishment event (h) is on the x-axis. All time-since-placement values are calculated as hours post placement + 2, to reflect the 4-hour averaging of enterococci. Decay of enterococci was exponential and occurred at a rate of 0.24 h<sup>-1</sup> (boxed equation). *Enterococcus* concentrations decayed below EPA single (blue) and geometric sample standards (red) by 1.3 and 5.8 hours, respectively. 23 hours post-placement, enterococci were almost undetectable in the surfzone.

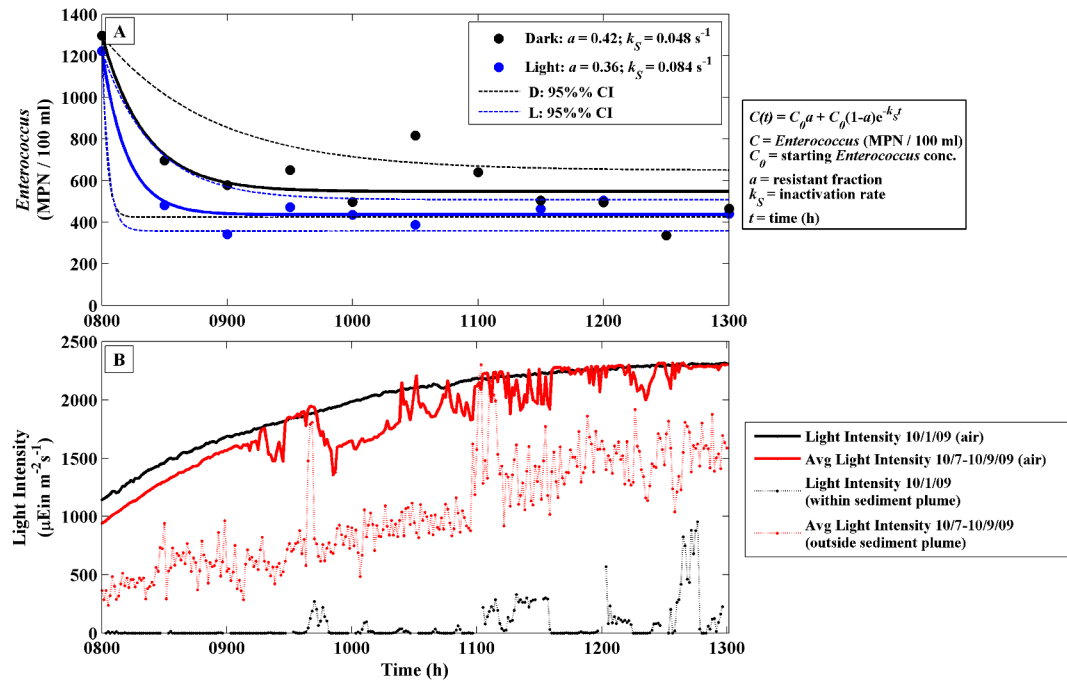


**Figure 5.8:** (A) Inactivation of enterococci in dark (black) and light (blue) microcosm treatments on 10/1/09. Inactivation was well modeled by an asymptotic exponential (see equation to the right). Fitted curves were not significantly different between light and dark treatments (see overlapping CI's). For both treatments  $\sim 61\%$  of nourishment associated enterococci were sensitive to inactivation, and decayed rapidly (avg  $0.055 \text{ s}^{-1}$ ). The remaining fraction was resistant and stable. (B) Solar insolation levels ( $\mu\text{Ein m}^{-2}\text{s}^{-1}$ ) versus time (h) from 0800 to 1300. Insolation on 10/1/09 within the sediment plume (black dashed line) is compared to average surfzone insolation levels when the plume is absent (red dashed line) for days with similar light intensities (black: light intensity 10/1/09, red: average intensity on alternate days). Note the extremely reduced insolation levels on 10/1/09 within the plume.

## Appendix 5.1: Supplementary Tables

**SI Table 5.1:** Sediment Placement Schedule

<b>Date</b>	<b>Volume of Placement (cubic yards)</b>	<b>Start Time</b>	<b>End Time</b>
09/21/09	3,892	0740	1700
09/22/09	4,116	0715	1640
09/23/09	3,528	0700	1640
09/24/09	4,312	0700	1640
09/25/09	5,124	0700	1640
09/28/09	4,564	0700	1640
09/29/09	2,240	0700	1300
10/01/09	5,236	0700	1615
10/02/09	1,988	0700	1300

SI Table 5.2: Spearman's Correlation Coefficients for Parameters Measured at BFSB

	chlorophyll	<i>Enterococcus</i>	sands	fines	nitrate	silicate	phosphate	nitrite	ammonium	tide height	alongshore velocity	temp.
chlorophyll	1	0.234	-0.269	0.236	-0.406**	0.250	0.129	-0.062	-0.153	-0.409**	-0.282*	0.054
<i>Enterococcus</i>		1	-0.076	<b>0.353**</b>	-0.130	<b>0.311**</b>	<b>0.221*</b>	0.135	-0.110	0.032	-0.121	-0.037
sand			1	<b>0.337**</b>	0.061	-0.066	-0.134	0.167	-0.128	<b>0.399**</b>	0.040	-0.014
fines				1	<b>-0.463**</b>	<b>0.297**</b>	0.085	0.175	<b>-0.426**</b>	-0.012	-0.053	0.106
nitrate					1	-0.032	0.169	0.137	<b>0.532**</b>	0.191	<b>0.269**</b>	<b>-0.295**</b>
silicate						1	<b>0.465**</b>	-0.199	-0.012	<b>-0.247*</b>	-0.154	0.098
phosphate							1	<b>-0.209*</b>	<b>0.456**</b>	<b>-0.216*</b>	0.089	<b>-0.396**</b>
nitrite								1	-0.045	0.143	-0.021	0.169
ammonium									1	0.014	0.154	<b>-0.382**</b>
tide height										1	-0.259	0.002
alongshore velocity											1	-0.331
temp.												1

\*\* significant:  $p < 0.01$  level\* significant:  $p < 0.05$  level

**SI Table 5.3:** Best-fit Generalized Linear Models for chlorophyll a at BFSB

	<b>Parameters</b>	<b>k<sup>1</sup></b>	<b>Log L</b>	<b>BIC<sup>4</sup></b>	<b>% DE</b>
<b>Model 1</b>	Nitrate <sup>2</sup>	3	-101.79	219.90	33.86
	Tide Height <sup>2</sup>				
<b>Model 2</b>	Nitrate <sup>2</sup>	4	-100.17	220.72	37.34
	Tide Height <sup>2</sup>				
	Nitrate x Tide height <sup>3</sup>				

1: Total number of model variables (includes intercept)

2: Parameter is significant at  $p < 0.01$  level (Chi squared significance test)

3: Parameter is marginally significant  $p < 0.1$  (Chi squared significance test)

4: Only models within 2 IC units of the best-fit model are shown



**SI Table 5.4:** Best-fit Generalized Linear Models for *Enterococcus* at BFSB

	<b>Parameters</b>	<b>k<sup>1</sup></b>	<b>Log L</b>	<b>BIC<sup>3</sup></b>	<b>% DE</b>
<b>Model 1</b>	Fine Sediment <sup>2</sup>	2	-66.75	142.85	9.72

1: Total number of model variables (includes intercept)

2: Parameter is significant at  $p < 0.01$  level (Chi squared significance test)

3: Only models within 2 IC units of the best-fit model are shown

**SI Table 5.5:** Biochemical Confirmation of *Enterococcus* in Nourishment Sediments from 10/1/09

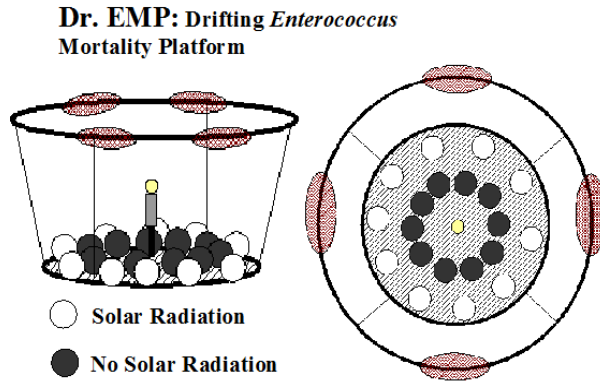
Enterolert well: Pos/Neg	Isolate #	BHIA*1	Gram stain	BHIB <sup>2</sup> w NaCl	BHIB 45 % C	BEA <sup>3</sup>	Cat <sup>4</sup>	PYR <sup>5</sup>	LAP <sup>6</sup>	Conf. ENT <sup>7</sup>	% False Pos/Neg
P	1	G	Gram +	G	G	+	-	+	+	Y	false + wells: 20% false + isolates: 18%
	2	G	Gram +	G	G	+	-	+	+	Y	
	3	G	Gram +	G	G	+	-	+	+	Y	
P	1	G	Gram +	G	G	+	-	+	+	Y	
	2	G	Gram +	G	G	+	-	+	+	Y	
	3	G	Gram +	G	G	+	-	+	+	Y	
P	1	G	Gram +	G	G	+	-	+	+	Y	
	2	G	Gram +	G	G	+	-	+	+	Y	
	3	G	Gram +	G	G	+	-	+	+	Y	
P	1	G	Gram +	G	NG	+	-	+	-	N	
	2	G	Gram +	G	NG	+	-	+	-	N	
P	1	G	Gram +	G	G	+	-	+	+	Y	
P	1	G	Gram +	G	G	+	-	+	+	Y	
	2	G	Gram +	G	G	+	-	+	+	Y	
P	1	G	Gram +	G	G	+	-	+	+	Y	
	2	G	Gram +	G	G	+	-	+	+	Y	
P	1	G	Gram +	G	G	+	-	+	+	Y	
	2	G	Gram +	G	G	+	-	+	+	Y	
P	1	G	Gram +	G	NG	+	-	+	-	N	
	2	G	Gram +	G	NG	+	-	+	-	N	
N	1	NG								N	
	2	NG								N	
	3	NG								N	
N	1	NG								N	
	2	NG								N	
	3	NG								N	
N	1	G	Gram -	NG	NG	+	+	-	+	N	
	2	G	Gram -	NG	NG	+	+	-	+	N	
N	1	G	Gram -	G	G	+	+	+	+	N	
	2	G	Gram -	G	G	+	+	+	+	N	
N	1	NG								N	
	2	NG								N	
N	1	NG								N	
	2	NG								N	
N	1	G	Gram -	G	G	+	+	+	+	N	
N	1	G	Gram -	G	NG	+	+	-	+	N	
	2	G	Gram -	G	NG	-	+	-	+	N	
N	1	NG								N	
	2	NG								N	

\*G: growth and NG: no growth; <sup>1</sup>BHIA stands for Brain Heart Infusion Agar;

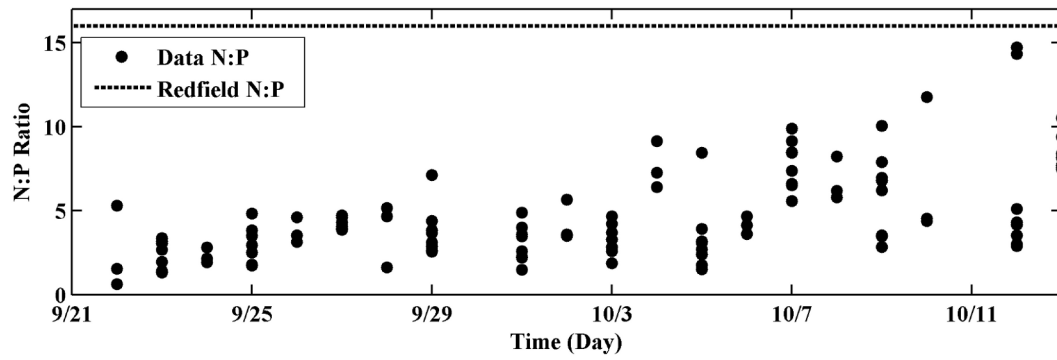
<sup>2</sup>BHIB stands for Brain Heart Infusion Broth; <sup>3</sup>BEA stands for Bile Esculin Agar; <sup>4</sup>Cat stands for Catalase;

<sup>5</sup>PYR stands for pyrrolidonyl aminopeptidase; <sup>6</sup>LAP stands for lucine arylamidase; <sup>7</sup>ENT = enterococci

## Appendix 5.2: Supplementary Figures

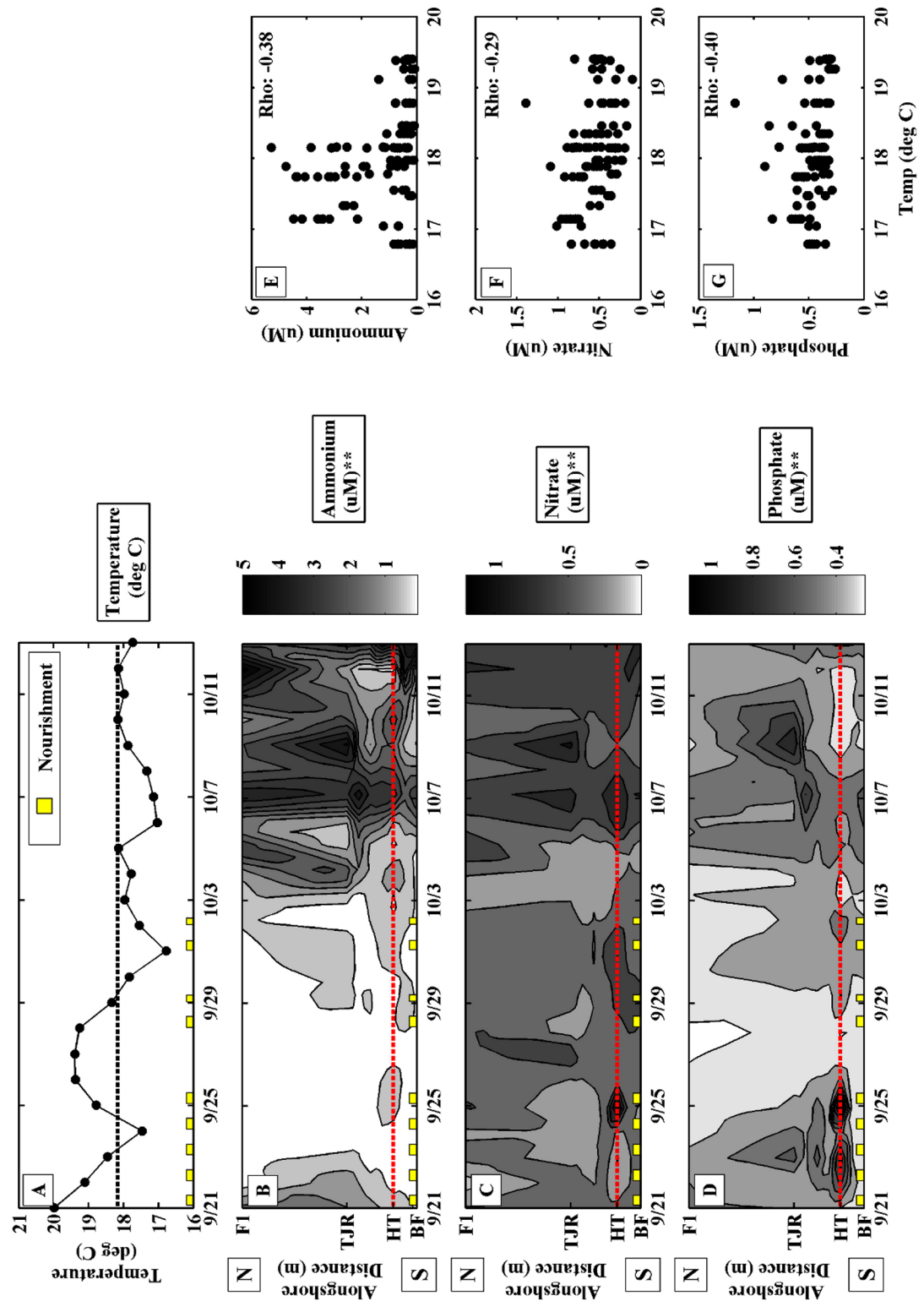


**SI Figure 5.1:** DrEMP (the Drifting *Enterococcus* Mortality Platform) is a field-deployable instrument for measuring *Enterococcus* growth/mortality rates in the surfzone. The platform holds silica microcosm chambers (opaque or transparent) for use in monitoring rates with or without ambient light. Opaque spheres are shown in black and transparent spheres are shown in white. The platform can hold a light and/or temperature sensor (one sensor is shown in yellow in the diagram). The platform is suspended by floats (shown in red) and can be deployed as a water following drifter or as a tethered mooring.



**SI Figure 5.2:** Ratio of nitrogen (nitrate, nitrite, and ammonium) to phosphate at BFSB. Note that this ratio is consistently below the Redfield ratio of 16:1, suggesting a nitrogen limited system.

**SI Figure 5.3:** Plots of (A) 130 m cross-shore averaged surfzone temperature ( $^{\circ}\text{C}$ ) and all parameters significantly correlated with temperature at the  $p < 0.05$  (\*) or  $p < 0.01$  (\*\*) level; (B) ammonium ( $\mu\text{M}$ ), (C) nitrate ( $\mu\text{M}$ ), and (D) phosphate ( $\mu\text{M}$ ). The  $x$ -axis for A-D is time (days). The  $y$ -axis is temperature ( $^{\circ}\text{C}$ ) (A) or alongshore distance (m) (B-D). A red dashed line marks the beach nourishment location (HT) (B-D), and yellow boxes indicate individual nourishment events. Subplots (E-G) show direct correlations between temperature ( $x$ -axis) and (E) ammonium, (F) nitrate, or (G) phosphate ( $y$ -axis). Spearman's correlation coefficients (Rho) are shown in the upper right hand corner of each correlation plot.



## CHAPTER 6.

### SUMMARY AND CONCLUSIONS

The goal of this dissertation was to evaluate different processes (both physical and biological) that regulate concentrations of fecal indicator bacteria (FIB) in the nearshore, and explore the contribution of these process to coastal FIB survivorship. The overarching conclusion of this work is that the importance of physical transports and FIB mortality can be spatially (CH 2-3) or temporally (CH 5) variable, and that measurements of both are necessary for accurately predicting the extent and intensity of nearshore FIB pollution (CH 2-5). This conclusion may seem self-evident, but very few studies have quantitatively evaluated these processes, making it difficult to identify the dominant controls on FIB concentrations in different systems (Boehm 2003; Kim et al., 2004; Boehm et al., 2005; Thupaki et al., 2010). Our ability to build accurate dynamics-based or predictive statistical models for use in future beach management programs rests on our ability to identify these processes, and understand the interactions among them.

One unique aspect of this dissertation is the evaluation of FIB dynamics both in knee-deep surfzone waters (traditional monitoring method), and seaward of the surfzone, where FIB have been sampled less frequently (CH 2-3). Our analyses showed that early morning FIB concentrations can exceed EPA single sample standards in the outer surfzone (and up to 100 m beyond), which has health-risk implications for surfers and paddle boarders who frequent these waters. Furthermore, the processes controlling FIB loss in these areas were different. Physics (advection and horizontal

diffusion) contributed significantly to FIB loss in the surfzone, as has been reported in other studies of dynamic beaches (Boehm 2003; Kim et al., 2004; Boehm et al., 2005). These processes were less important, however, seaward of the surfzone, suggesting that offshore FIB loss at dynamic beaches may be dominated by mortality rather than physics.

Notably, this conclusion rests upon the assumption that our physical model accurately captures dominant along and cross-shore physical processes in both locations. For the limited duration and alongshore spatial extent of our Huntington Beach sampling program (5 h and ~1000 m), we believe that this assumption is reasonable. Over greater spatial and temporal scales, however, rip-cell dilution may contribute significantly to coastal FIB loss and would be necessary to include in physical models (Boehm 2003; Boehm et al., 2005). This process is unlikely to have been dominant during our study because observed FIB decay was constant at all alongshore sampling stations. If surfzone FIB were periodically ejected in rip-cell plumes, decay would have been temporally variable in the alongshore.

In addition to the aforementioned spatial variability in the contribution of mortality and physical transports to nearshore FIB loss, it is also likely that the role of these processes may be temporally variable. During the Sediment Fate and Transport study (CH 5), microcosm experiments showed that mortality rates of sediment-associated FIB were temporally variable. Initial FIB mortality was rapid, after which mortality rates were near zero, suggesting the presence of a stable population. In the surfzone, however, FIB loss never leveled off. This suggests that FIB concentrations at Border Fields State Beach were initially controlled by a combination of mortality



and physical transports, and that following die-off (or VBNC inactivation) of a significant fraction of FIB upon seawater immersion, FIB loss was primarily physically driven.

Observations of temporally variable FIB mortality rates, although infrequently included in FIB models, are becoming increasingly common. When observed, the traditional explanation for multi-rate FIB loss has been the co-occurrence of multiple FIB species (*Enterococcus*) or strains (*E. coli*) with different intrinsic mortality rates (Velz et al., 1984; Easton et al., 2005). While this explanation could be applied to FIB mortality in the microcosm experiments discussed above, it does not explain the biphasic decay observed in our laboratory microcosms (CH 4) that were performed using a single strain of *Enterococcus faecium*, both in the presence and absence of phytoplankton. The processes driving biphasic decay in pure FIB cultures are not yet well understood, which is a concern because these processes may also underlie the biphasic patterns observed in the environment (despite the prevalence of the multi-species hypothesis). Biphasic mortality has the potential to enhance FIB persistence in coastal systems beyond what is predicted under exponential decay because, over time, the fraction of FIB with slower mortality becomes dominant and lingers. The health-risk implications of this process will depend, in part, on the identity of the resistant fraction (antibiotic resistant strain, non-fecal or fecal species, etc.) and whether or not the majority of pathogens also exhibit biphasic mortality, as has been observed for some species of *Salmonella* and *Clostridium*, both of which can cause disease in humans (You et al., 2006; Maraccini et al., 2012; Hellweger et al., 2009).

The seawater microcosm experiments performed in CH 4 not only highlighted

biphasic loss as an appropriate mortality formulation for FIB, but also identified a hitherto unrecognized biotic control on the survivorship of the fecal indicator *Enterococcus*: marine phytoplankton. Bloom concentrations of the dinoflagellate *Lingulodinium polyedrum* were found to halve *Enterococcus* mortality rates in dark seawater microcosms. This emphasizes that ambient marine communities can play an important role in regulating FIB dynamics in coastal systems. Biotic controls on FIB are often left out of marine dynamics-based FIB models because they are considered insignificant relative to solar radiation, temperature effects, and physics. While this may be true in some instances (Bohem, 2003; Bohem et al., 2005), the results of our FIB-phytoplankton model simulations suggest that the presence of phytoplankton can enhance FIB survivorship by ~21%, when viewed in the context of realistic physical processes (alongshore advection and horizontal diffusion). These results suggest that the role of biotic communities on FIB survivorship in seawater may need to be reevaluated. Current work in freshwater systems emphasizes the role of protistan grazing on FIB mortality (Grant and Sanders, 2010; Surbeck et al., 2010), and work in sediments has shown that FIB survivorship is strongly dependent on autochthonous bacterial assemblages (Feng et al., 2010). It is likely that biological controls are just as prevalent in seawater. These processes may have gone unnoticed, however, due to the complexity of FIB sources, transports and growth/decay in marine systems, which can vary with weather, tides, irradiance, and any number of dissolved compounds or organisms. This can make any one relationship difficult to disentangle from others, and favor the identification of processes that are readily measured in high resolution using existing instrumentation: irradiance, temperature, pH, salinity, and dissolved

oxygen.

In both our Huntington Beach and Border Fields State Beach field programs, although mortality emerged alongside physical transports as an important factor controlling FIB dynamics, the specific mechanisms governing FIB mortality were consistently difficult to identify. At Huntington Beach this may have been due in part to our sampling design, which traded temporal duration of sampling for high spatial resolution. The true impacts of processes that are cyclical (like solar radiation) are hard to interpret when less than a full cycle is evaluated. It is also likely that our ability to discriminate between different FIB mortality mechanisms was hampered by our limited number of high-resolution measurements in addition to fecal indicators. Specifically, the mortality forms evaluated in this study would have been better constrained if measurements of parameters like solar penetration, protistan grazing rates, and/or reactive oxygen species, had been made. These measurements could have been used to inform the shape of the cross-shore gradients in bacterial stressors in our ADG or ADGI models, which, in the absence of such measurements, were approximated using a tanh function.

In a way, the absence of high-resolution measurements of this sort at Huntington Beach reflects the way I viewed fecal indicators at the start of my dissertation. FIB were terrestrial organisms that were not likely to persist (or grow) in marine waters, and had extra-enteric mortality that was irradiance-dominated. As my research has progressed, however, my view of FIB has become increasingly ecological, with FIB seen less as a pollutant and more as part of an ecosystem. This means competition, predation, facilitation, and all manner of ecological principles

apply to FIB, as well as abiotic stressors like irradiance-induced mortality. Even irradiance-induced mortality is not likely to be as simple as initially envisioned, as absolute irradiance is far less important than true irradiance penetration, which is a function of water depth, turbidity, bubbles, plankton concentration, etc., all of which are linked to turbulent surfzone dynamics (Alkan et al., 1995). It is possible to take absolute irradiance measurements and simulate this complexity using models, as was done in CH 2's ADGI model (advection + diffusion + cross-shore variable solar mortality), but this process only produces estimates of what an irradiance penetration field might look like. The more we simulate, the greater our model error, and the less we are able to distinguish among individual processes affecting FIB survivorship. Clever sampling of the specific factors that directly affect FIB (irradiance penetration instead of absolute irradiance, community grazing rates instead of grazer concentration, etc.) is likely to significantly increase our ability to detect and distinguish between different processes affecting FIB survivorship in marine systems.

Notably, however, even when high-resolution field measurements of this sort are made, the identification of dominant mechanisms controlling FIB mortality can be difficult. At Border Field State Beach irradiance penetration was measured directly, allowing evaluation of solar effects on FIB mortality (CH 5). As it turned out, however, irradiance penetration during these experiments was near zero (presumably due to turbidity associated with nourishment sediments). This means that, while we could say definitively that irradiance-induced mortality did not dominate FIB loss in these experiments, we still don't know what the dominant factor was. This example underscores the notion that FIB survivorship in marine systems is incredibly complex,

and co-monitoring a sufficient number of environmental variables to identify those that dominate mortality in any given system is a daunting task. Interdisciplinary and multi-institutional experiments are likely to be invaluable in this regard, as a wide range of variables are measured contemporaneously by different researchers for a single system, increasing our chances of capturing the processes that contribute most prominently to FIB loss in those systems (Hamilton et al., 2004; Boehm et al., 2009).

Because they represent a combined research effort, interdisciplinary field programs are also more likely than other field programs to have the manpower and time to make field-based rate measurements. As indicated by our 1-per-day FIB-phytoplankton correlation assessments in CH 4, measurements of concentration (especially those that are widely spaced in time) may be difficult to use for assessing relationships among organisms, even when those relationships are known exactly. By measuring FIB growth/mortality rates directly we sidestep problems associated with source dynamics; FIB concentration at any one time could be high or low independent of environmental conditions, simply due to source load. It is the rate at which those introduced concentrations change that is a function of environmental variables like solar radiation, temperature, phytoplankton, protists, etc. For this reason, rate measurements are likely to increase our understanding of FIB survivorship in marine systems more than measurements of FIB concentration. Our use of DrEMP in CH 5 is just one example of a field-deployable system for FIB rate estimation in marine systems. Other systems that allow for continuous flow-through of nutrients and other dissolved compounds, have been used successfully to measure FIB growth/mortality rates in freshwater lakes and streams (Schumacher, 2003). Such systems may prove

difficult to implement in the surfzone, however, due to the turbulent conditions.

In light of the aforementioned complexity of FIB dynamics in coastal systems, the success of our simple dynamics-based models at Huntington Beach (CH 2-3) and our one-parameter generalized linear model (GLM) at Border Fields State Beach (CH 5) in capturing FIB variability, is both surprising and comforting. The success of these models suggests that although FIB dynamics are complex, it is likely that these dynamics are dominated by a mere handful of the many possible parameters affecting FIB. It is notable that in both systems, the parameters identified as important were different. Furthermore, the important parameters varied spatially – in the cross-shore at Huntington Beach and the alongshore at Border Fields State Beach. In fact, at Border Fields State Beach, our model was really only successful at one spatial location (which happened to contain the majority of the FIB signal). The factors affecting background, lower frequency FIB contamination during this study remain unknown.

By increasing our understanding of both the identity of, and interplay among processes that control FIB concentrations in coastal marine systems, the studies in this dissertation bring us closer to our goal of constructing informed water-quality monitoring programs and predictive models that allow us to effectively track FIB in marine systems. In order to translate between FIB and health risk, however, it is necessary to evaluate the survivorship of marine pathogens in much the same way this study evaluated FIB. Although many in the field of water quality have become disenchanted with FIB as indicators of health risk (due to observations of environmental growth and/or the existence of non-fecal bacterial reservoirs like sand), we currently know too little about pathogen persistence in marine systems to infer that

these processes render FIB ineffective as indicators. Recently, *Staphylococcus* (a non-fecal pathogen) was observed to be correlated with *Enterococcus* in both seawater and sediment at several Southern California beaches (Goodwin et al., 2012). Because the sources of *Staphylococcus* and *Enterococcus* are likely to be different, this correlation may reflect similar environmental survivorship and/or reservoirs, linking FIB to pathogens.

Notably, not all pathogens are likely to be correlated with FIB in marine waters. Thus, the connection between FIB and health risk is likely to be a function of the specific pathogens we are concerned with. Human viruses are often the poster child of where FIB fail because they do not replicate in the environment and are often uncorrelated with FIB concentrations (Jiang and Chu, 2004; Choi and Jiang, 2005; Boehm et al., 2009). This being said, Choi and Jiang (2005) showed that viral loads in two Southern California rivers were not only uncorrelated with FIB, but with health risk, due to tendency of our current genetic identification methods to detect non-infectious, as well as infectious, viral particles. Ironically, at this time we may understand more about what FIB mean for health risk, than specific pathogens. Future efforts should focus on synthesizing FIB dynamics and pathogen dynamics in an environmental context (similar to what was done here with FIB alone) and linking all of this back to human health risk. Beach managers have the unenviable job of translating complex environmental information into discrete, binary closure decisions. We have an obligation as scientists in a water quality field, to help make this process as painless as possible.

### Literature Cited

- Alkan, U.; Elliot, D. J.; Evison, L. M. 1995. Survival of enteric bacteria in relation to simulated solar radiation and other environmental factors in marine waters. *Water Res.* 29, 2071-2081.
- Boehm, A. B. 2003. Model of microbial transport and inactivation in the surfzone and application to field measurements of total coliform in northern Orange County, California. *Environmental Science and Technology.* 37, 5511-5517.
- Boehm, A. B.; Keymer, D. P.; Shellenbarger, G. G. 2005. An analytical model of enterococci inactivation, grazing, and transport in the surfzone of a marine beach. *Water Research.* 39, 3565-3578.
- Boehm, A.; Yamahara, K.; Love, D. C.; Peterson, B. M.; McNeill, K.; Nelson, K. L. 2009. Covariation and photoinactivation of traditional and novel indicator organisms and human viruses at a sewage impacted marine beach. *Environmental Science and Technology.* 43, 8046-8052.
- Choi, S; Jiang, S. C. 2005. Real-time PCR quantification of human adenoviruses in urban rivers indicates genome prevalence but low infectivity. *Applied and Environmental Microbiology.* 71: 7426-7433.
- Easton, J. H., J. J. Gauthier, M. M. Lalor, and R. E. Pitt. 2005. Die-off of pathogenic *E. coli* O157:H7 in sewage contaminated waters. *Journal of the American Water Resources Association.* 41:1187-1193.
- Feng, F.; Goto, D.; Yan, T. 2010. Effects of autochthonous microbial community on the die-off of fecal indicators in tropical beach sand. *FEMS Microbial Ecology.* 74: 214-225.
- Goodwin, K. D.; McNay, M.; Cao, Y.; Ebentier, P; Madison, M.; Griffith, J. F. 2012. A multi-beach study of *Staphylococcus aureus*, MRSA, and enterococci in seawater and beach sand. *Water Research.* in press.
- Grant, S. B.; Sanders, B. F. 2010. Beach boundary layer: A framework for addressing recreational water quality impairment at enclosed beaches. *Environmental Science and Technology.* 44: 8804-8813.
- Hamilton, P.; Jones, B; Largier, J; McGee, C.; Noble, M.; Orzech, K; Robertson, G; Rosenfield, L.; Xu, J. 2004. USGS 04-1019. Huntington Beach shoreline contamination investigation phase III. Coastal circulation and transport patterns: the likelihood of OCSD's plume impacting the Huntington Beach shoreline. Edited by Noble, M. and Xu, J.



- Hellweger, F. L.; Bucci, V.; Litman, M. R.; Gu, A. Z.; Onnis-Hayden, A. 2009. Biphasic decay kinetics of fecal bacteria in surface water not a density effect. *Journal of Environmental Engineering*. 135: 372-376.
- Jiang, S. C.; Chu, W. 2004. PCR detection of pathogenic viruses in Southern California urban rivers. *Journal of Applied Microbiology*. 97: 17-28.
- Kim, J. H.; Grant, S. B.; McGee, C. D.; Sanders, B. F.; and Largier, J. L. 2004. Locating sources of surf zone pollution: a mass budget analysis of fecal indicator bacteria at Huntington Beach, California. *Environmental Science and Technology*. 38: 2626-2636.
- Maraccini, P. A.; Ferguson, D. M.; Boehm, A. B. 2012. Diurnal variation in *Enterococcus* species composition in polluted ocean water and a potential role for the enterococcal carotenoid in protection against photoinactivation. *Applied and Environmental Microbiology*. 78: 305-310.
- Schumacher, J. G. 2003. Survival, transport, and sources of fecal bacteria in streams and survival in land-applied poultry litter in the Upper Shoal Creek Basin, Southwestern Missouri, 2001– 2002', *Technical Report*, USGS Water-Resources Investigations Report 03–4243, Rolla MO.
- Surbeck, C. Q.; Jiang, S. C. Grant, S. B. 2010. Ecological control of fecal indicator bacteria in an urban stream. *Environmental Science and Technology* 44, 631-637.
- Thupaki, P.; Phannikumar, M. S.; Beletsky, D.; Schwab, D. J.; Nevers, M. B.; Whitman, R. L. 2010. Budget analysis of *Escherichia coli* at a southern Lake Michigan beach. *Environmental Science and Technology*. 44: 1010-1016.
- Velz, C. J. 1984. Applied stream sanitation, 2nd ed. John Wiley & Sons, Inc., New York, NY.
- You, Y.; Rankin, S. C.; Aceto, H. W.; Benson, C. E.; Toth, J. D.; Dou, Z. 2006. Survival of *Salmonella enterica* serovar Newport in manure and manure-amended soils. *Applied and Environmental Microbiology*. 72: 5777–5783.